

Aus dem Bereich Med. Physiologie
Theoretische Medizin und Biowissenschaften
der Medizinischen Fakultät
der Universität des Saarlandes, Homburg/Saar

The Role of Synaptobrevin2 in Exo-Endocytosis in Primary Mouse Cytotoxic T Lymphocytes

**Dissertation zur Erlangung des Grades eines Doktors der Naturwissenschaften
der Medizinischen Fakultät
der UNIVERSITÄT DES SAARLANDES
2016**

vorgelegt von: Hawraa Bzeih
geb.am: 05.04.1989 in Tyre, Lebanon

Tag des Promotionskolloquiums:

Dekan:

Vorsitzender:

Berichtersteller:

To my beloved family

TABLE OF CONTENT

TABLE OF CONTENT	I
LIST OF ABBREVIATIONS	VI
ACKNOWLEDGMENTS	IX
ZUSAMMENFASSUNG	11
I. INTRODUCTION	13
I.1 The Immune system	13
I.1.1 Innate vs. adaptive immune systems	13
I.1.2 Cytotoxic T Lymphocytes (CTLs)	14
I.1.2.1 Immunological synapse	15
I.1.2.2 Cytotoxic granules (CGs) of CTLs.....	18
I.2 Soluble <i>N</i>-ethylmaleimide-sensitive factor attachment protein receptor (SNARE) proteins	19
I.2.1 Function of SNARE proteins	21
I.2.1.1 Docking	21
I.2.1.2 Priming	22
I.2.1.3 Fusion	23
I.3 Endocytosis	23
I.3.1 Clathrin-mediated endocytosis (CME).....	24
I.3.1.1 Mechanism of clathrin-mediated endocytosis (CME).....	24
I.3.1.2 Constitutive versus ligand-induced CME.....	27
I.3.2 Clathrin-independent endocytosis (CIE)	27
I.3.2.1 Dynamin-dependent CIE	28

I.3.2.2	Dynamin-independent CIE.....	28
I.4	The endosomal pathway: from the plasma membrane to the endosomal system	29
I.4.1	Rab proteins binding to membranes.....	29
I.4.2	Acidification of endosomes.....	30
I.4.3	From the plasma membrane to the early endosomes and back	31
I.4.4	From the early endosomes to late endosomes	32
I.5	Immune diseases associated with the SNARE machinery dysfunction.....	33
I.6	Synaptobrevin2 (Syb2).....	34
I.7	Aim of this work	36
II.	MATERIALS AND METHODS	37
II.1	Materials:	37
II.1.1	Chemicals.....	37
II.1.2	Solutions for cell culture	39
II.1.2.1	RPMI 1640 (10% FCS).....	39
II.1.2.2	IMDM (10% FCS)	39
II.1.2.3	Isolation Buffer	39
II.1.2.4	Erythrolysis buffer (100 ml).....	39
II.1.3	Solutions for cell fixation and staining	39
II.1.3.1	Paraformaldehyde (15% PFA, 10 ml)	39
II.1.3.2	Quenching Solution (0.1 M Glycine)	40
II.1.3.3	Permeabilization Solution (50 ml, 0.1% Triton)	40
II.1.3.4	Blocking Solution (50 ml, 2% BSA).....	40
II.1.3.5	Mounting Medium.....	40
II.1.4	Solutions for cloning	40
II.1.4.1	LB-Medium.....	40

II.1.4.2	Loading Buffer	41
II.1.5	Solutions for Western blot	41
II.1.5.1	Lysis buffer (5 ml).....	41
II.1.5.2	TBS (10x).....	41
II.1.5.3	TBST (0.05%) (1L).....	41
II.1.6	Bacteria and Cell Lines	42
II.1.6.1	Bacteria	42
II.1.6.2	Cell Lines	42
II.1.7	Mouse Strains.....	42
II.1.8	Kits.....	42
II.1.8.1	Kits for cloning.....	42
II.1.8.2	Kits for cell culture.....	42
II.1.9	Antibodies	43
II.1.10	Plasmids	43
II.1.10.1	Plasmids for Rab proteins.....	43
II.1.10.2	pMAX with a new multiple cloning site (MCS):	43
II.2	Methods	46
II.2.1	Positive isolation of CD8 ⁺ T lymphocytes	46
II.2.2	RNA extraction	46
II.2.3	RNA quality check.....	47
II.2.4	cDNA synthesis.....	47
II.2.5	Brain and CTL protein lysate preparation.....	47
II.2.6	Western blot.....	48
II.2.7	Co-Immunoprecipitation.....	49
II.2.7.1	IP using anti-Synaptobrevin2 antibody:	49
II.2.8	Labeling of anti-RFP antibodies with fluorescent dyes	50
II.2.9	Electroporation of CTLs with different Rab protein constructs	51
II.2.10	Coating coverslips.....	51

II.2.11 Live imaging	52
II.2.11.1 LSM microscope	52
II.2.11.2 Acidification of endocytosed Syb2-containing (endo-Syb2) vesicles	52
II.2.12 Imaging using structured illumination microscope (SIM)	53
II.2.12.1 SIM microscope	53
II.2.12.2 Fixation and labeling of cells	54
II.2.13 Image analysis.....	55
II.2.14 Software	55
III. RESULTS	56
III.1 SNAP-23 is a t-SNARE required for cytotoxic granule (CG) fusion in mouse CTLs.....	56
III.2 Proteins present on endocytosed Syb2-containing (endo-Syb2) vesicles.....	59
III.2.1 SNAP-23 is endocytosed with endo-Syb2 in the same vesicle	59
III.2.2 ZAP70 is endocytosed with endo-Syb2 in the same vesicle	61
III.2.3 H ⁺ V-ATPase is present on endo-Syb2 vesicles.....	63
III.2.4 H ⁺ V-ATPase is colocalized with endo-Syb2 vesicles 1-2 min following exposure of Syb2-mRFP at the plasma membrane shown by live imaging	65
III.3 Trafficking of endo-Syb2 vesicles through the endosomal pathway	66
III.3.1 Endo-Syb2 vesicles reach early endosomes within 15 min of target cells' addition.....	67
III.3.2 Endo-Syb2 vesicles show no colocalization with recycling endosomes	68
III.3.3 Endo-Syb2 vesicles reach late endosomes 30-60 min after CTL:target cell conjugation	69
III.4 Acquisition of granzyme B by endo-Syb2 vesicles	70
III.4.1 Endo-Syb2 vesicles do not acquire granzyme B at Rab5-containing early endosomes	71
III.4.2 Endo-Syb2 vesicles colocalize with granzyme B at the late endosomes 60 min after CTL:target cell conjugation.....	73

IV.	DISCUSSION	76
IV.1	SNAP-23 is a t-SNARE required for CG fusion in mouse CTLs.....	76
IV.2	H⁺ V-ATPase is endocytosed along with Syb2, the v-SNARE of CGs, into early endosomes	78
	IV.2.1 SNAP-23 and ZAP70 are endocytosed along with endo-Syb2 into early endosomes	79
IV.3	Syb2 reaches the early endosomes within 15 min after addition of target cells	81
IV.4	Endo-Syb2 traffics through early endosomes and late endosomes but not recycling endosomes	83
IV.5	Endo-Syb2 vesicles acquire granzyme B at the late endosomes to become a fully mature vesicle	84
IV.6	Model for Syb2 endocytosis	86
V.	OUTLOOK.....	88
VI.	SUMMARY	89
	LITERATURE	91
	CURRICULUM VITAE.....	ERROR! BOOKMARK NOT DEFINED.
	PUBLICATIONS	103

List of Abbreviations

°C	Degrees Celsius
APC	Antigen-presenting cell
ApE	A-plasmid Editor
ATP	Adenosine triphosphate
AU	Airy Units
a.u.	Arbitrary units
βME	β-Mercaptoethanol
Bp	Base pair
BSA	Bovine serum albumin
[Ca ²⁺] _i	Intracellular calcium concentration
CD	Cluster of differentiation
CG	Cytotoxic granule
CTL	Cytotoxic T lymphocyte
DMSO	Dimethyl sulfoxide
DNA	DeoxyriboNucleic Acid
dNTP	DeoxyriboNucleotide TriPhosphate
DH5α	<i>Escherichia coli</i> competent cells: F ⁻ endA1 glnV44 thi-1 recA1 relA1 gyrA96 deoR nupG purB20 φ80dlacZΔM15 Δ(lacZYA- argF)U169, hsdR17(rK ⁻ mK ⁺), λ ⁻
DPBS	Dulbecco's phosphate buffered saline
<i>E. coli</i>	<i>Escherichia coli</i>
EDTA	Ethylenediaminetetraacetic acid
EGTA	Ethylene glycol tetraacetic acid
EtBr	Ethidium Bromide
FCS	Fetal calf serum
G	Gram
GPCR	G-protein coupled receptor
Hr	Hour
HEPES	4-(2-Hydroxyethyl)-1-piperazineethanesulfonic acid

LIST OF ABBREVIATIONS

HPLC	High performance liquid chromatography
ICAM-1	Intercellular adhesion molecule 1
IMDM	Iscove's Modified Dulbecco's medium
KO	Knockout
LAMP	Lysosomal associated membrane proteins
LB	Loading buffer
LB-medium	Lysogeny Broth-medium
LDS	Lithium dodecyl sulfate
LFA-1	Lymphocyte function-associated antigen 1
LSM	Laser scanning microscopy
M	Mol/L
m-	Milli
MHC	Major histocompatibility complex
Min	Minute(s)
MW	Molecular weight
n-	nano
NSF	<i>N</i> -ethylmaleimide-sensitive fusion factor
ORF	Open reading frame
Ori	Origin of replication
P	Probability value
p-	Pico
PBS	Phosphate buffer saline
PCR	Polymerase chain reaction
Pen/Strep	Penicillin/Streptomycin
PFA	Paraformaldehyde
<i>Pfu</i>	<i>Pyrococcus furiosus</i> polymerase
pH	Potential Hydrogen
Rcf	Relative centrifugal force
RNA	Ribonucleic Acid
Rpm	Round per minute

LIST OF ABBREVIATIONS

RPMI	Roswell Park Memorial Institute
S	Second(s)
SAP	Shrimp alkaline phosphatase
SEM	Standard error of the mean
SMAC	Supra molecular activation clusters
SNAP-23	Synaptosomal-associated protein-23
SNAP-25	Synaptosomal-associated protein-25
SNARE	Soluble <i>N</i> -ethylmaleimide-sensitive factor attachment protein receptor
SV	Synaptic vesicle
Syb2	Synaptobrevin2
TAE	Tris-Acetate-EDTA
TCR	T cell receptor
Tris	Tris(hydroxymethyl)aminomethane
t-SNARE	Target-SNARE
U	Units
UV	Ultra Violet
VAMP	Vesicle-associated membrane protein
v-SNARE	Vesicular-SNARE
WT	Wild type

ACKNOWLEDGMENTS

My great gratitude goes to my supervisor Prof. Jens Rettig for his continuous support, encouragement and great scientific discussions during my entire PhD. Without his guidance and motivation I would have not been able to complete my thesis. I would always be grateful to him for being such a great advisor and mentor.

I would also like to thank Dr. Varsha Pattu for her direct supervision and her scientific input to my work. I would like to thank Dr. Elmar Krause, Dr. Ulrike Hahn and Dr. Mahantappa Halimani for their support and guidance for performing new experiments especially in the beginning of my PhD.

I would like to thank Dr. David Stevens, Dr. Varsha Pattu, Dr. Elmar Krause, Dr. Ute Becherer and Dr. Claudia Scherra for their contribution to my work through discussions and for helping me with my thesis. I extend my gratitude to Prof. Olaf Pongs for his great ideas and support during the last period of my PhD.

I would like to thank Prof. Richard Zimmermann and all his group especially Dr. Martin Jung for helping me with performing experiments at his laboratory. I thank also Prof. Markus Hoth and all his group members for helping me especially during the beginning of my PhD. I would like to thank Prof. Dieter Bruns and all his lab members for general discussions and for inviting me as research scientist as a member of GRK1326 that gave me that chance to start my PhD in Germany.

I would like to thank Dr. Emmanuelle Cordat, Prof. Johannes Herrmann and all IRTG1830 members for great discussions during the meetings; and especially Dr. Cordat for allowing me to work in her laboratory during my research stay in Canada. I thank also IRTG1830 for funding and Dr. Gabrielle Amoroso for her amazing support through my entire PhD.

I would like to thank my friends and all my lab members including Ali shaib, Marwa Sleiman, Hsin-Fang Chang, Olga Ratai, Praneeth Chitirala, Keerthana Ravichandran and Angelina Staudt for being very kind and helpful. I especially thank Ali Shaib, Marwa Sleiman, Ali Harb, Ahmed

Shaaban and Mazen Makke for always being there for help regarding science and for being such good friends, making my stay in Germany memorable.

I thank Anja Ludes, Katrin Sandmeier, Manuela Schneider, Anne Weinland, Margarete Klose, Jacqueline Vogel and Tamara Paul for excellent technical help. I extend my thanks to Bernadette Schwarz and Josephine Kretschmer for their assistance and help especially with the paperwork.

Last but not least, I would like to thank my family and my husband Ali for their support and encouragement through my entire PhD making it much easier for me to be abroad and away from them.

ZUSAMMENFASSUNG

Zytotoxische T Lymphozyten (CTLs) töten Zielzellen durch die Freisetzung von Substanzen aus sogenannten zytotoxischen Granulen (CGs). Da CTLs in der Lage sind, mehrere Zielzellen sequentiell zu töten, werden sie auch als „Serial Killers“ bezeichnet. Voraussetzung für diesen Prozess ist ein schnelles Erneuern von CGs. Diese Erneuerung könnte durch komplette *de novo* Synthese erfolgen oder aber durch Recycling noch verwendbarer Komponenten mit partieller Neusynthese. Um das Recycling besser zu verstehen, haben wir den endocytotischen Weg von Synaptobrevin2 (Syb2), dem v-SNARE von CGs von Maus-CTLs untersucht. Diese Untersuchungen wurden an CTLs von Syb2-mRFP Knockin (Sybki) Mäusen durchgeführt. Durch Exozytose an die Oberfläche gelangtes Syb2-mRFP (weiterhin abgekürzt als Syb2) wurde mit anti-mRFP Antikörpern markiert und so die folgende Endozytose und Prozessierung in den CTLs untersucht.

Wir begannen unsere Studie am Zeitpunkt der Fusion CGs mit der Plasmamembran. Durch Co-Immunopräzipitationsexperimente konnten wir zeigen das Syb2 mit dem synaptosomal-assoziierten Proteinkin-23 (SNAP-23) während der SNARE-Komplexbildung assoziiert. Diese Interaktion dürfte der Fusion von CGs mit der Plasmamembran dienen. SNAP-23 ist als wahrscheinlich ein t-SNARE der CG Fusion. Nach der Fusion von CGs mit der Plasmamembran erscheint das an Syb2 fusionierte mRFP auf der Zelloberfläche. Die Benutzung Fluoreszenzmarkierter anti-RFP Antikörper erlaubt dann das Verfolgen von Syb2 während des endozytotischen Prozesses. Wir konnten verschiedene Proteine identifizieren, die, zumindest bis zur Fusion mit Early Endosomes (frühen Endosomen), zusammen mit Synaptobrevin2 im selben Vesikel auftraten und somit gleichzeitig endozytiert wurden. Proteine, die mit Synaptobrevin2 endozytiert wurden sind das t-SNARE SNAP23, das zeta-Kette- assoziierte-70 kDA-Tyrosin-Phosphoprotein (ZAP70) und das CG-Membranprotein H⁺ V-ATPase. Diese Ergebnisse wurden mit hochauflösender Fluoreszenzmikroskopie erhoben, wobei Proben vor der Untersuchung zu unterschiedlichen Zeitpunkten nach Stimulation fixiert wurden. Die Endozytose der V-ATPase zusammen mit Syb2 wurde außerdem durch *live cell* Experimente verifiziert, bei denen das Ansäuern endozytierter und Syb2-enthaltender Vesikel innerhalb von nur 1-2 Minuten nach Stimulation der Zellen gezeigt werden konnte. Endozytiertes Syb2 erreichte 15 min nach dem

initialen Stimulus Early Endosomes (frühe Endosomen), wie durch Kollokalisierung mit eGFP-RAB5 (einem Early Endosome Marker) gezeigt wurde. Nach 60 min schließlich erreichte endozytiertes Syb2 die Late Endosomes (späte Endosomen, Marker eGFP-RAB7). Hingegen konnten wir kein endozytiertes Syb2 in Recycling Endosoms (Marker eGFP-Rab11) finden. Um herauszufinden, ob Vesikel, die endozytiertes Syb2 enthalten, zu neuen zytotoxischen Granulen heranreifen, haben wir untersucht, ob diese Vesikel das als Marker für reife zytotoxische Granulen geltende apoptotische Protein GranzymB aufnehmen. Wir fanden, dass GranzymB mit Syb2 nach 60 min kollokalisiert, also nach derselben Zeit der maximalen Kollokalisierung mit Late Endosomes.

Unsere Studie identifiziert SNAP-23 als t-SNARE, das mit dem V-SNARE Syb2 interagiert um die Fusion von CGs zu initiieren. Außerdem wird gezeigt, dass exozytiertes Syb2 zusammen mit anderen Komponenten von CGs endozytiert wird und während der Reifung lediglich fehlende Proteine wie Granzym B neu eingebaut werden. Dieser Prozess könnte für das „Serial Killing“ von CTLs wichtig sein.

I. Introduction

I.1 The Immune system

I.1.1 Innate vs. adaptive immune systems

The immune system consists of two main branches: the innate and the adaptive immune systems. The skin and epithelial tissues constitute the first line of defense of the innate system. They function to prevent the entry of pathogens into the host tissue by rapidly eliminating them, carried out by the action of innate immune cells such as neutrophils, phagocytes and natural killer (NK) cells. When a pathogen escapes the action of innate immune cells, the highly specific and more effective cells of the adaptive immune system comes into action (Medzhitov and Janeway, 2000). The adaptive immune system consists of humoral and cellular responses. The humoral response is generated by B lymphocytes that upon activation differentiate into plasma cells, which produce antibodies against the invading pathogen. These specific antibodies neutralize extracellular microbes and prevent their entry into host cells allowing cells of the innate immune system to phagocytose and eliminate them. The second response known as the cellular response is performed by another subset of lymphocytes known as T lymphocytes, these are either CD4⁺ (T_h cells) or CD8⁺ cells (known as cytotoxic T lymphocytes (CTLs) upon activation). Initially, lymphocytes are synthesized as naïve cells. Such cells possess a specific receptor for a specific antigen but are not functionally active. Upon encounter with an appropriate antigen, presented as an antigen-MHC complex on the surface of an antigen presenting cell (APC), peptides presented by MHC class I are recognized by CD8⁺ cells and peptides presented by MHC class II are recognized by B cells and CD4⁺ cells, the lymphocyte carrying the corresponding receptor is activated and induced to proliferate in a process known as clonal expansion. This activation process produces copies of lymphocytes carrying the same receptor (clones), which are then able to carry out their effector function against their target. Effector CD4⁺ cells produce cytokines that activate phagocytes and other lymphocytes including B cells and CD8⁺ cells. Activated CD8⁺ cells or CTLs are then able to induce death of target cells (Figure 1) (Abbas et al., 2015) (Dempsey et al., 2003; Gasteiger and Rudensky, 2014).

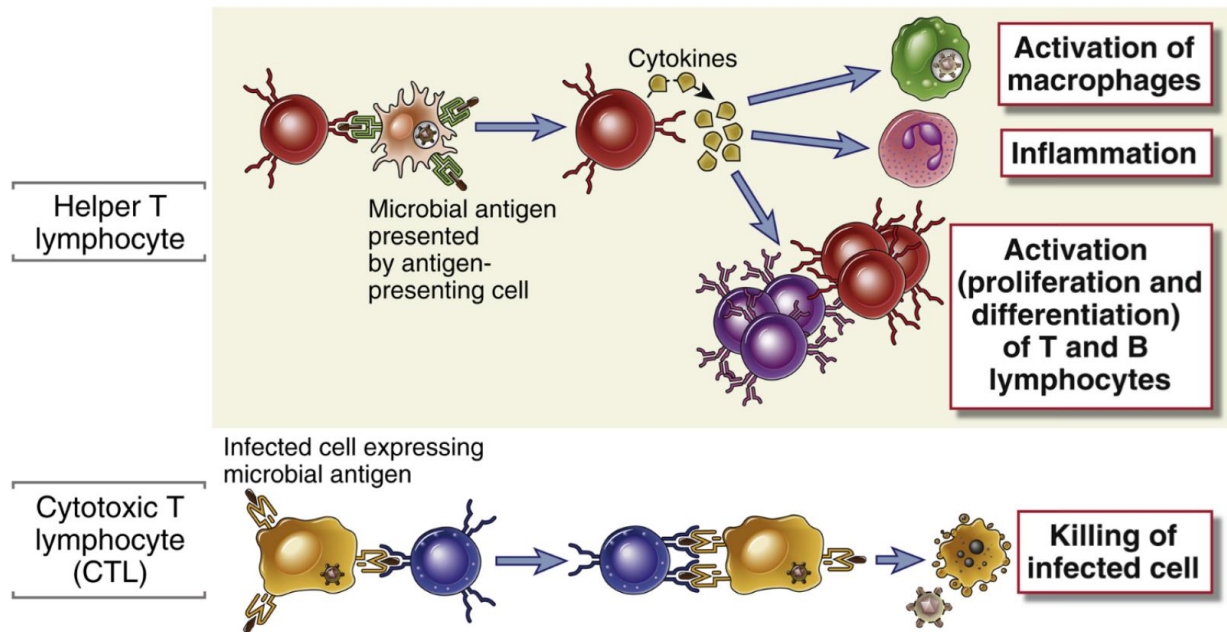


Figure 1. Cellular response of the adaptive immune system.

Different types of pathogens activate different subsets of T cell lymphocytes. $CD4^+$ T cells differentiate into helper T lymphocytes (Th) (upper panel) upon encounter with an APC carrying bacterial antigens on MHC class II. Th cells then produce cytokines that activate innate immune cells and other lymphocytes. $CD8^+$ T cells differentiate into cytotoxic T lymphocytes (CTLs) (lower panel) when the T cell receptors (TCR) recognize viral antigens bound to MHC class I presented by an APC. This process activates CTLs, so upon encounter with an infected cell they release cytotoxic proteins that lead to target cell apoptosis. APC, antigen-presenting cell; MHC, major histocompatibility complex (Abbas et al., 2015).

I.1.2 Cytotoxic T Lymphocytes (CTLs)

Activated $CD8^+$ T cells or cytotoxic T lymphocytes are known as the killer cells of the adaptive immune system. They derive their name from their ability to kill virally-infected and tumor cells by releasing the content of their cytotoxic granules (CGs), perforin and granzyme, which are then taken up by the target cell resulting in its death (Zhang and Bevan, 2011).

Naïve $CD8^+$ T cells carry T cell receptors (TCRs), which are specific to a single peptide. There are millions of T cell clones, i.e. carrying TCRs with different specificity against a wide spectrum of pathogens. Initial activation of naïve $CD8^+$ T cells require that they get in contact with an antigen presenting cell (APC), which presents an appropriate peptide on an MHC class I molecule. The foreign peptides presented by MHC class I molecules are derived from cytosolic pathogens such as viruses. For this reason, $CD8^+$ T cells which recognize these peptide-MHC I complexes, usually mediate the response to a viral infection (Figure 1, lower panel). Upon TCR

recognition of a specific peptide presented as an MHC I-peptide complex, CD8⁺ T cells which patrol the blood and lymphatic systems decrease their rate of migration, and remain in the region of contact with their APCs. This usually occurs in the peripheral lymphoid organs. This cessation of motion is the result of interaction of cell-cell adhesion molecules (Dustin and Springer, 1989). Once a CD8⁺ T cell is activated it increases the expression of activation markers, upregulates the expression of cytotoxic proteins, secretes cytokines and proliferate to induce a more efficient clearance of the pathogen. Activated or effector CTLs have a short life, but some remain as memory cells which can initiate a faster and stronger response upon a repeated encounter to the same antigen specific to their TCR (Abbas et al., 2015).

I.1.2.1 Immunological synapse

The TCR-pMHC I (peptide-MHC I) interaction leads to the formation of a close contact between the CD8⁺ T cell and the APC (target cell). This contact is called the immunological synapse (IS). The initial IS, also known as the signaling synapse, is long lasting and is formed to activate a naïve CD8⁺ T cell against a specific pathogen thus inducing effector CTL differentiation. The second IS is short lived, lasting for about 20 to 30 min. It is formed between a fully activated CTL and its target: in this case the CTL polarizes its newly formed CGs towards the IS directly upon contact with their target where the CGs fuse with the plasma membrane and release their content, inducing target cell death. Both types of synapses are structurally similar, with compartmentalization into three areas, a central area called central supra molecular activation cluster (cSMAC) surrounded by a peripheral ring called the pSMAC which is surrounded by a distal area called the dSMAC (Figure 2) (Grakoui et al., 1999; Monks et al., 1998). Upon initial contact of the CTL with the target cell, their contact area is rich with polymerized actin (Ryser et al., 1982), which then moves rapidly (after around one minute) towards the periphery of the newly formed IS to clear the center for the TCR microclusters which translocate laterally from the pSMAC upon actin network reorganization (Campi et al., 2005; Varma et al., 2006). A second wave of TCR arrives at the IS later with the polarizing centrosome about 4 to 6 minutes after IS formation (Das et al., 2004; Ritter et al., 2015). The polarizing centrosome (Kupfer and Singer, 1989) also directs the accumulating CGs on the microtubules towards the CTL-target contact site (Geiger et al., 1982; Ritter et al., 2015; Stinchcombe et al., 2001b; Stinchcombe et al., 2006) where they fuse with the CTL plasma membrane in a specialized secretory domain within the cSMAC, releasing their toxic cargo (Peters et al., 1989) (See Figure 2). The

INTRODUCTION

interaction between the TCR and the peptide-MHC I complex presented on the APC or target cell accounts for the 13 nm distance between the two interacting cells (Choudhuri et al., 2005). Other components of the cSMAC include members of the Src-family kinases, Lck and Fyn, which interact with the cytosolic domain of the CD3 receptor. These molecules are recruited in the first minutes of TCR-peptide interaction and can be used as the markers for early IS formation (Beal et al., 2009). The pSMAC contains adhesion molecules like lymphocyte function-associated antigen 1 (LFA-1), found on the T cell surface, which interacts with intercellular Adhesion Molecule 1 (ICAM-1) located on the target cells' membrane, inducing the formation of a tight contact between the CTL and the target cell (Monks et al., 1998; Potter et al., 2001). The cytosolic tail of LFA-1 binds to talin, causing its aggregation at the cSMAC. The reorganized actin clusters at the periphery of the IS to form the dSMAC, which is also the site for the accumulation of the phosphatase CD45 that is responsible for the activation of many signaling proteins (Freiberg et al., 2002).

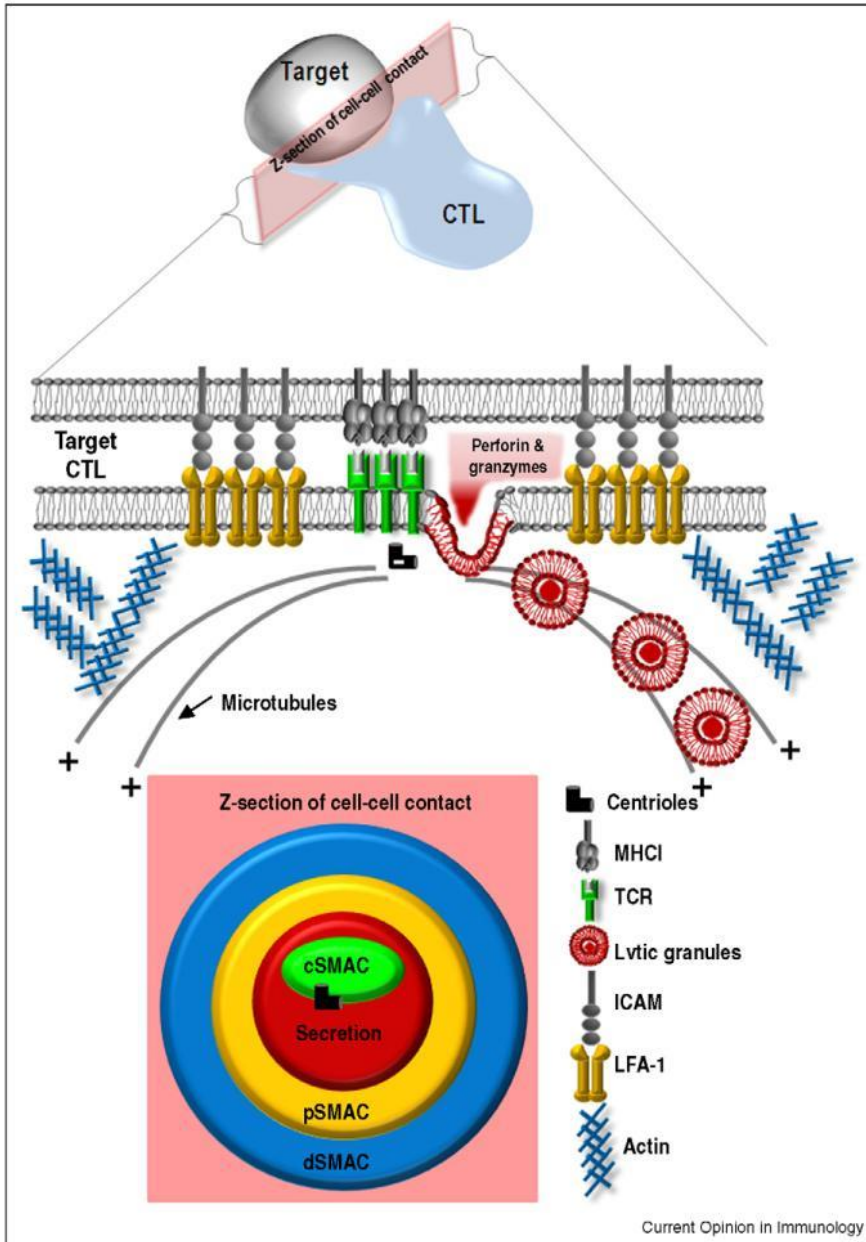


Figure 2. Organization of the immunological synapse (IS).

The contact formed between the CTL and the target cell, the IS, is shown here in detail. In the central area called cSMAC (central SMAC), the TCR clusters on the T cell membrane binding to the peptide-MHC I complex on the target cell membrane (green). The lytic granules or CGs fuse in the area around the TCR (red). The pSMAC (peripheral SMAC) surrounds the cSMAC and it contains the adhesion molecule LFA-1 on the CTL membrane, binding to ICAM on the target cell membrane and surrounded by actin localized to the dSMAC (distal SMAC). CTL, cytotoxic T lymphocyte; ICAM, Intercellular Adhesion Molecule; LFA-1, lymphocyte function-associated antigen 1; SMAC, supra molecular activation cluster (Jenkins and Griffiths, 2010).

I.1.2.2 Cytotoxic granules (CGs) of CTLs

CTLs are able to kill target cells because they contain organelles called cytotoxic granules (CGs) that contain cytotoxic proteins. CGs are also known as secretory lysosomes because they harbor many of the protein content found in or on conventional lysosomes (Burkhardt et al., 1990; Peters et al., 1991), such as the lysosomal transmembrane proteins, acid hydrolases and others. Among the membrane proteins of CGs, are the lysosomal associated membrane proteins (LAMP-1 and LAMP-2, and LAMP-3 or CD63), Fas-ligand (FasL), the V-type H⁺ ATPase, and the v-SNARE synaptobrevin2 (Syb2). Most membrane proteins are recognized by one of the adaptor proteins (AP-1, -2, and -3) depending on their location whether on endosomes, the plasma membrane, or the Golgi respectively, where they are then exported to reach the CGs via lysosomes. LAMP proteins are heavily glycosylated and constitute up to 50% of the lysosomal membrane proteins (Fukuda, 1991); the N-glycosylated regions of LAMP proteins are exposed to the lumen of lysosomes. They are thought to be responsible for the protection of the lysosomal membrane from the action of the luminal soluble hydrolases. LAMP-1 and -2 (also called CD107a and b, respectively) are frequently used as markers for degranulation of lysosomes in CTLs (Betts et al., 2003). FasL, another membrane component of CGs, is incorporated into the CTL membrane upon CG fusion; it is then cleaved by extracellular proteases producing a soluble FasL which can bind to the Fas receptor (CD95) on the surface of the target cell inducing its apoptosis (Dhein et al., 1995). The V-ATPase (see below) is involved in maintaining the acidic pH of CGs (pH 5.5-4.5) (Burkhardt et al., 1990) that is required to keep the cytotoxic proteins in an inactive state in the vesicle. As a requirement for fusion, CGs require a vesicle-associated SNARE protein (v-SNARE, see also I.2); Matti et al showed that Syb2 was the v-SNARE required for fusion in mouse CTLs (Matti et al., 2013); Syb2 localized to CGs containing granzyme B, which are characterized by an electron dense core. The author and his colleagues also found that CG fusion is aborted in CTLs treated with tetanus toxin that cleaves Syb2 (Matti et al., 2013).

CGs also contain a number of soluble proteins. The cytotoxic proteins perforin and granzyme, the lysosomal hydrolases such as cathepsins and the chondroitin sulfate proteoglycans (serglycin) are found in CGs. Serglycin gives the CGs their electron dense structure and it binds the cytotoxic proteins to keep them inactive while still inside the vesicle (Blott and Griffiths, 2002; de Saint Basile et al., 2010). Cytotoxic proteins are initially synthesized as inactive

precursors. Perforin, the pore forming protein, is synthesized as a 70-kDa inactive precursor with N-terminal glycosylation that is processed into the active form upon entry into the CGs. Activation of perforin entails the removal of a 10-20 amino acid stretch from the C-terminus exposing a phospholipid-binding C2 domain. Perforin is then able to bind lipid membranes via this domain in a calcium-dependent manner (Uellner et al., 1997). Perforin's C-terminus and its N-linked glycans are important for its traffic from the ER to the Golgi and finally to the CGs (Brennan et al., 2011). Calreticulin, a calcium binding protein, plays an important role in inhibiting the function of perforin inside the CG, along with the serglycin complex (Fraser et al., 2000; Masson et al., 1990). The other family of CG cytotoxic proteins, granzymes, belongs to the group of serine esterases. There are about eight identified granzymes in mouse CTLs (A, B, C, D, E, F, G and H) (Masson and Tschopp, 1987). Granzyme B, for example, is synthesized as a pro-enzyme that is activated at the CGs by the cleavage of an N-terminal dipeptide by a group of redundant lysosomal hydrolases (cathepsins) (D'Angelo et al., 2010). Granzymes A and B, as well as some lysosomal proteins such as cathepsin B, are targeted to the CGs via mannose-6-Phosphate receptor (Griffiths and Isaaz, 1993).

Upon CG fusion and release of cytotoxic proteins, perforin is thought to aid in granzyme penetration into the target cell either by forming pores in the target's plasma membrane (Podack and Hengartner, 1989) or by being endocytosed into the target in vesicles together along with granzyme, and then forming pores in the vesicle membrane to allow for access of granzyme into the target's cytosol (Shi et al., 1997). Also cathepsin B, a soluble enzyme of CGs, relocates to the CTL membrane upon CG fusion, thus protecting the CTL from self-suicide by cleaving the cytotoxic proteins that are directed back towards the CTL (Balaji et al., 2002).

I.2 Soluble *N*-ethylmaleimide-sensitive factor attachment protein receptor (SNARE) proteins

Intracellular fusion processes occur via coordinated molecular fusion machinery in order to ensure cargo transfer in eukaryotic cells. Cargo-containing vesicles' fusion with the membrane of the destination organelle provides the cargo at the correct place and time. For example, release of cytotoxic proteins into the immunological synapse (IS) occurs by fusion of CG membrane with the plasma membrane (PM) of the CTL. This fusion process, like intracellular fusion

INTRODUCTION

processes, occurs by the concerted action of a group of proteins involved in membrane fusion called SNARE (soluble *N*-ethylmaleimide-sensitive factor attachment protein (SNAP) receptor) proteins (Hanson et al., 1997; Lin and Scheller, 1997). SNAREs are sorted to different membranes depending on the group to which they belong. Early classification determined two groups of SNAREs, v-SNAREs (located to the vesicle membrane or donor membrane) and t-SNAREs (located to the target membrane). SNARE proteins interact with each other via the highly conserved SNARE motif (α -helix, ~ 60 amino acids) contributed from each SNARE protein. The crystal structure of the core SNARE complex determined by Sutton and his colleagues (Sutton et al., 1998) provided more insight into the nature of interaction between the different SNARE motifs showing the tight interaction between the arginine (R) or glutamine (Q) amino acids at the zero layer of the formed SNARE complex (Figure 3). A new terminology based on the central functional residue of the SNARE motif of each SNARE protein involved in the complex, whether it's an R (termed R-SNAREs) or a Q (termed Q-SNAREs) amino acid (Fasshauer et al., 1998) was then developed. Q-SNAREs can be further classified as Qa-, Qb-, Qc- or Qb,c-SNAREs depending on how their α -helix is positioned within the trans-SNARE complex. R-SNAREs and most Q-SNAREs contribute one α -helix to the SNARE complex except for the Qb,c-SNARE proteins which contribute 2 α -helices. One R- and two or three Q-SNAREs (Qa, Qb,c or Qa, Qb, Qc) on opposing membranes form a trans-SNARE complex bringing the two membranes into close proximity, inducing membrane fusion thus forming the transient cis-SNARE complex (Hanson et al., 1997; Weber et al., 1998). The cis-SNARE complex is then disassembled due to the ATPase activity of *N*-ethylmaleimide-sensitive fusion factor (NSF) protein, which binds the complex through α -SNAP (Sollner et al., 1993a; Sollner et al., 1993b).

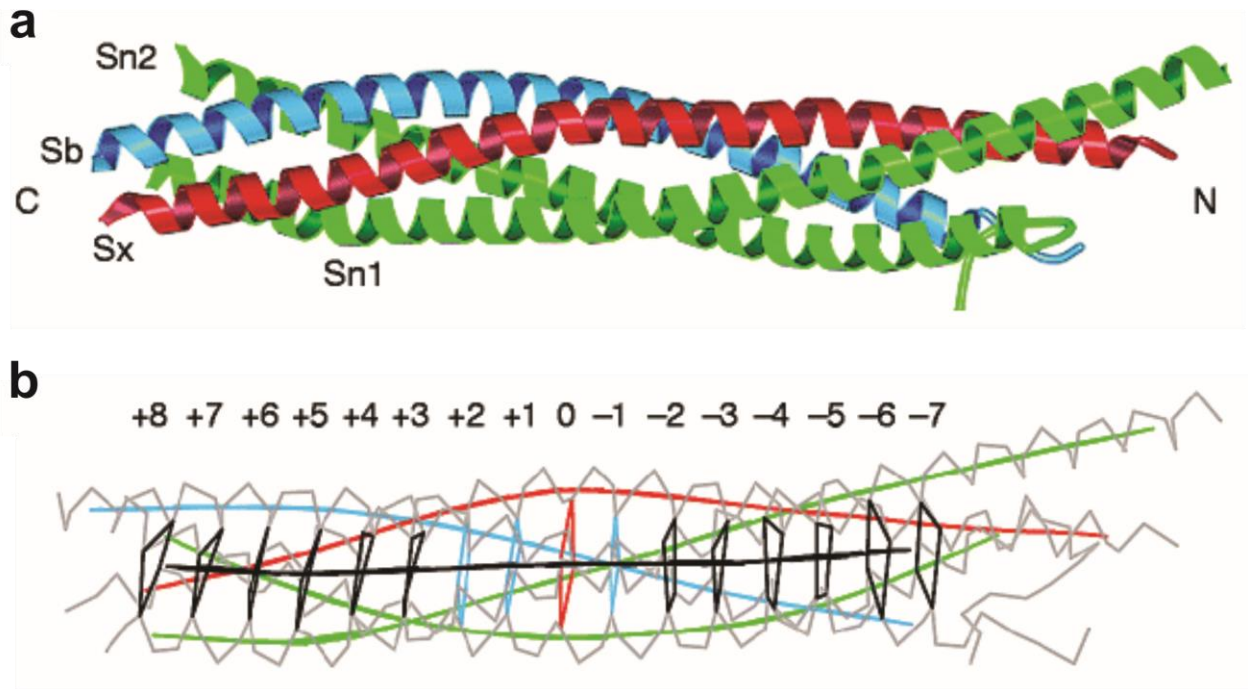


Figure 3. Topology of the SNARE complex fusion machinery.

a, Ribbon illustration of the SNARE complex: blue, synaptobrevin2 (Sb); red, syntaxin-1A (Sx); green, SNAP-25B (Sn1 and Sn2). **b**, Organization of SNARE proteins within the SNARE complex. C α traces (grey), local helical axes (blue, red and green for synaptobrevin2, syntaxin-1A and SNAP-25B, respectively), the superhelical axis (black), and layers (0, red; -1, +1 and +2, blue; all others black) of the complex are shown. Virtual bonds between corresponding C α positions represent the different layers (Sutton et al., 1998).

I.2.1 Function of SNARE proteins

The first indication that SNARE proteins mediate membrane fusion was their identification as targets for clostridial botulinum and tetanus toxins including Syb2 (Schiavo et al., 1992), SNAP-25 (Blasi et al., 1993a), and STX1 (Blasi et al., 1993b). These three proteins were found to form a complex together that is dissociated by the ATPase NSF protein (Sollner et al., 1993a). This discovery led to the suggestion that SNARE proteins bring opposing membranes closer together and induce their fusion. Although SNARE proteins constitute the minimal fusion machinery, many other proteins are required for the regulation of the exocytosis process at the different steps of docking, priming and fusion.

I.2.1.1 Docking

Docked or tethered vesicles are located close to the plasma membrane, however they are not fusion competent until they are primed, i.e. they are able to fuse directly in response to elevated

calcium signals. Although the proteins involved in docking are still poorly identified, it is thought that members of the *sec1/Munc18* family might be involved in docking (Becherer and Rettig, 2006). *Munc18-1* deletion abolishes secretion in neurons and neuroendocrine cells. This effect is probably mediated by different interactions in different cell types, as the number of large dense core vesicles (LDCVs) at the plasma membrane is reduced in chromaffin cells (Voets et al., 2001), however the number of synaptic vesicles at the active zone is not affected (Verhage et al., 2000). *Munc18-1* can bind directly to syntaxin and regulate its availability for interaction with other SNARE proteins or its stability and turnover (Dulubova et al., 1999).

1.2.1.2 Priming

Priming docked vesicles, i.e. rendering them fusion competent is better understood than docking. Priming is initiated by the formation of the ternary SNARE complex composed of one R-SNARE and two or three Q-SNAREs. The SNARE complex is characterized by its stability as it is known to be SDS-resistant and shows high thermostability (Fasshauer et al., 1997). The *Munc13*'s are critical for the priming process (Brose et al., 2000). There are four isoforms of the *Munc13* family, *Munc13-1*, -2, -3 and -4. In hippocampal neurons for example, where only *Munc13-1* and *Munc13-2* are expressed, vesicle fusion is entirely abolished in *Munc13-1/2* double KO mice (Varoqueaux et al., 2002). *Munc13-1* is thought to mediate the release of *Munc18-1* binding to syntaxin-1, aided by Rab3-interacting molecule (RIM), making it available to freely interact with the other SNARE proteins (Rizo and Sudhof, 2002; Sassa et al., 1999). Mutations in *Munc13-4* cause familial hemophagocytic lymphohistiocytosis 3 (FHL3) in human patients (Feldmann et al., 2003). CGs of CTLs isolated from FHL3 patients are able to dock at the IS but fail to fuse with the plasma membrane of the CTL, a requirement for killing of the target cell, consistent with a priming defect (Feldmann et al., 2003). *Munc13-4* is an effector protein of Rab27a in mast cells, where it localizes to and regulates the function of secretory lysosomes in these cells (Neeft et al., 2005). *Munc13-4* was also identified as a binding partner of Rab27a in platelets, which mediates the secretion of their dense core granules (Shirakawa et al., 2004).

Rab proteins are small GTPases that are involved in the regulation of vesicle fusion and thus SNARE proteins function. Each Rab protein has several effector proteins; it is mainly through their effectors that Rab proteins are able to regulate SNARE protein function. Rab3, a regulator

of synaptic vesicle fusion, acts with its effector proteins, e.g. RIM (Wang et al., 1997) and Rabphilin-3A (Shirataki et al., 1993) probably by regulating the availability of vesicles thereby determining their fusion efficiency. Though Rab3 is not expressed in CTLs, the related protein Rab27 is present and was shown to be involved in CG fusion in these cells (Menasche et al., 2000). Mutations in Rab27a lead to a disease known as Griscelli syndrome type II (GS2) (Menasche et al., 2000), which might develop to haemophagocytic syndrome (HS), a disease that is caused by increased activation of immune cells. CTLs from GS2 patients show reduced killing activity and reduced CG exocytosis, however they show no defect in polarization of the granules towards the IS (Stinchcombe et al., 2001a).

I.2.1.3 Fusion

The SNARE proteins involved in the formation of the SNARE complex are critically important for fusion. The zippering of the SNARE proteins proceeds from the N-terminus towards the C-terminus of each of the SNARE proteins forming a coiled-coil complex (Sorensen et al., 2006), which is thought to provide the driving force for vesicle fusion (Sollner et al., 1993b). Zippering of the SNARE proteins is triggered by an increase in intracellular calcium concentrations, bringing the vesicle membrane and plasma membrane closer together. The transmembrane domains of Syb2 and syntaxin are thought to transmit the energy initiated by the SNARE complex formation into the phospholipid membranes and induce their deformation thus facilitating membrane fusion (Jahn and Scheller, 2006). The membrane embedded region of syntaxin lines the fusion pore and its timing and dilation is thought to be regulated by Syb2 (Han et al., 2004). After fusion, the vesicle membrane is in continuity with the plasma membrane and the SNAREs then form transiently the cis-SNARE complexes before they are disassembled by the ATPase NSF (Sollner et al., 1993a).

I.3 Endocytosis

Eukaryotic cells have established endocytosis during their evolution to select for molecules entering the cell from the sea of molecules in the extracellular medium, rather than by entering through channels or pumps as in prokaryotes. Intercellular communication and communication between cells and the surrounding environment is initiated by ligands that bind to surface receptors to initiate a signaling cascade via activation of receptor-interacting proteins or via

endocytosis of the ligand-bound receptor to initiate intracellular signaling. Endocytosis of signaling receptors regulates cell activity by controlling the number of receptors available at the plasma membrane. The endocytosis of any cargo from the plasma membrane into the cell requires a selection mechanism that occurs at the plasma membrane. Many different endocytic pathways taken by different cargoes have been found, and they are widely classified as either clathrin-mediated endocytosis (CME), including constitutive and ligand-induced endocytosis, or clathrin-independent endocytosis (CIE). The latter can be dynamin-dependent or dynamin-independent in contrast to CME that is always dynamin-dependent. This classification is based on the requirement of the endocytosed vesicles for the function of the large GTPase dynamin to be pinched-off from the plasma membrane (Le Roy and Wrana, 2005; McMahon and Boucrot, 2011).

I.3.1 Clathrin-mediated endocytosis (CME)

I.3.1.1 Mechanism of clathrin-mediated endocytosis (CME)

Clathrin-mediated endocytosis (CME) is one of the best-characterized routes of receptor-mediated endocytosis. CME represents the process of cargo protein recycling from the plasma membrane via a clathrin-coated vesicle, with the aid of adaptor proteins, as clathrin, the main coat component, forms a scaffold around the vesicle (Figures 4, 6A) (Pearse, 1975). CME proceeds through five different stages whereby different sets of proteins are involved at each stage (Figure 4) (McMahon and Boucrot, 2011). Stage I, nucleation, is the formation of the nucleation module by a group of proteins called FCH domain only (FCHo) proteins, intersectins and epidermal growth factor receptor (EGFR) substrate 15 (EPS15) where these proteins define the site at the plasma membrane to which clathrin will be recruited. Depletion of any of these proteins prevents the formation of the clathrin-coated pit (CCP). The FCHo proteins contain an F-BAR domain with membrane-bending activity that then recruits the scaffold proteins intersectins and EPS15 (Henne et al., 2010; Stimpson et al., 2009). FCHo proteins also interact with Phosphatidylinositol 4,5-bisphosphate (PI(4,5)P₂) present at the plasma membrane, which in turn interacts with the adaptor protein AP2 at its α subunit N-terminus and μ 2 subunit (Collins et al., 2002; Rohde et al., 2002). AP2 is the main adaptor protein for CME (Keen, 1987; Pearse and Robinson, 1984) and its function is restricted to the plasma membrane (Gaidarov and Keen, 1999). AP2 initiates the second stage of CME known as cargo selection by binding to the cargo

INTRODUCTION

protein directly or indirectly through cargo-specific adaptor proteins. AP2 is one of several AP complexes that are composed of several subunits: two large subunits ‘ α and $\beta 2$ ’ each having a core and an appendage domain, a medium subunit ($\mu 2$) and a small subunit (σ) (Kirchhausen et al., 1989). AP2 binds to its protein cargoes via its $\mu 2$ and σ subunits by recognizing certain target sequences present on the cargoes; these are short peptide motifs present mainly on integral membrane proteins, the most common are the tyrosine-based motif ‘Yxx ϕ ’ (Ohno et al., 1995) and the dileucine (D/ExxxLL) motif (Rapoport et al., 1998). ANTH-domain containing brain-specific AP180 and ubiquitous CALM proteins, found to be responsible for endocytosis of Syb2 in the central nervous system (CNS), are examples of cargo specific adaptor proteins (Koo et al., 2011a). Other adaptor proteins like epsin and Dab2 are also involved in specific target recognition along with AP2 to which they bind via its appendage domains. Clathrin recruitment follows cargo selection i.e. AP2 binding to its cargo and to PI(4,5)P2 at the plasma membrane marking the start of the third stage of CME. AP2 interacts with soluble clathrin components via defined motifs in the $\beta 2$ and appendage domains (Owen et al., 2000), which may displace some of the other accessory binding adaptor proteins. Clathrin is composed of three heavy chains and three light chains that polymerize once they are recruited by AP2 to form a lattice around the nascent vesicle forming a clathrin-coated pit (CCP) (Fotin et al., 2004). The pit invagination is then deepened to form a vesicle that is still bound to the plasma membrane via its neck. In the fourth stage of CME, the large GTPase, dynamin, is recruited to the site of vesicle scission by BAR-domain containing proteins via interactions with its proline-rich domain (PRD) and pleckstrin homology (PH) domain (Ferguson et al., 2009). Dynamin then polymerizes around the nascent vesicle neck, acting as a mechanochemical enzyme, by inducing its pinching off from the plasma membrane after GTP hydrolysis (Marks et al., 2001; Sweitzer and Hinshaw, 1998). Many reports have shown that inhibiting dynamin function at this stage, by using inhibitors such as dynasore (Macia et al., 2006) or by using different dynamin mutants, produces invaginated clathrin-coated pits that cannot pinch off to form a vesicle. Dynamins function to cleave the clathrin-coated vesicle. This is then followed by the disassembly of the clathrin coat from the nascent vesicle, marking the last stage of CME (uncoating), allowing it to fuse with acceptor membranes, where the coat components can be recycled for the fission of new vesicles. Several proteins are involved in the uncoating process including the ATPase heat shock cognate 70 kDa (HSC70) (Schlossman et al., 1984) that is recruited by the neuronal cofactor auxilin (Ungewickell et al., 1995) and the abundant cyclin G-associated kinase (GAK) (Umeda et al.,

INTRODUCTION

2000) which bind to clathrin triskelia initiating clathrin coat disassembly in an ATP-dependent manner. The polyphosphoinositide phosphatase synaptojanin 1 might also be involved in clathrin coat disassembly (Cremona et al., 1999) as it can bind to accessory adaptor proteins on the clathrin-coated vesicle and probably weakens their binding to the vesicle membrane by changing its phosphoinositide composition. These cargo-carrying vesicles are now ready to enter the endocytic pathway. They sort the cargo, and according to the cell's need, it is either recycled back to the plasma membrane or trafficked to the lysosomes mainly for degradation.

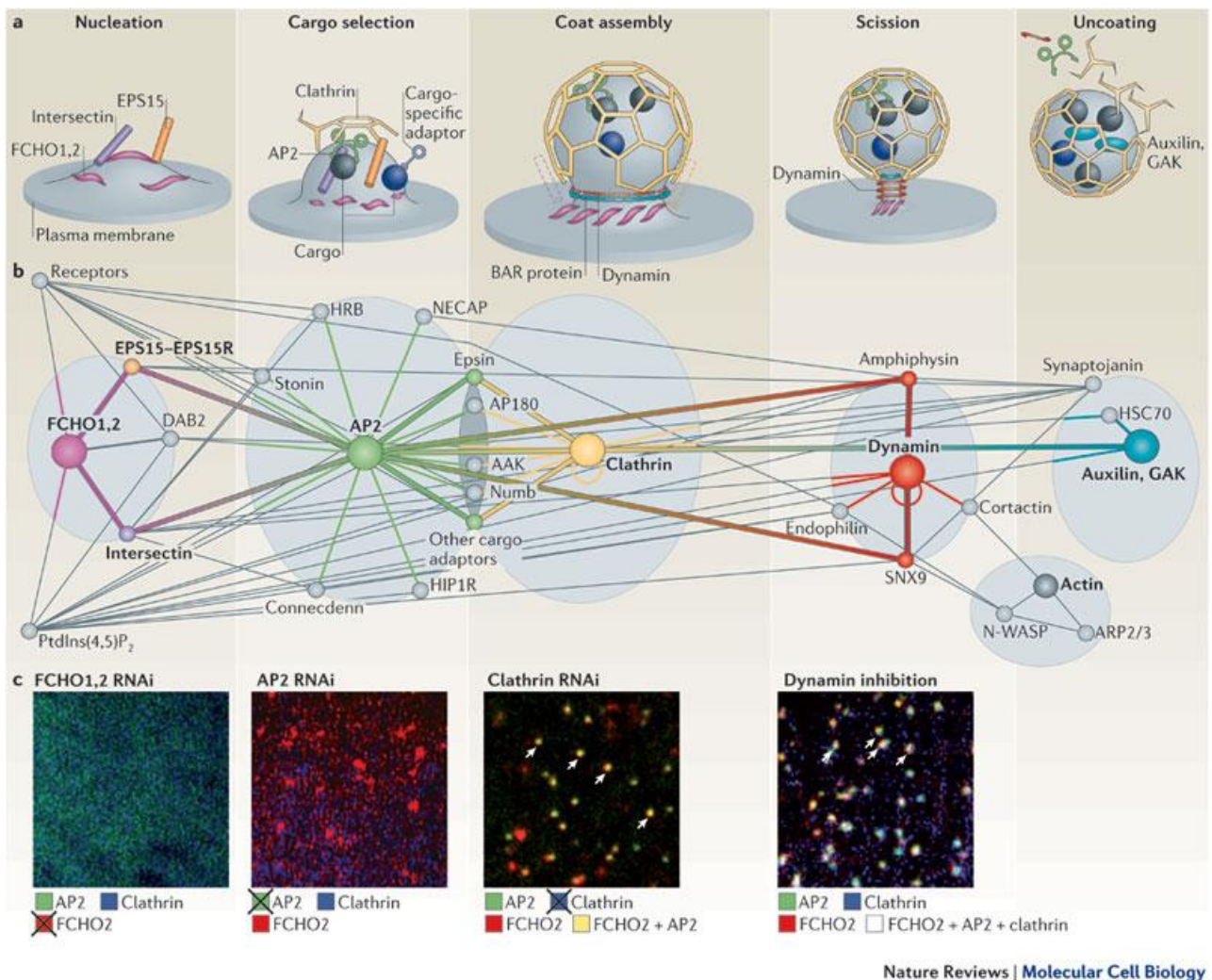


Figure 4. Clathrin-coated vesicle formation.

a, The five different steps required for clathrin-coated vesicle formation are shown in detail with the proteins involved at each step. Nucleation: The FCHO proteins binding to PtdIns(4,5)P₂ at the plasma membrane initiate nucleation of the plasma membrane as they recruit intersectins and EPS15 proteins and later AP2. Cargo selection: The AP2 binds directly to the cargo protein to be endocytosed through its different subunits or indirectly through cargo-specific adaptors. Coat assembly: cytosolic clathrin triskelia bind to AP2 bound to its cargo at the plasma

membrane and polymerize to form a clathrin coat around the nascent vesicle. Scission: Dynamin, a large GTPase protein, is recruited to the forming vesicle where it polymerizes around the vesicle neck to induce budding of the vesicle. Uncoating: The ATPase HSC70 is recruited to the newly formed clathrin-coated vesicle by auxilin or GAK proteins, where it then starts the ATP-dependent process of uncoating of the vesicle; released proteins can then be recycled and used in another round of clathrin-dependent endocytosis. b, A scheme showing the central players (shown in big circles) in each of the previously mentioned steps of clathrin-dependent endocytosis along with many of their interaction partners. c, Epithelial cells expressing different fusion proteins, FCHo2 tagged with red fluorescent protein (RFP), AP2 tagged on the $\sigma 2$ subunit with enhanced green fluorescent protein ($\sigma 2$ -eGFP) and clathrin tagged with blue fluorescent protein (BFP), are silenced for any of these proteins using siRNA against the protein shown on the top of the image. These experiments show the requirement of the transfected proteins for clathrin-coated vesicle formation in the sequence shown in (a). AAK, AP2-associated protein kinase 1; AP2, adaptor protein 2; ARP2/3, actin-related protein 2/3; DAB2, Disabled homologue 2; EPS15, EGFR substrate 15; FCHo, FCH domain only; GAK, G-associated kinase; HSC70, heat shock cognate 70; HIP1R, HIP1-related; N-WASP, neural Wiskott-Aldrich syndrome protein; NECAP, adaptin ear-binding coat-associated protein; PtdIns(4,5)P2, phosphatidylinositol(4,5)bisphosphate; SNX9, sorting nexin 9 (McMahon and Boucrot, 2011).

I.3.1.2 Constitutive versus ligand-induced CME

CME can be divided into constitutive and ligand-induced endocytosis. The constitutive pathway is mainly taken by non-signaling receptors as for the case of the ones involved in nutrient uptake such as transferrin-R (Watts, 1985) and LDL-R (Anderson et al., 1982). These receptors are continuously endocytosed and are then sorted in the endosomal pathway to be either transported back to the cell surface or to lysosomes for degradation.

In ligand-induced endocytosis, ligand binding induces the activation of the bound receptors, which induces their internalization, typically to lysosomes for degradation, and terminates their response. This is typical of signaling receptors like epidermal growth factor receptor (EGF-R) (Beguinet et al., 1984) and other receptor tyrosine kinases (RTKs). This process of endocytosis serves to remodel the plasma membrane protein composition and to relocalize specific receptors to certain membrane areas important for signaling.

I.3.2 Clathrin-independent endocytosis (CIE)

Endocytosis can be further classified according to the type of the vesicle a protein is incorporated into upon endocytosis (Le Roy and Wrana, 2005). Although the best-characterized mode of entry is clathrin-mediated endocytosis (CME), clathrin-independent endocytic (CIE) pathways exist as well. CIE is regulated differently from CME that allows for a wider regulatory spectrum of the cell's functional activities. There are several forms of CIE, requiring different proteins such as caveolin, flotillin, and ADP-ribosylation factor (ARF). Many different aspects of CIE still needs to be investigated. The mechanism of cargo selection in CIE can be protein-dependent, lipid-

dependent or both protein and lipid dependent. CIE can be further classified as dynamin-dependent and dynamin-independent, as it has been shown that dynamin is not restricted to CME pathways.

I.3.2.1 Dynamin-dependent CIE

Caveolae-mediated endocytosis is one of the best-characterized dynamin-dependent CIE pathways. A member of the caveolin (Cav) protein family marks a small region of the plasma membrane (50-80 nm), enriched in sphingolipids and cholesterol (Simons and Ikonen, 1997) (Nabi and Le, 2003), to be endocytosed into the cytosol as caveolae with a flask-shaped structure (Parton and Simons, 2007). Another dynamin-dependent CI pathway is known as RhoA-dependent pathway, initially discovered for the β -chain of the IL-2R, this pathway can also be used by other different proteins (Lamaze et al., 2001). Although endophilin is known to be involved in CME, it has been shown to be involved in dynamin-dependent CIE named fast endophilin-mediated endocytosis (FEME) (Boucrot et al., 2015). FEME produces tubulovesicular invaginations of the plasma membrane and is activated by ligand binding (activated within seconds of ligand binding), where it mediates the endocytosis of several G-protein-coupled receptors (GPCRs) and protein tyrosine kinases (Boucrot et al., 2015).

I.3.2.2 Dynamin-independent CIE

Dynamin-independent CIE has also been described. A fluid-phase uptake that is increased upon expressing dynamin-I mutant (Damke et al., 1995) or the temperature sensitive-form of dynamin (*shibire*) (Guha et al., 2003) involve ARF6 and CDC42 small GTPases. The latter is required for the uptake of cholera toxin B (CtxB) (Llorente et al., 1998) and ARF6 is required for the uptake of MHC class I (Radhakrishna and Donaldson, 1997) among other proteins (Kumari and Mayor, 2008). Another CI mechanism, mediated by lipid-raft associated proteins flotillin 1 and flotillin 2, is mediated by dynamin-dependent pathways for some proteoglycans (Ait-Slimane et al., 2009) and dynamin-independent pathways for certain glycosylphosphatidylinositol (GPI) anchored proteins (Glebov et al., 2006).

I.4 The endosomal pathway: from the plasma membrane to the endosomal system

I.4.1 Rab proteins binding to membranes

Rab proteins, involved in vesicle transport regulation (to and from the plasma membrane and between organelles) and determining organelle identity, constitute the largest family of the small GTPases, with about 63 different members in humans compared to only 11 members in *Saccharomyces cerevisiae*. The higher number of Rab proteins in humans reflect their requirement for the regulation of the more sophisticated transport systems in higher organisms (Zerial and McBride, 2001). GTP-bound ‘active’ Rab proteins bind membranes by means of a geranylgeranyl group added to the two consensus cysteines at their C-termini; upon GTP hydrolysis to GDP the GDP-bound ‘inactive’ Rab proteins are released from membranes. Rab Escort Protein (REB) presents the soluble Rab to an enzyme called Rab geranylgeranyl transferase (RabGGT) that transfers the geranylgeranyl group to the Rab protein allowing it to bind membrane. Guanine nucleotide exchange factors (GEFs) catalyze the exchange of GDP to GTP by interacting with specific amino acids of the Rab protein (Delprato et al., 2004). GTP is then hydrolyzed not only by the intrinsic GTPase activity of the Rab protein, but also by certain proteins called GTPase-activating proteins (Figure 5) (GAPs) (Haas et al., 2007).

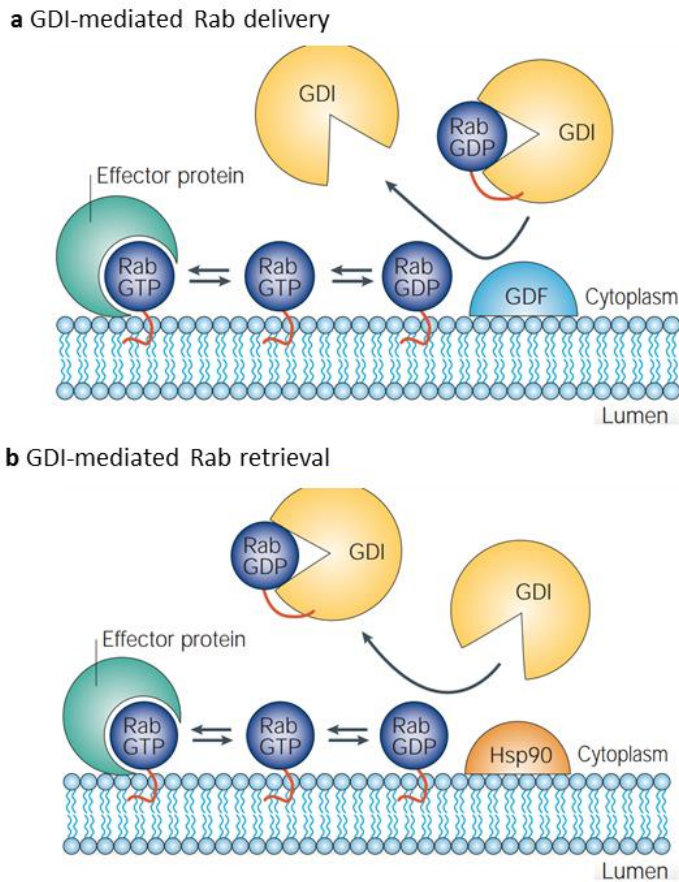


Figure 5. Rab proteins binding to and release from membranes.

(a) GDP-bound prenylated Rab proteins bind to GDI in the cytosol and are directed towards their target membrane. There, resident GDF catalyzes the attachment of Rab GTPase to the membrane. GEF proteins convert GDP-bound Rab to GTP-bound once they are bound to the membrane, where they can then interact with their effector protein. (b) After catalysis of the GTP to GDP, the GDP-bound Rab GTPase can be retrieved again by GDI protein. Hsp90 is thought to be involved in this interaction in neuronal cells. GDI, GDP-dissociation inhibitor; GDF, GDI-displacement factor; GEF, guanine-nucleotide exchange factor (Pfeffer and Aivazian, 2004).

I.4.2 Acidification of endosomes

Endosomes are characterized by a mildly acidic pH that gradually decreases as a cargo is traversed through the endocytic pathway. This acidic pH is maintained by an ATP-driven proton pump, the V-type H⁺ ATPase (where V stands for vacuolar) [reviewed in (Beyenbach and Wieczorek, 2006)]. The V-ATPase constitutes a large complex composed of 2 domains, the cytosolic V1 domain that undergoes ATP hydrolysis and the V0 domain an integral membrane protein that functions in proton translocation. Each of the two domains consists of different subunits, with 8 subunits making up V1 and 5 subunits for V0. Regulation of the V-ATPase function is mainly attributed to the reversible association and dissociation of the two domains (Forgac, 1998; Lafourcade et al., 2008; Trombetta et al., 2003). The endosomal pH helps, for example, to dissociate ligands from signaling receptors and thus prevents excessive signaling from these ligand-bound receptors. Ligands and receptors can then be sorted into different compartments in the sorting endosome to be further processed.

I.4.3 From the plasma membrane to the early endosomes and back

Routing through the endocytic pathway has been studied in great detail for many proteins. Generally the first stop for an endocytic vesicle using any pathway for entry into the cell is at the early endosomes (EEs) also known as sorting endosomes (Figure 6B) (Yamashiro and Maxfield, 1987). Serving as a focal point for endocytosed vesicles (Mayor et al., 1993), EEs are characterized by a slightly acidic pH (pH 6.5) (Maxfield and McGraw, 2004; Yamashiro et al., 1984) that allows for the dissociation of ligands bound to receptors as in the case of signaling-receptors' endocytosis. Rab5 a small GTPase and its main effector early endosomal antigen 1 (EEA1) mark the early endosomes; they are required for the transport and fusion of vesicles with EEs and for sorting proteins to their different fates (Bucci et al., 1992; Christoforidis et al., 1999). Rab5 availability is maintained on EEs by the GTP/GDP cycle of the GTPase and also by the continual homotypic fusion events between different Rab5-positive endosomes (Rink et al., 2005). Early endosomes show a pleomorphic structure with different tubular and vesicular structures, protein composition and probably different acidity that might also imply differential functions of sorting proteins either to recycling pathway or to degradative pathway (Gruenberg, 2001; Mellman, 1996; Raiborg et al., 2002). Ligands of signaling receptors are usually sorted to the degradative pathway whereas their receptors can be used for several rounds of recycling before being degraded (Basu et al., 1981; Fehlmann et al., 1982). For example, epidermal growth factor (EGF) dissociates from its receptor (EGFR) once they reach the EEs, where both can be trafficked further to be degraded in the late endosomes, or EGF can be degraded while the EGFR is recycled back to the plasma membrane through recycling endosomes for another round of signaling [reviewed in (Tomas et al., 2014)]. The transferrin receptor, the classical endocytic receptor for recycling to the plasma membrane, is endocytosed upon binding of its ligand as diferric transferrin (transferrin with two bound atoms of ferric iron (Fe^{3+})). After uncoating of the clathrin-coated vesicles carrying the transferrin-transferrin receptor complex, they can fuse with two different populations of EEs. In the acidic environment of the EEs, ferric ions are dissociated from transferrin though it remains bound to its receptor. From the EEs the complex is then either recycled in a Rab4-dependent fast route directly to the plasma membrane (2.5 minute) or through a Rab4/Rab11-dependent slower route via the recycling endosomes (7.5 minute) (Hopkins and Trowbridge, 1983; Sonnichsen et al., 2000; Stein and Sussman, 1986). Rab11 interacts with Myosin Vb via Rab11 family interacting protein 2 which regulates protein recycling from the plasma membrane (Hales et al., 2002).

I.4.4 From the early endosomes to late endosomes

After sorting into EEs from the plasma membrane, proteins may be further trafficked into Rab7-containing late endosomes (LEs) for further processing, depending on the cargo protein (Figure 6B) (Schmid et al., 1988). LEs are derived from the vesicular domains of EEs, where most of the proteins destined for degradation have accumulated; in this region Rab5 is gradually lost probably by converting to the GDP-bound form and is then replaced by Rab7 which accumulates in this region to generate LEs (Rink et al., 2005). As mentioned before, the pH drops further in LEs to values below 6. This might be because the V1 domain of the V-ATPase associates more readily with the V0 domain localized to LE membrane thereby forming more functional pumps at this site (Lafourcade et al., 2008). It is also thought that the V-ATPases are localized to the vesicular regions of EEs, so when these regions transform to LEs, the V-ATPases are then more concentrated which might contribute to the lower acidity of LEs (Huotari and Helenius, 2011). This decrease in the pH in LEs is required for the inactivation of internalized pathogens, for proper sorting of certain cargo proteins and for regulating the activity of hydrolytic enzymes. Rab7 regulates transport between late endosomes and lysosomes by interacting with Rab-interacting lysosomal protein (RILP) which results in recruitment of the dynein-dynactin motor complex (Jordens et al., 2001). Further maturation of LEs result in fusion of these organelles with lysosomes. This is considered to be a dead-end pathway for most proteins where they are degraded by the function of lysosomal enzymes. The fusion between LE and lysosomes generates ‘endolysosome’ where most of protein degradation takes place; these organelles differ from conventional lysosomes, which contain a characteristic dense core (Huotari and Helenius, 2011).

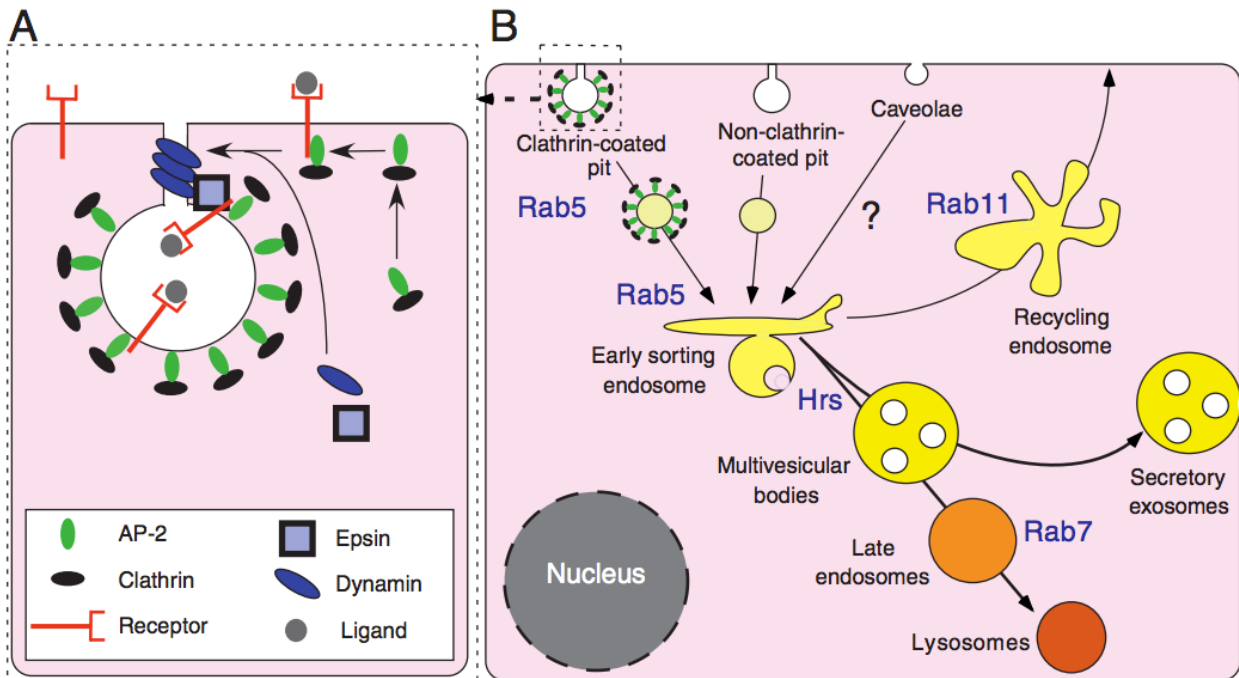


Figure 6. Sorting of endocytosed vesicle components through the endocytic pathway.

A, A clathrin-coated vesicle carrying cargo-bound receptors with the adaptor proteins mainly AP2. Dynamin surrounds the vesicle neck, as it is ready to be pinched off. B, A general scheme of the pathway followed by a vesicle following endocytosis, whether by clathrin-dependent, clathrin-independent or caveolae-dependent mechanism. Most endocytosed vesicles fuse first with the early endosomes (sorting endosomes, Rab5-positive endosomes), from where they are either recycled back to the plasma membrane by recycling endosomes (Rab11-positive endosomes) or trafficked further to late endosomes (Rab7-positive endosomes) through multivesicular bodies and then to lysosomes (Le Borgne et al., 2005).

I.5 Immune diseases associated with the SNARE machinery dysfunction

The main function of CTLs is to kill virally-infected and tumor cells by releasing cytotoxic proteins to be endocytosed by target cells inducing their death. Malfunction in the exocytosis of cytotoxic granules (CGs) leads to the inability to kill target cells. Several human diseases caused by mutations in proteins associated with the SNARE fusion machinery have been described. Familial hemophagocytic lymphohistiocytosis (FHL) is an immune disorder caused by mutation of genes involved in the lysosomal secretory pathway. FHL is classified into different types depending on the corresponding mutated gene, PRF1 gene in FHL2 (Stepp et al., 1999), Munc13-4 gene in FHL3 (Feldmann et al., 2003), STX11 in FHL4 (zur Stadt et al., 2005) and Munc18-2 in FHL5 (Cote et al., 2009). FHL patients present with symptoms related to hyperactivation of immune cells (such as macrophages and T cells) which is probably due to the

cells' inability to clear infections (Sieni et al., 2014). Symptoms also include hepatosplenomegaly, fever, bone marrow hemophagocytosis and neurological abnormalities. FHL usually shows early onset in life and if left untreated, it is usually fatal (Sieni et al., 2014). Griscelli syndrome 2 (GS2) caused by mutations in the small GTPase Rab27a (Menasche et al., 2000) is also associated with defects in cytotoxic granule secretion. GS2 patients show hypopigmentation and immune abnormalities (hemophagocytosis) due to defects in melanosome exocytosis from melanocytes and CG granules from CTLs, respectively (Menasche et al., 2000). Rab27a is expressed in lymphocytes and melanocytes explaining the defects present with GS2 (Chen et al., 1997). Mice lacking Rab27a, known as *ashen mice*, also present with reduced killing activity of their CTLs, but do not develop hemophagocytosis. Chediak-Higashi syndrome (CHS) is an autosomal recessive disease caused by mutations in lysosomal trafficking regulator protein (LYST) (Barbosa et al., 1996), which manifests with albinism and a lymphocyte killing-dysfunction. The normally produced lysosomes fuse to form giant organelles but are not able to fuse with the plasma membrane (Baetz et al., 1995).

In addition to these diseases caused by the inability of granule exocytosis, several other immune disorders are associated with deficiency of endocytosis of components required for the fusion machinery (Mosesson et al., 2008), resulting in their exhaustion and a loss of exocytotic function. Understanding the mechanism of endocytosis of the different proteins involved in the fusion machinery would thus give us insight into their mechanism of action and disturbances leading to disease.

I.6 Synaptobrevin2 (Syb2)

Synaptobrevin2 (Syb2) is a component of the SNARE complex involved in CG fusion. Syb2, also known as VAMP2, for vesicle associated membrane protein 2, was discovered in the late 1980's (Baumert et al., 1989) as a protein component of synaptic vesicles (SVs). Shortly afterwards, Syb2, was shown to be the target for tetanus toxin and some botulinum toxin subtypes (Link et al., 1992) (Schiavo et al., 1992). Since these toxins are specific blockers of synaptic transmission, Syb2 was considered to be a critical player in SV fusion.

Syb2 binds to the vesicle membrane via a C-terminal hydrophobic domain. An adjacent linker joins the transmembrane domain (TMD) with the SNARE motif and a short proline-rich N-

terminal sequence (Archer et al., 1990; Fasshauer et al., 1998). Syb2 is the most abundant protein of synaptic vesicles (Takamori et al., 2006). When a vesicle undergoes exocytosis, its membrane becomes a part of the plasma membrane. In order to prevent excessive increase in the plasma membrane surface area and to compensate for loss of synaptic vesicles and their components, vesicles are recycled via endocytosis. The mechanism of endocytosis at synapses has been investigated in neurons where it is mainly clathrin-dependent (Granseth et al., 2006). Despite extensive studies on endocytosis of synaptic vesicle (SV) membrane, the mechanism of SV membrane retrieval remains controversial. Depending of the strength of the stimuli, different modes of endocytosis may be used (Kononenko and Haucke, 2015). The main models for endocytosis at synapses include the retrieval of SV membrane by CME directly after fusion, or the formation of clathrin-coated SVs from an endosome-like vacuole (ELV), that is formed in a clathrin-independent ultra-fast endocytosis (Watanabe et al., 2014).

AP180, a brain specific adaptor protein and its homologue the more ubiquitous adaptor protein clathrin assembly lymphoid myeloid leukemia (CALM), were identified as adaptor proteins specific for the endocytosis of Syb2 (Koo et al., 2011a). Syb2 was shown to interact directly with the ANTH domain of AP180 and CALM adaptor proteins at the N-terminal half of its SNARE motif, which is probably important for the retrieval of free Syb2 that has dissociated from its SNARE partners (Koo et al., 2011a; Koo et al., 2011b).

Syb2 has been shown to be expressed in several types of immune cells and to regulate the fusion of different types of vesicles in these cells. For example, in neutrophils, Syb2 migrates to the plasma membrane upon activation of these cells (Brumell et al., 1995). Syb2 is also expressed in macrophages (Pitzurra et al., 1996) and eosinophils (Shukla et al., 2000), where cleaving Syb2 inhibits degranulation. Matti et al found that Syb2 is the v-SNARE required for fusion of CGs of mouse CTLs (Matti et al., 2013). Given the Syb2 expression in immune cells and its involvement in exocytosis of different types of vesicles, we need to learn more about its endocytosis in these cells. Studying the endocytosis of Syb2 in CTLs would not only allow for the description of the endocytic pathway of Syb2, but it would also give us insight into the mechanism of CG endocytosis in CTLs.

I.7 Aim of this work

Little is known about the endocytosis of CG components in CTLs. Trafficking of molecules to and from the plasma membrane is critical for the proper functioning of cells, indicating the importance of understanding the mechanism of endocytosis involving critical components such as the CGs of CTLs.

In neurons, different endocytic pathways have been described with ultrafast and slow endocytosis (ranging from milliseconds to seconds) involving different proteins with different mechanisms of endocytosis; either the synaptic vesicle is endocytosed directly without diffusing with the plasma membrane, or the synaptic vesicle components are endocytosed individually or in case of excessive stimulus, bulk endocytosis takes place. The latter allows for a large area of the plasma membrane to be endocytosed forming an endosome-like vacuole (ELV), where clathrin-coated vesicles would bud from it inside the cytosol.

The work presented here investigates the mechanism of CG endocytosis via the trafficking of CG membrane components in mouse CTLs following exocytosis. Syb2 endocytosis has been shown to be critical for the serial killing function of CTLs (Chang et al., 2016). Syb2, the v-SNARE required for fusion of CGs (Matti et al., 2013), is therefore used as a marker to follow the endocytic pathway of CG membrane components. CTLs from *sybki* (Syb2-mRFP knock-in) mice were utilized in our study to follow the fluorescently-labelled Syb2 using a specific anti-RFP antibody. Studying the endocytosis of CG membrane components will give us insight into the efficacy of CTL function such as the ability to kill multiple target cells.

II. Materials and Methods

II.1 Materials:

II.1.1 Chemicals

Product	Company
Agar	Roth
BSA	Sigma-Aldrich
β -Mercaptoethanol	Roth
Chloroform	Sigma-Aldrich
cOmplete Mini, EDTA-free Protease Inhibitor Cocktail Tablets	Roche
Dithiothreitol	Sigma-Aldrich
dNTP-Mix	Fermentas
DPBS	Life Technologies
Ethanol 100%	Roth
EtBr	Life Technologies
EDTA	Sigma-Aldrich
EGTA	Sigma-Aldrich
FCS	Life Technologies
Formaldehyde	PolyScience
Glucose	Merck
Glutamax	Life Technologies
Glycerol	Roth
Glycine	Roth
HEPES	Sigma-Aldrich
HPLC water	Life Technologies
IMDM	Thermo Scientific
Isopropanol	Roth
Kanamycin K-1377	Sigma-Aldrich

MATERIALS AND METHODS

Product	Company
KCl	Merck
λ Marker	Roche
Methanol 100%	Roth
MgATP	Sigma-Aldrich
NaCl	Merck
NaCHO ₃	Merck
Nonfat dried milk powder	AppliChem Panreac
NuPAGE 10% Bis-Tris Gel 1.0mm	Fisher Scientific
NuPAGE LDS sample buffer 4x	Invitrogen
NuPAGE MES SDS Running Buffer 20x	Fisher Scientific
NuPAGE Transfer Buffer 20x	Fisher Scientific
PCR-buffer	Sigma-Aldrich
Pen/strep	Gibco
Peptone	Roth
<i>pfu</i> -Polymerase Buffer	Fermentas
Phenol	Sigma-Aldrich
Polyornithine	Sigma-Aldrich
Ponceau S solution 0,1%	Sigma-Aldrich
Protein G Agarose	Thermo Scientific
Protran BA 83 Nitrocellulose Membrane	Fisher Scientific
Restore Western Blot Stripping Reagent	Fisher Scientific
RPMI	Sigma-Aldrich
Roti Nanoquant 5x	Roth
Spectra Multicolor Broad Range LAD	Fisher Scientific
Streptomycin	Life Technologies
Sucrose	Merck
Super Signal West Dura Extended	Fisher Scientific
Triton X-100	Roth
Tris-hydrochloride	Roth
TRIzol	Life Technologies
Tween 20	Roth
Water	Sigma-Aldrich

II.1.2 Solutions for cell culture

II.1.2.1 RPMI 1640 (10% FCS)

RPMI, 500 ml

FCS, 50 ml, (10%)

Pen/Strep, 5.5 ml, (1%)

Hepes from 1 M stock, 5.5 ml, (10 mM)

II.1.2.2 IMDM (10% FCS)

IMDM, 500 ml

FCS, 50 ml, (10%)

Pen/Strep, 2.75 ml, (0.5%)

β -mercaptoethanol, 1.936 μ l, (50 μ M)

II.1.2.3 Isolation Buffer

PBS, 500 ml

BSA, 0.5 g, (0.1%)

EDTA from 0.5 M stock solution, 2 ml, (2 mM)

II.1.2.4 Erythrolysis buffer (100 ml)

H₂O, 100 ml

NH₄Cl, 0.829 g, (155 mM)

KHCO₃, 0.1 g, (10 mM)

EDTA from 50 mM stock, 260 μ l, pH 7.4 (0.1 mM)

II.1.3 Solutions for cell fixation and staining

II.1.3.1 Paraformaldehyde (15% PFA, 10 ml)

PFA, 1.5 g

Sigma H₂O, 10 ml

NaOH, 20 µl

pH 7.4

II.1.3.2 Quenching Solution (0.1 M Glycine)

Glycine, 0.375 g

PBS, 50 ml

II.1.3.3 Permeabilization Solution (50 ml, 0.1% Triton)

Triton x-100, 50 µl

PBS 1x, 50 ml

II.1.3.4 Blocking Solution (50 ml, 2% BSA)

BSA, 1 g

Triton x-100, 50 µl

PBS, 50 ml

II.1.3.5 Mounting Medium

Mowiol 4-88, 2.4 g

Glycerol, 6 g

H₂O double distilled, 6 ml

Tris-Buffer, 12 ml

pH 8.5

II.1.4 Solutions for cloning

II.1.4.1 LB-Medium

Peptone, 8g

Yeast extract, 4g

NaCl, 4 g

H₂O, 800 ml

II.1.4.2 Loading Buffer

Sucrose, 4g

Bromophenol blue

Sigma H₂O, 10 ml

II.1.5 Solutions for Western blot

II.1.5.1 Lysis buffer (5 ml)

Tris-Cl, 50 mM

NaCl, 150 mM

PMSF, 250 μ M

Triton x-100, 1%

Deoxycholic acid, 1 mM

EDTA, 1 mM

DTT, 1 mM

H₂O, up to 5 ml

1 tablet protease inhibitor cocktail

II.1.5.2 TBS (10x)

NaCl, 87.7 g

1 M Tris-Cl (pH 7.5), 100 ml

H₂O, up to 1 L

II.1.5.3 TBST (0.05%) (1L)

10x TBS, 100 ml

Tween 20, 500 μ l

H₂O, 900 ml

II.1.6 Bacteria and Cell Lines

II.1.6.1 Bacteria

DH5 α : F⁻ endA1 glnV44 thi-1 recA1 relA1 gyrA96 deoR nupG purB20 ϕ 80dlacZ Δ M15 Δ (lacZYA-argF) U169, hsdR17(rK-mK+), λ ⁻. Invitrogen, Life Technologies

II.1.6.2 Cell Lines

P815 cell line from DSMZ. DSMZ no. ACC 1

II.1.7 Mouse Strains

C57Bl/6N (Black 6), Stock No: 005304, The Jackson Laboratory

Synaptobrevin2-mRFP knock-in mouse (sybki) (Matti et al., 2013)

II.1.8 Kits

II.1.8.1 Kits for cloning

EndoFree Plasmid Maxi Kit, Qiagen

EndoFree Plasmid Mini Kit, Qiagen

QIAprep Spin Miniprep Kit, Qiagen

QIAquick Gel Extraction Kit, Qiagen

QIAquick PCR Purification Kit, Qiagen

II.1.8.2 Kits for cell culture

Dynabeads FlowComp mouse CD8 kit, Thermo Fisher

Dynabeads mouse T-activator CD3/CD28 for T-cell expansion and activation, Thermo Fisher

II.1.9 Antibodies

Antibody for STX11 has been produced in our lab earlier (Halimani et al., 2014). Antibody against $\alpha 3$ subunit of the H^+ V-ATPase was a kind gift from Prof. Thomas Jentsch (FMP, berlin). Antibodies used from commercial sources include anti-CALM antibody (sc-6433; Santa Cruz), hamster anti-mouse CD3e antibody (clone 145-2C11; BD Pharmingen), anti-granzyme B antibody (4275S, Cell Signaling), mouse anti-Syb2 antibody (104211, clone 69.1; synaptic systems), rabbit anti-RFP antibody (Genway Biotech), rabbit anti-SNAP-23 antibody (111203; synaptic systems), anti-ZAP70 antibody (clone 1E7.2; Merck Millipore) and all AlexaFluor secondary IgG antibodies (Invitrogen). The anti-RFP antibody was labeled with the different Alexa fluorophores (Alexa405, 488 and 647) and pHrodo green STP ester (ThermoFischer Scientific) using a commercially available mAb labeling kit from Invitrogen.

II.1.10 Plasmids

II.1.10.1 Plasmids for Rab proteins

Plasmids for eGFP-Rab5/7/11 have been previously described (Halimani et al., 2014). Briefly, each Rab protein was amplified with a primer that had BamHI and EcoRI restriction sites at both ends, where the PCR product was then ligated to a vector already containing eGFP-C1 to the N-terminus of the Rab protein.

II.1.10.2 pMAX with a new multiple cloning site (MCS):

'pMAX-minus eGFP' was used as a template to generate a new pMAX vector with an improved multiple cloning site (MCS). The vector was cut with KpnI and NheI to introduce the new MCS sequence consisting of the following restriction sites KpnI-ClaI-EcoRI-HindIII-XbaI-BglII-BamHI-NotI-NheI, with overhangs for KpnI and NheI (ClaI is also known as Bsu15I, shown in the map). The sequence of the two oligonucleotides was as follows, Positive strand:

5' CATCGATGAATTCAAGCTTCTAGAGATCTGGATCCGCCGCGCCGCG 3'

Negative strand:

5' CATGGTAGCTACTTAAGTTCGAAGATCTCTAGACCTAGGCGGCGCCGCGCGATC 3'

MATERIALS AND METHODS

The two oligonucleotides were ordered with a 5'-phosphate modification on each strand. Before ligation into the pMAX the two oligonucleotides were hybridized; 2 µg from each oligo were mixed together in an eppendorf, then water was added to make a final volume of 50 µl. The eppendorf was put in a beaker containing boiling water for 2-3 minutes. Then, the whole beaker was put in an empty icebox, covered with a lid to allow the temperature to decrease slowly. The oligonucleotides were kept for 3.5 hrs in the icebox. The measured DNA concentration was 150 ng/µl; 10 ng were used for the ligation reaction with 190 ng from the pMAX vector cut with KpnI and NheI. Ligation was done overnight at room temperature. Then the ligation product was transformed into DH5a bacteria. Positive clones were checked by digestion with HindIII, as HindIII is not present in the original vector. Thus, if the MCS is inserted into the vector then HindIII should linearize the vector; otherwise the vector shouldn't be cut. All clones checked contained the HindIII restriction site and thus the new MCS. Clones 5 and 6 shown in figure 7A were taken for sequencing and further for Maxiprep after checking the sequence.

The pMAX vector was fully sequenced using the following three primers,

1. 5' GGCTATTGGCCATTGCATACG 3'
2. 5' GGACAAACCACAACACTAGAATGC 3'
3. 5' GAAGAACTCGTCAAGAAGGCG 3'

The sequencing showed that the insert was correctly inserted into the vector. The exceptionally small size of the pMAX (2848 bp) vector along with the new inserted MCS (Figure 7B), allowed for pMAX to be used as a vector for most of the future cloning in the lab.

MATERIALS AND METHODS

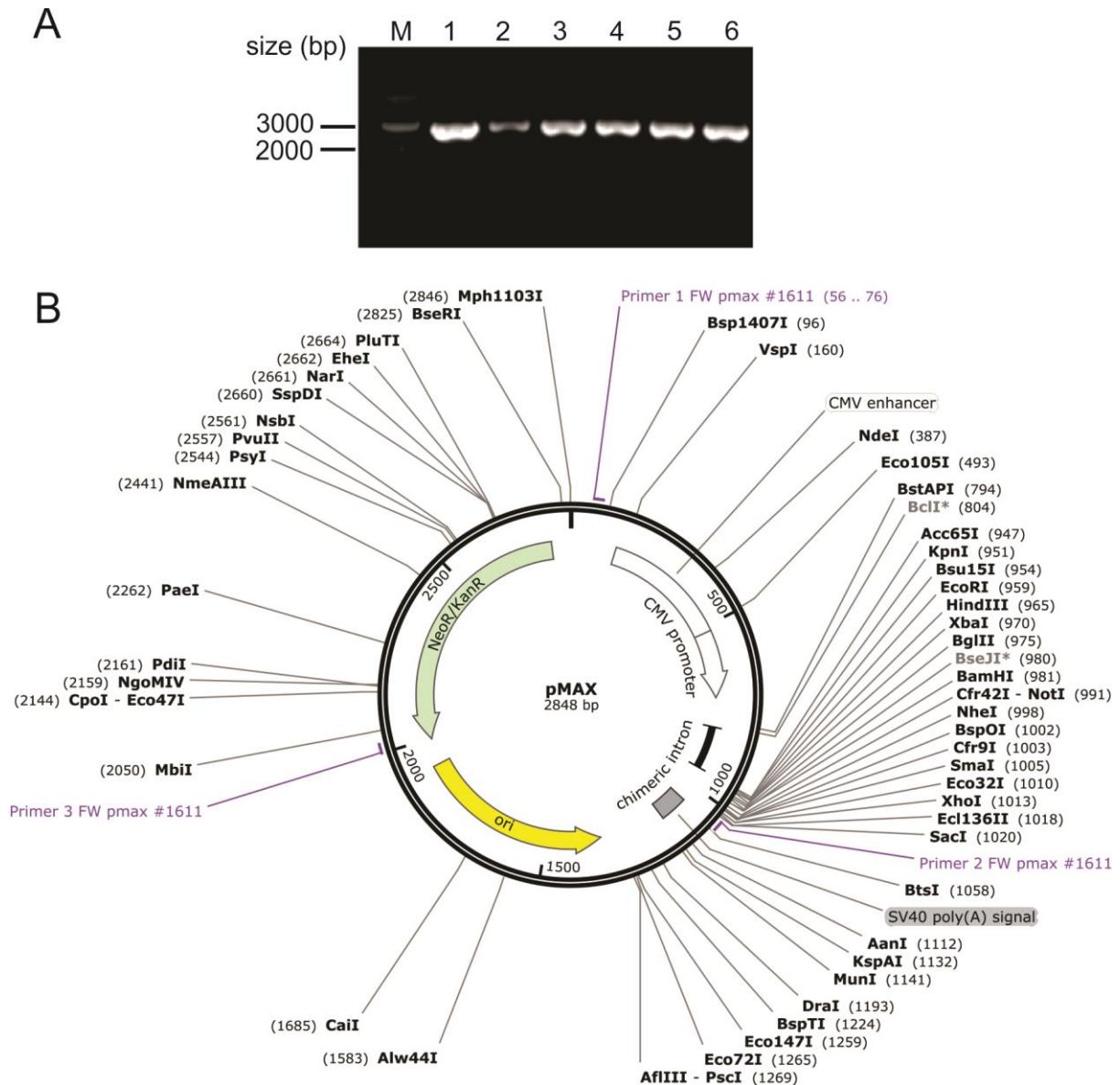


Figure 7. pMAX vector with the new MCS.

A, clones of pMAX with the new MCS, digested with HindIII and run on an agarose gel. The gel shows a single band for all the clones indicating a linearized vector. Numbers on top of the gel indicate the clone number; M, marker. B, vector map of the pMAX showing the new restriction sites added (only single cutter endonucleases are shown). Map was done with SnapGene Viewer.

II.2 Methods

II.2.1 Positive isolation of CD8⁺ T lymphocytes

The spleen was isolated from 8-12 week old mice, smashed on a 70 µm filter; splenocytes were collected in a falcon tube and centrifuged. The erythrocytes were next lysed with an erythrolysis buffer. Splenocytes were again washed with RPMI medium. CD8⁺ T lymphocytes were then positively isolated from the splenocytes using ‘Dynabeads FlowComp Mouse CD8’ kit according to the manufacturer's instructions. Briefly, 50*10⁶ splenocytes were resuspended in 500 µl isolation buffer (see Materials and Methods), with 25 µl anti-CD8 antibody provided in the kit. Cells were kept on ice for 10 min, and then washed to remove unbound antibody by centrifuging cells at 350 *g for 8 min. The pellet was resuspended in 1 ml isolation buffer and 75 µl of FlowComp Dynabeads were added (provided in the kit). The suspension was incubated for 15 minutes while rotating at 4 °C. The cells were then exposed to the magnet for about 2 minutes, to separate bead-bound cells from free cells. The latter were removed and the bead-bound cells were washed with isolation buffer and put in the magnet for another 2 minutes. The washed bead-bound cells were resuspended in 1 ml release buffer provided in the kit for 10 min rotation at RT. Afterwards the cells were exposed to the magnet for 2 minutes, cells were then collected by centrifugation at 350 *g for 8 min. CD8⁺ T lymphocytes were resuspended in IMDM medium at a concentration of 10⁶ cells per ml, then plated in a 24-well plate with mouse T cell-Activator CD3/CD28 Dynabeads at a ratio of 1:0.8 per well.

II.2.2 RNA extraction

Cytotoxic T lymphocytes (CTLs) (5*10⁶ cells) were washed with PBS and resuspended in 1 ml trizol. Isolation proceeded as recommended by the manufacturer’s protocol. Briefly, cells were lysed by sonication and kept on ice. Cells were centrifuged at 12000 *g for 10 min at 4 °C, and the supernatant was transferred to a new eppendorf tube. 200 µl chloroform (per 1 ml trizol) were added to the supernatant, mixed and incubated for 2-3 minutes at RT and centrifuged at 12000 *g for 15 min at 4 °C. Different phases appear at this step; the top aqueous phase (which contains the RNA) was carefully transferred to a fresh tube. In order to precipitate the RNA, 500 µl isopropanol (per 1 ml trizol) were added and incubated for 10 minutes at RT, the sample was then centrifuged again at 12000 *g for 10 min at 4 °C. After discarding the supernatant, the RNA pellet was washed with 1 ml 70% ethanol (per 1 ml trizol) then centrifuged at 7500 *g for 5 min

at 4 °C. Then the supernatant was discarded and the RNA pellet was allowed to air-dry at RT; color should change from white to transparent. The pellet was then dissolved in 30 µl DEPC-treated H₂O.

II.2.3 RNA quality check

In order to determine the integrity of the RNA, the optical density of the samples was measured using an Eppendorf Biophotometer plus. Samples were diluted with RNase-free water, and absorbance was measured at 260/280 nm. Reading between 1.8 and 2.0 indicates high quality of the RNA. Running the RNA samples on an agarose gel can also determine whether the RNA is degraded or not. Figure 8 shows two bands corresponding to the different subunits of the ribosomal RNA (28S and 18S) that confirms the integrity of the RNA.

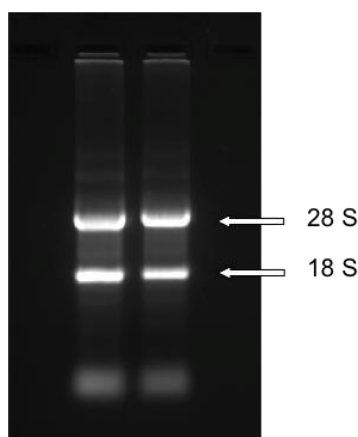


Figure 8. RNA quality check on an agarose gel.

Two different RNA samples from two different mice are run on a gel to check for the quality of the RNA.

II.2.4 cDNA synthesis

cDNA (complementary DNA) synthesis kit was used to synthesize cDNA from RNA isolated from activated CTLs by reverse transcription. First 1 µl total RNA (from 1 µg/µl sample), 1 µl random primers (1 µM) and 1 µl dNTPs (10 mM) were mixed and kept for 5 minutes at 65 °C in order to linearize the RNA secondary structures. Then 4 µl first strand buffer (5x), 1 µl RNaseOUT (RNase inhibitor), 2 µl DTT (0.1 M stock) and 1 µl SuperScript II reverse transcriptase were added to the mixture and incubated for 1 hr at 42 °C.

II.2.5 Brain and CTL protein lysate preparation

Whole brain was isolated from adult mice (8-12 weeks old). Brain was homogenized in protein lysis buffer (see Materials and methods). Homogenate was then centrifuged twice at 1000 *g for 5 minutes at 4 °C to pellet unlysed tissue and cellular debris. The supernatant was then collected,

aliquoted, snap-frozen in liquid nitrogen and then stored at -80 °C. An aliquot was taken to measure protein concentration using Eppendorf Biophotometer plus. About 10×10^6 CTLs were lysed in lysis buffer (100 μ l for 10^7 cells). Cells were then incubated for 30 min on a shaker at 4 °C. Then cells were centrifuged at 10,000 *g for 10 min at 4 °C. The supernatant was collected, and protein concentration was measured. The lysate was aliquoted, snap-frozen and stored at -80 °C until use.

II.2.6 Western blot

In order to check the expression of several proteins, CTL protein lysate was used for Western blot. First, a reducing agent (β -mercaptoethanol) was added to the 4x LDS sample buffer at a 10% ratio. The LDS sample buffer was then added to the desired concentration of protein lysate at a final ratio of 1x, water was added, if necessary, to a final volume of 35 μ l if using a 10-well polyacrylamide gel. The prepared samples were then boiled at 99 °C for 5 min and then were loaded onto the gel. Pre-cast gels from Invitrogen were used (10% bis-tris polyacrylamide gels). MES running buffer (20x) was diluted with distilled water to obtain 1x running buffer. The wells of the gel were first washed with the running buffer, and then samples were loaded. Running was done at 120 V for 1:30 or 2 hrs depending on the proteins to be detected. Buffer for transfer was diluted to 1x from a 20x solution obtained from Invitrogen; methanol was also added to the transfer buffer at a final concentration of 20%. After running, the gel was transferred to a nitrocellulose membrane soaked in 1x transfer buffer. The transfer was done for 2 hrs at RT at 200 mA. The membrane was incubated for about a minute with Ponceau S solution to check for the quality of the transfer. The membrane was washed with TBST (0.05% tween) for 2 times, 5 minutes each (to wash out the Ponceau S staining) and then blocked with 5% nonfat dry milk for 2 hrs at RT. Afterwards the membrane was incubated with the primary antibody for 1 hr at RT or overnight at 4 °C, depending on the antibody used. The blot was then washed for 5 times, 5 minutes each. The secondary antibody coupled to HRP (horseradish peroxidase) was added (dependent on the species used to generate the primary antibody; mouse, rabbit, goat...) for 1 hr at RT. The blot was washed 5 times (5 minutes each). ECL reagent was prepared fresh and added to the blot to visualize the bands using the gel doc system.

II.2.7 Co-Immunoprecipitation

Fresh lysates prepared from brain or CTLs were used for co-immunoprecipitation (Co-IP). Freshly washed (PBS, 0.1 % triton) Protein G Agarose beads were used to immunoprecipitate the protein of interest with its interacting partners. After determining the protein concentration, the required amount of protein lysate was taken for immunoprecipitation (IP). The lysates were incubated with 20 μ l of Protein G Agarose beads on a shaker for 1 hr at 4 °C and then were centrifuged at 1000 *g for 2 minutes. The supernatant (containing the precleared lysates) was then split into two fractions, the first fraction was incubated with the primary antibody for the protein of interest, and the second fraction was incubated with an IgG control antibody. Samples were incubated for 2 hrs while kept on a shaker at 4 °C. At this step, the primary antibody should bind to its target bound to interacting proteins in the lysate solution. After 2 hrs, 30 μ l prewashed Agarose beads were added to both sets and further incubated for 1 hr on a shaker at 4 °C. At this point, the antibody bound to protein complexes should bind to the Agarose beads. The samples were then centrifuged at 1000 *g for 2 minutes, then the supernatant was collected and the Agarose beads were washed with 1 ml washing buffer (PBS, 0.1 % triton) twice. The antibody-protein complexes bound to the Agarose beads were eluted with 30 μ l 1x LDS sample buffer with 10% β ME. The total lysates (input), supernatant and the elution from the Agarose beads were then tested for the expression and/or enrichment of the corresponding protein by Western blot.

II.2.7.1 IP using anti-Synaptobrevin2 antibody:

WT CTLs were stimulated with anti-CD3/CD28 coated-beads for different time points to induce SNARE complex formation. After stimulation, cells were separated from the beads and lysed in lysis buffer (see solutions; section II.1.5.1). After measuring protein concentration, 150 μ g of protein lysates (for each antibody) were used for Co-IP. Lysates were precleared as described above, then were incubated with 2 μ l anti-Syb2 antibody (1mg/ml), or with 2 μ l mouse IgG antibody (1mg/ml) for 2 hrs on a shaker at 4 °C. Pre-washed Agarose beads were then added, and incubated with the samples for one extra hour. The samples were then centrifuged. The supernatant was collected and the Agarose beads were washed twice with washing buffer and then eluted in 1x LDS sample buffer with 10% β ME. 50 μ g of total lysate, 50 μ g of the supernatant and the whole elution from the beads were run on a polyacrylamide gel. The gel was transferred to a nitrocellulose membrane as described above. Then the membrane was probed

with different antibodies to check for proteins that co-immunoprecipitated with Syb2. Anti-SNAP-23 antibody was used with 1:1000 dilution in 5% milk (dissolved in TBST), incubated for 1 hr at RT, washed as described and then incubated with an anti-rabbit HRP conjugated secondary antibody (same for anti-CALM antibody). Anti-Stx11 antibody was also used to check whether Stx11 was co-immunoprecipitated with Syb2. It was used with a dilution of 1:500 in 5% BSA and incubated with the membrane overnight at 4 °C. After checking for the different antibodies, the membrane was stripped and reprobed with anti-Syb2 antibody at a 1:1000 dilution in 5% milk, overnight at 4 °C. The membrane was then incubated with anti-mouse secondary-HRP antibody at a 1:1000 dilution for 1 hr at RT.

II.2.8 Labeling of anti-RFP antibodies with fluorescent dyes

In order to study the acidification of syb2-mRFP-containing (endo-Syb2) vesicles, a pH-sensitive dye, pHrodo green STP ester (increases in fluorescence with decreasing pH) (Miksa et al., 2009) and a pH-insensitive dye, Alexa405 were conjugated to anti-RFP antibody. The conjugation was performed using an antibody-labeling kit from Invitrogen according to the provider's protocol. Briefly, 1 M solution of sodium bicarbonate was freshly prepared and 10 µl were added to a 100 µl anti-RFP antibody (1mg/ml). The mixture was then added to the vial containing Alexa Fluor dye (Alexa405) and pHrodo green STP ester, mixed together and incubated for 1 hr at RT. During incubation, the purification column was prepared by adding 1.5 ml resin to the column and spinning it down at 1100 *g for 3 min. The reaction mixture was added to the column and centrifuged for 5 min at 1100 *g. The eluate containing the conjugated antibody is then ready to be used.

For the anti-RFP antibody labeled with either of the Alexa Fluor dyes (Alexa-405/488/647) only, the procedure was similar except that only the Alexa Fluor dye was used for labeling the antibody.



Figure 9. Endocytosis of fluorescently-labeled antibody.

A scheme showing endocytosis of a fluorescently-labeled antibody with a pH-dependent dye. The antibody binds its ligand and both are then endocytosed together. In the endocytosed vesicle the pH drops which induces the dye to fluoresce, thus the fate of the receptor and antibody can be followed. Source: promega.com (pH-Ab reactive dyes for screening antibody internalization).

II.2.9 Electroporation of CTLs with different Rab protein constructs

CD3/CD28 beads were removed from day 2 activated CTLs. CTLs were transfected overnight (12 hrs) with 6 μg of either of the following constructs, eGFP-Rab5, eGFP-Rab7 or eGFP-Rab11. Electroporation was performed using Nucleofection kit (LONZA). Briefly, $2\text{-}3 \times 10^6$ cells were washed with PBS. Cells were then resuspended in 100 μl nucleofection solution with the corresponding plasmid DNA. Cells were kept in medium provided with the kit overnight at 37 °C and with 5% CO_2 .

II.2.10 Coating coverslips

For all experiments, coverslips used were coated with 0.1 mg/ml polyornithine for 30 min at RT (glass coverslips were precleaned with 70% ethanol prior to coating). For studying acidification of endocytosed vesicles, anti-CD3-coated coverslips were used as a stimulation that mimics an antigen presenting cell or a target cell. For this experiment coverslips were first coated, as mentioned, with polyornithine, then with 30 $\mu\text{g}/\text{ml}$ anti-CD3 antibody (diluted from 1 mg/ml stock) in a final volume of 30 μl for one coverslip (25 mm). The antibody was kept on the coverslips for 2 hrs at 37 °C, then the solution was aspirated and the coverslips were ready to be used.

II.2.11 Live imaging

II.2.11.1 LSM microscope

Live imaging experiments were performed using Zeiss laser scanning microscope 780 (LSM 780). LSM 780 is a confocal light microscope with the ability to acquire images either simultaneously or sequentially. It is equipped with a 32-channel GaAsP detector with active cooling and oversampling of photon counting to deliver highest sensitivity for better signal to noise ratio. This detector is also equipped with two side PMTs that expand the spectral working range and allow for imaging of samples with different signal intensities. The setup is equipped with an incubator chamber that can be kept at 37 °C with 5% CO₂ as well, which can be used for live imaging experiments. A 63x oil immersion objective with a NA of 1.4 Plan-Apochromat was used for live imaging experiments. The ZEN software was used to acquire movies and images. Different wavelengths were used for exciting samples, 405 nm with a Diode 405 nm laser and 488, 561 and 633 nm with a multiple band beam splitter for 488/561/633 nm and a pinhole size of 1 airy unit (AU). To cover the range of the cell, confocal z-stacks were taken with a step size of 0.5 μm.

II.2.11.2 Acidification of endocytosed Syb2-containing (endo-Syb2) vesicles

In order to study acidification of endo-Syb2 vesicles an anti-RFP antibody that is coupled to Alexa405 and pHrodo green dyes (anti-RFP405/pHrodo) (1 mg/ml) was used. Alexa405 is a pH-insensitive dye, so it will fluoresce immediately when the antibody is bound to Syb2-mRFP molecules at the plasma membrane, however pHrodo green is a pH-sensitive dye that is not fluorescent in neutral environment but it increases in fluorescence with increasing acidity (Miksa et al., 2009), i.e. even when the anti-RFP antibody is bound to the syb2-mRFP, no signal from pHrodo will be detected in neutral environment. Only upon endocytosis and acidification of these endocytosed vesicles will the signal from pHrodo be visible.

II.2.11.2.1 Live imaging with anti-CD3-coated coverslips

Sybki CTLs (CTLs isolated from Syb2-mRFP knock-in mice) were added to anti-CD3-coated coverslips at a concentration of 0.2×10^6 in 100 μl IMDM medium; CTLs were allowed to settle and imaged using LSM microscope, in the presence of anti-RFP405/pHrodo antibody (1 mg/ml). The signal from Alexa405 appeared an average of one minute earlier than that of pHrodo.

Acquisition frequency was 1 Hz. Movies were taken with a z-stack of 12 planes with a step size of 0.5 μm . The total number of cells analyzed was 34 cells from two different mice, with a total number of 48 endocytic events.

II.2.11.2.2 Live imaging with P815 target cells

Sybki CTLs were added to polyornithine-coated coverslips at a concentration of 0.2×10^6 in 90 μl IMDM medium, allowed to settle and imaged using LSM microscope. 10 μl of P815 target cells were then added to the coverslip at a final concentration of 0.1×10^6 , along with anti-CD3 antibody (1 mg/ml) and anti-RFP405/pHrodo (1 mg/ml). Acquisition frequency was 2 Hz. Movies were taken with a z-stack of 12 planes with a step size of 0.5 μm . The total number of cells analyzed was 9 cells from four different mice, with a total number of 15 endocytic events.

II.2.12 Imaging using structured illumination microscope (SIM)

II.2.12.1 SIM microscope

In 1873 Ernst Abbe discovered that the resolution of microscopes is limited by the following formula: $d = \lambda/2NA$, where d , is the diffraction limit of light; λ , is the wavelength of light; and NA , is the numerical aperture of the objective (Abbe, 1873). Several microscopes were developed later that defy Abbe's diffraction limit. The structured illumination microscope (SIM) is a super-resolution microscope that defies the diffraction limit of light. Illuminating the sample with a series of excitation light patterns generates a grid pattern similar to that generated by the moiré effect. The grid pattern is tilted in a certain angle to acquire successive images from the illuminated area (5 or 3 rotations). The produced series of images are then processed and reconstructed to generate a high-resolution image (Gustafsson, 2005). The axial resolution of the reconstructed images ranges between 150 and 300 nm.

Images were acquired using ZEN software. An oil-immersion 63x objective with a NA of 1.4 Plan-Apochromat was used to image different samples. Different wavelengths were used for exciting samples; the setup is equipped with several lasers, for example the lasers used included, an HR Diode 405, 488 and 642 nm lasers and an HR DPSS 561 nm laser. Thirty stacks were taken for each image with a step size of 0.2 μm to cover about 6 μm of the cell.

II.2.12.2 Fixation and labeling of cells

CD8⁺ T lymphocytes isolated from sybki or WT mice were activated for 3 days with beads as described above. Cells were used for fixation either as resting cells, i.e. without P815 target cells or as conjugated cells, i.e. with P815 target cells.

II.2.12.2.1 Resting cells

Activated CTLs were removed from beads, washed with isolation buffer and then resuspended in IMDM medium at a concentration of 4×10^6 cell/ml. Then 50 μ l CTLs were put on polyornithine-coated glass coverslips (1mg/ml). Cells were allowed to adhere to the coverslip for 15 minutes at 37 °C with 5% CO₂. Then cells were washed once with PBS and then ice-cold 4% PFA was immediately added to the cells for 20 minutes. Fixed cells were washed twice with PBS and once with PBS containing 0.1 M glycine (quenching solution) for 3 minutes. The cells were again washed twice with PBS and kept at 4 °C. Cells were then ready for labeling.

Fixed cells were permeabilized with PBS containing 0.1% triton for 20 minutes. Then cells were blocked with blocking solution (PBS with 0.1% triton, 2% BSA) for another 30 minutes. During this time the antibody dilutions were prepared in blocking buffer. After adding the primary antibody the coverslips were incubated for 1 hr at RT, and afterwards washed for 5 times (5 min each) with PBS (0.1% triton). Coverslips were then incubated with the corresponding secondary antibody, diluted in blocking buffer, for 1 hr at RT. The coverslips were washed for 5 times (5 min each) and mounted on glass slides in 4 μ l mounting medium (for 12 mm coverslips). Coverslips were allowed to dry for about 15 minutes and then kept at 4 °C, until imaged on the SIM microscope.

II.2.12.2.2 Conjugated cells

Sybki CTLs were removed from beads and washed with isolation buffer then resuspended in IMDM medium at a concentration of 8×10^6 cell/ml (transfected cells were treated the in same way, except that they were already removed from beads before transfection). P815 target cells were also washed with isolation buffer and then resuspended in IMDM medium at a concentration of 8×10^6 cells/ml, with anti-CD3 antibody at a concentration of 0.3 μ g/ μ l. CTLs were then mixed with target cells just before adding them to the coverslips (1:1 ratio). Cells were incubated at 37 °C with 5% CO₂ for different time points, and then fixed with ice-cold 4% PFA.

After fixation cells were treated as described above, if labeling with different antibodies was required, otherwise the coverslips were mounted directly after washing with PBS.

II.2.13 Image analysis

Images studied for colocalization of anti-RFP647 with the different Rab GTPases were analyzed using JACoP plugin in Fiji. Manders' coefficient was calculated by JACoP. To analyze the experiments for granzyme B uptake into endocytosed-Syb2-containing (endo-Syb2) vesicles (carrying anti-RFP405 antibody), three-color colocalization analysis was performed. Fiji was used to obtain the number of colocalized Rab5/7 and endo-Syb2 pixels that also contained granzyme B. This was done by applying a threshold and converting all three channels individually to binary images such that all fluorescent pixels are in the foreground having a bit value of 255. First, the Rab5 and endo-Syb2 binary images were merged to obtain a resulting RGB image with the following parameters: background-Yellow (255,255,000); Rab5 green only (000,255,000); endo-Syb2 red only (255,000,000); colocalized pixels Black (000,000,000). Applying a color threshold based on hue saturation and brightness to this image results in an image (Rab plus endo-Syb2) in which the colocalized pixels are in the foreground. The number of colocalized pixels was calculated by dividing the raw integrated density by the mean intensity of the resulting image (Rab plus endo-Syb2). Next, Rab plus endo-Syb2 images were merged with the granzyme B binary image, and the resulting image was processed as described above to obtain the colocalized pixels between all three channels: Rab5/7, endo-Syb2, and granzyme B over time (Chang et al., 2016).

II.2.14 Software

A plasmid Editor (ApE), version 1.17, M. Wayne Davis.

CorelDRAW, version 16.1.0.843, Corel Corporation.

ImageJ, National Institutes of Health, Federal Government of USA.

Office 2013, Microsoft.

SigmaPlot Version 13, Systat Software, Inc.

SnapGene Viewer 2.8, GSL Biotech LLC

Zeiss Efficient Navigator (Zen) 2012, Carl Zeiss.

III. Results

III.1 SNAP-23 is a t-SNARE required for cytotoxic granule (CG) fusion in mouse CTLs

Our group have previously identified Syb2 as the v-SNARE and STX11 as a t-SNARE required for fusion in CTLs (Halimani et al., 2014; Matti et al., 2013). Studies on other types of immune cells like neutrophils (secretion of specific and tertiary granules) (Mollinedo et al., 2006), macrophages (TNF α secretion) (Pagan et al., 2003), mast cells (specialized secretory granules) (Guo et al., 1998; Paumet et al., 2000) and platelets (lysosome release) (Chen et al., 2000) have shown that SNAP-23 is a t-SNARE required for vesicle fusion in these cells. In order to define the identity of t-SNAREs in mouse CTLs, we performed immunoprecipitation using anti-Syb2 antibody and checked for the co-immunoprecipitation of SNAP-23 and STX11 along with Syb2. Also, because recent experiments have shown that CALM is an adaptor protein required for Syb2 endocytosis from mouse CTLs (Chang et al., 2016), we examined whether CALM co-immunoprecipitates with Syb2. To induce CG fusion and thus SNARE complex formation, CTLs from WT mice were activated with anti-CD3/CD28-coated beads for 0, 15, 30 or 60 minutes.

After running the Western blot for the IP samples, the membrane was probed with anti-Syb2 antibody. As shown in (Figure 10A) Syb2 was immunoprecipitated with anti-Syb2 antibody, at all time points of stimulation; no band was seen with IP using control IgG antibody. Syb2 was detected in the input samples (Figure 10A, right side), however it was barely visible in the IP-supernatant, indicating that almost all Syb2 was immunoprecipitated from the input samples. Both blots were probed for other proteins that might be co-immunoprecipitated along with Syb2. Probing with anti-SNAP-23 antibody showed that SNAP-23 was co-immunoprecipitated with Syb2 only after 30 and 60 min of CTL stimulation (Figure 10A, left blot). SNAP-23 can also be detected in the input samples and also the IP-supernatant. Though STX11 could be detected in the lanes corresponding to the input and IP-supernatant, anti-STX11 antibody didn't show any band of STX11 that co-immunoprecipitated with Syb2. GAPDH was used as a loading control for the input and IP-supernatant samples (Figure 10A, left blot). Figure 10B also shows a Western blot for IP using Syb2 antibody from unstimulated CTLs or CTLs stimulated for 30

RESULTS

min. Syb2 can be detected in the IP fraction and input but is not detected in the IP with control IgG antibody. The same membrane was probed with anti-CALM antibody to check whether CALM is co-immunoprecipitated with Syb2 under these conditions. A band corresponding to CALM is detected only in the input samples and the supernatant but not the IP samples.

SNAP-23 is phosphorylated by a protein called SNARE kinase (SNAK) (Cabaniols et al., 1999) and is present in the cell in a phosphorylated and unphosphorylated forms. In order to detect both phosphorylated-SNAP-23 (p-SNAP-23) and un-phosphorylated-SNAP-23 (SNAP-23) we repeated the IP with anti-Syb2 antibody, but allowed the blot to run for longer time to better separate p-SNAP-23 and SNAP-23. In this experiment, WT CTLs were only stimulated for 15 and 30 min with anti-CD3/CD28-coated beads. Again Syb2 could be detected in the IP with anti-Syb2 antibody but not with the control IP (Figure 10B). Syb2 was also detected in the input samples but not in the IP-supernatant. When probing the blot with anti-SNAP-23 antibody, two bands corresponding to p-SNAP-23 and SNAP-23 could be detected in the input, but not in the IP with CTLs stimulated for 15 min. However after 30 min stimulation, a clear band of SNAP-23 could be detected to be co-immunoprecipitated with Syb2, which corresponded to the un-phosphorylated form of SNAP-23.

Our data show that SNAP-23 is a t-SNARE involved in CG fusion in mouse CTLs, and only the un-phosphorylated form of SNAP-23 was incorporated into the SNARE complex. In spite of this, STX11 and CALM did not co-immunoprecipitate with Syb2, probably because the binding of Syb2 with these proteins is not favoured under the current experimental conditions. It could also be that the endogenous interaction between Syb2 and CALM for example is transient thus allowing only a small fraction of Syb2 to be bound to CALM at a time, rendering it undetectable in a Western blot.

RESULTS

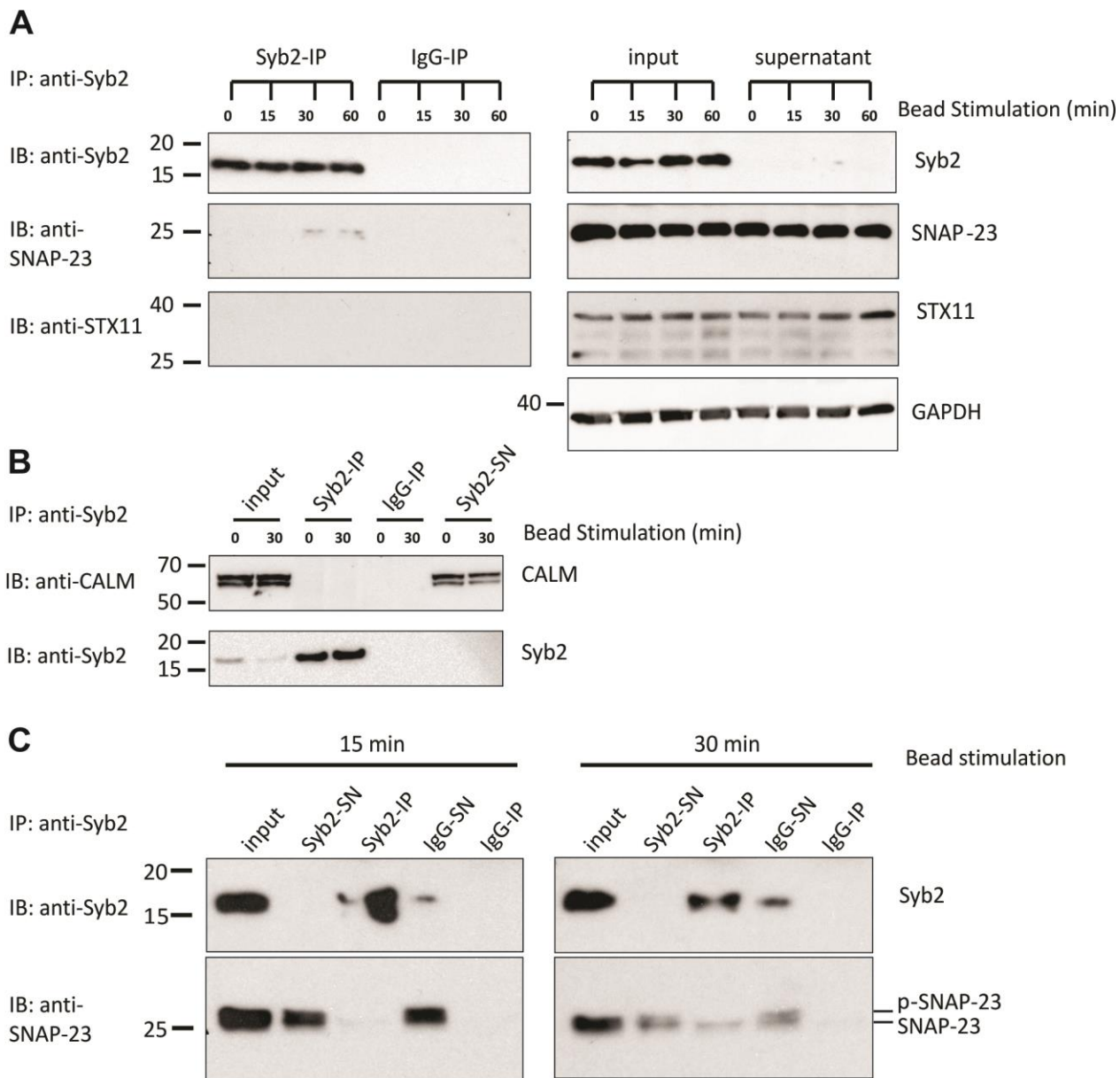


Figure 10. Co-immunoprecipitation of Syb2 with SNAP-23, STX11 and CALM.

Lysates from stimulated WT CTLs were used for immunoprecipitation with anti-Syb2 antibody, or with a control mouse IgG antibody. A, A Western blot of the IP samples, the input from each time point and the supernatant after each IP probed with Syb2 antibody (upper blots), with SNAP-23 antibody (middle blots), or with STX11 antibody (lower blots). SNAP-23 was immunoprecipitated with Syb2 after 30 and 60 min of CTL stimulation, however, STX11 did not co-immunoprecipitate with Syb2. The membrane from input and supernatant samples was stripped and reprobed with GAPDH antibody as a loading control. B, Co-IP done using anti-Syb2 antibody with either unstimulated CTLs or stimulated for 30 min. Western blot for the IP samples did not detect CALM in the IP fraction, although it can be detected in the input samples and the supernatant. Syb2 is present in the IP samples and can be detected in the input but not in the IP with the control IgG. C, A similar experiment to that in (A) is shown, however here CTLs were stimulated for only 15 and 30 minutes. Blots were probed with anti-Syb2 (upper blots) and anti-SNAP-23 (lower blots) antibodies; notice that here SNAP-23 is present in two bands, in both the input and supernatant, which represent the phosphorylated and un-phosphorylated forms of SNAP-23. Only the lower band i.e.

the un-phosphorylated form of SNAP-23 is immunoprecipitated with Syb2. CALM: clathrin assembly lymphoid myeloid leukemia, IP: immunoprecipitation, SN: supernatant, SNAP-23: synaptosomal-associated protein 23, STX11: syntaxin-11, Syb2: synaptobrevin2.

III.2 Proteins present on endocytosed Syb2-containing (endo-Syb2) vesicles

After fusion of CGs, the vesicle components diffuse in the plasma membrane, where the SNARE proteins are in the cis-SNARE complex (all proteins are in the same membrane). The complex is dissociated by the ATPase NSF allowing individual SNARE proteins to be free at the plasma membrane where they are endocytosed and reused for further rounds of fusion. We have confirmed the results from Chang et al, which shows that endocytosis of Syb2 occurs in mouse CTLs (Chang et al., 2016) (see results below). To study endocytosis of Syb2, we used CTLs isolated from Syb2-mRFP knock-in (sybki) mice. Thus anti-RFP antibodies were used to track Syb2-mRFP. The anti-RFP antibodies were coupled to Alexa405, 488 or 647 dyes and either was then added to the extracellular medium containing CTLs. The epitope of the anti-RFP antibody is located in the vesicle lumen (i.e. the mRFP fused to Syb2 faces the vesicle lumen) and is thus exposed to the extracellular medium upon CG fusion. Endocytosis of Syb2-mRFP results in import of the bound antibody as well, marking the endocytosed Syb2-mRFP (endo-Syb2) with the fluorescent dye. Endo-Syb2 can then be tracked using the Alexa dye fluorescence. Endocytosis of Syb2 is important for the serial killing function of CTLs because it allows for the replenishment of CG v-SNAREs (Rothstein et al., 1978). In order to determine what other proteins may be endocytosed with Syb2, we used antibodies against these candidate proteins and looked at colocalization in endocytosed vesicles.

III.2.1 SNAP-23 is endocytosed with endo-Syb2 in the same vesicle

We have shown that SNAP-23 (synaptosomal-associated protein of 23 kDa) is a t-SNARE required for fusion in mouse CTLs. Therefore, we investigated whether SNAP-23 is endocytosed along with Syb2 in the same vesicle. For that purpose, sybki CTLs (magenta) were conjugated with target cells in the presence of anti-RFP488 (green) and fixed after 5, 10 and 15 min of target cell addition (Figure 11A). Afterwards, conjugated cells were washed, permeabilized and labeled with an anti-SNAP-23 antibody, followed by the corresponding secondary antibody coupled to Alexa647 (red, see Figure 11A). The third column shows a merged image of SNAP-23 and anti-RFP488 (colocalization is detected in yellow). Quantification of colocalization between endo-

RESULTS

Syb2 vesicles (containing anti-RFP647) and anti-SNAP-23 was performed using the JACoP (Just Another Colocalization Plugin) plugin from FIJI. The Manders' coefficient obtained by JACoP is shown as a dot plot (Figure 11B) for the different time points. Manders' coefficient was used instead of Pearson's coefficient because the colocalization studied here is from one channel to the other and not between both channels (Bolte and Cordelieres, 2006), i.e. colocalization of anti-RFP488 (endo-Syb2) with anti-SNAP23 and not the other way around. SNAP-23 showed a very good colocalization with anti-RFP488 based on Manders' coefficient values at all time points tested here (Figure 11B). These results indicate that SNAP-23 is endocytosed with Syb2 in the same vesicle at least until they fuse with early endosomes (section III.3.1).

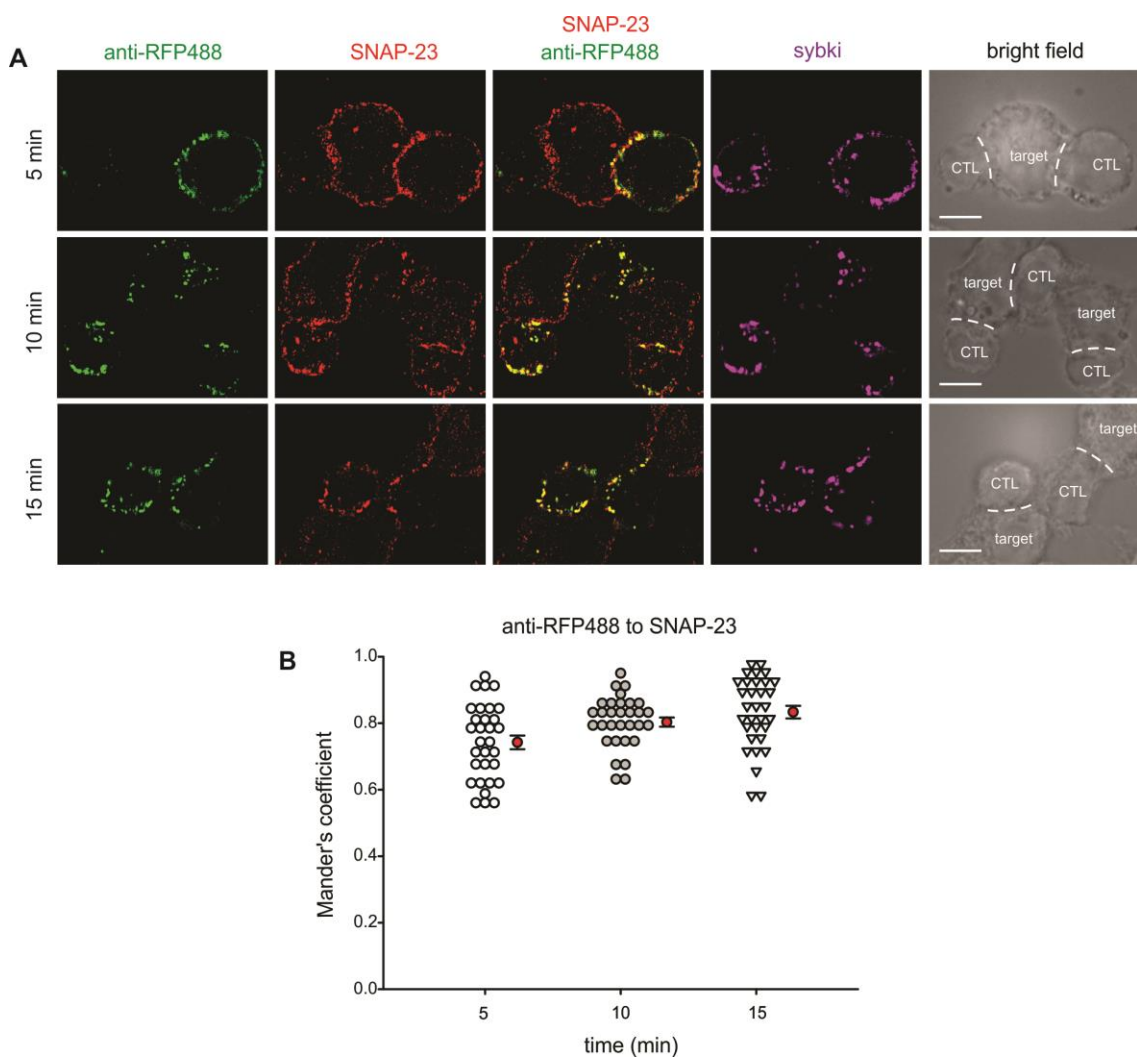


Figure 11. SNAP-23 is present on the same vesicles like endo-Syb2.

A, SIM images of sybki CTLs (magenta) conjugated with P815 target cells in the presence of anti-RFP488 (green) antibody and fixed after 5, 10 and 15 min. Fixed cells were labeled with SNAP-23 (red). The third column shows a

merged image of the anti-RFP488 channel with that of SNAP-23 (colocalization is seen in yellow). B, Quantification of colocalization between the endo-Syb2 vesicles and SNAP-23 using Manders' coefficient is shown as dot plot for the different time points for CTL:target cell conjugation. Data are from three independent experiments. Scale bar: 5 μ m. Sybki: Synaptobrevin2-mRFP knock-in, SNAP23: Synaptosomal-associated protein 23 kDa

III.2.2 ZAP70 is endocytosed with endo-Syb2 in the same vesicle

Zeta-chain associated 70 kDa tyrosine phosphoprotein (ZAP70) is involved in initiating T cell receptor (TCR) responses in CTLs. It acts upstream in the signaling pathway leading to T cell activation, as it phosphorylates several proteins recruited to the forming IS to activate further downstream events (Wang et al., 2010). Due to its crucial function at the IS, we investigated ZAP70 endocytosis and whether it colocalizes with endo-Syb2. For this purpose, sybki CTLs (magenta) were conjugated with target cells in the presence of anti-RFP488 (green) and fixed after 5, 10 and 15 min (Figure 12A). Afterwards, conjugated cells were washed, permeabilized and labeled with an anti-ZAP70 primary antibody, followed by the corresponding secondary antibody coupled to Alexa647 (red, see Figure 12A). The third column shows a merge between the images from ZAP70 and anti-RFP488 (colocalization is detected in yellow). Quantification of colocalization between endo-Syb2 vesicles (containing anti-RFP488) and anti-ZAP70 was calculated using JACoP plugin from FIJI. The Manders' coefficient obtained by JACoP is shown as a dot plot (Figure 12B) for the different time points. ZAP70 shows a very good colocalization with anti-RFP488 based on Manders' coefficient values from all time points checked here (Figure 12B). As with SNAP-23, ZAP70 is endocytosed with Syb2 in the same vesicle at least until they fuse with early endosomes (section III.3.1).

RESULTS

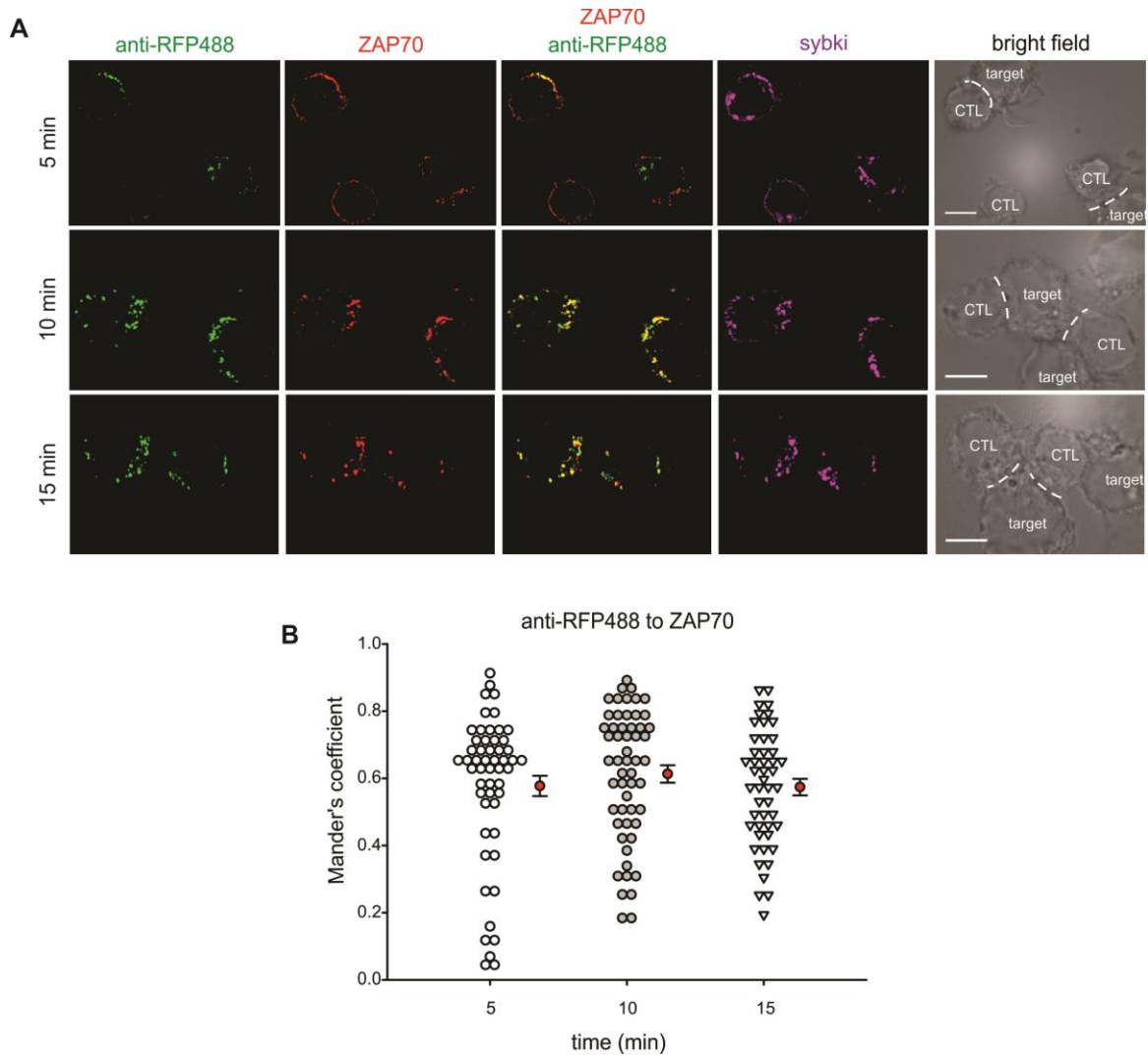


Figure 12. ZAP70 is endocytosed in the same vesicle with endo-Syb2.

A, SIM images of sybki CTLs (magenta) conjugated with P815 target cells in the presence of anti-RFP488 (green) antibody and fixed after 5, 10 and 15 min. Fixed cells were labeled with ZAP70 (red). The third column shows a merged image of the anti-RFP488 channel with that of ZAP70 (colocalization is seen in yellow). B, Quantification of colocalization between the endo-Syb2 vesicles and ZAP70 using Manders' coefficient is shown as dot plot for the different time points for CTL:target cell conjugation. Data are from three independent experiments. Scale bar: 5 μ m. Sybki: Synaptobrevin2-mRFP knock-in, ZAP70: zeta-associated protein of 70 kDa.

III.2.3 H⁺ V-ATPase is present on endo-Syb2 vesicles

Since an acidic pH is a key feature of CGs, we investigated whether the H⁺ V-ATPase would be endocytosed directly with Syb2 in the same vesicle. Therefore, we investigated using high-resolution microscopy whether the H⁺ V-ATPase is localized on nascent endo-Syb2 vesicles. Figure 13A shows SIM images of sybki CTLs (magenta) incubated with P815 target cells in the presence of anti-RFP488 antibody (green) and fixed after 5, 10 or 20 minutes of target cell addition, then stained with an antibody against $\alpha 3$ subunit of the H⁺ V-ATPase (red). The $\alpha 3$ signal corresponding to the V-ATPase shows colocalization with endo-Syb2 vesicles even at the 5 minute time-point of conjugation with target cells (Figure 13A, third column; colocalization can be detected in yellow). Colocalization of endo-Syb2 vesicles (containing anti-RFP488) with $\alpha 3$ subunit of the V-ATPase, quantified using Manders' coefficient (Figure 13B), demonstrated a high degree of co-localization at all the given time points starting as early as 5 min of CTL:target cell incubation. This result indicates that the V-ATPase is already endocytosed along with Syb2, as the colocalization of fluorescent anti-RFP with the V-ATPase occurs at time points earlier than co-localization with early endosomes, which are the first organelles that nascent endocytosed vesicles fuse with (section III.3.1).

RESULTS

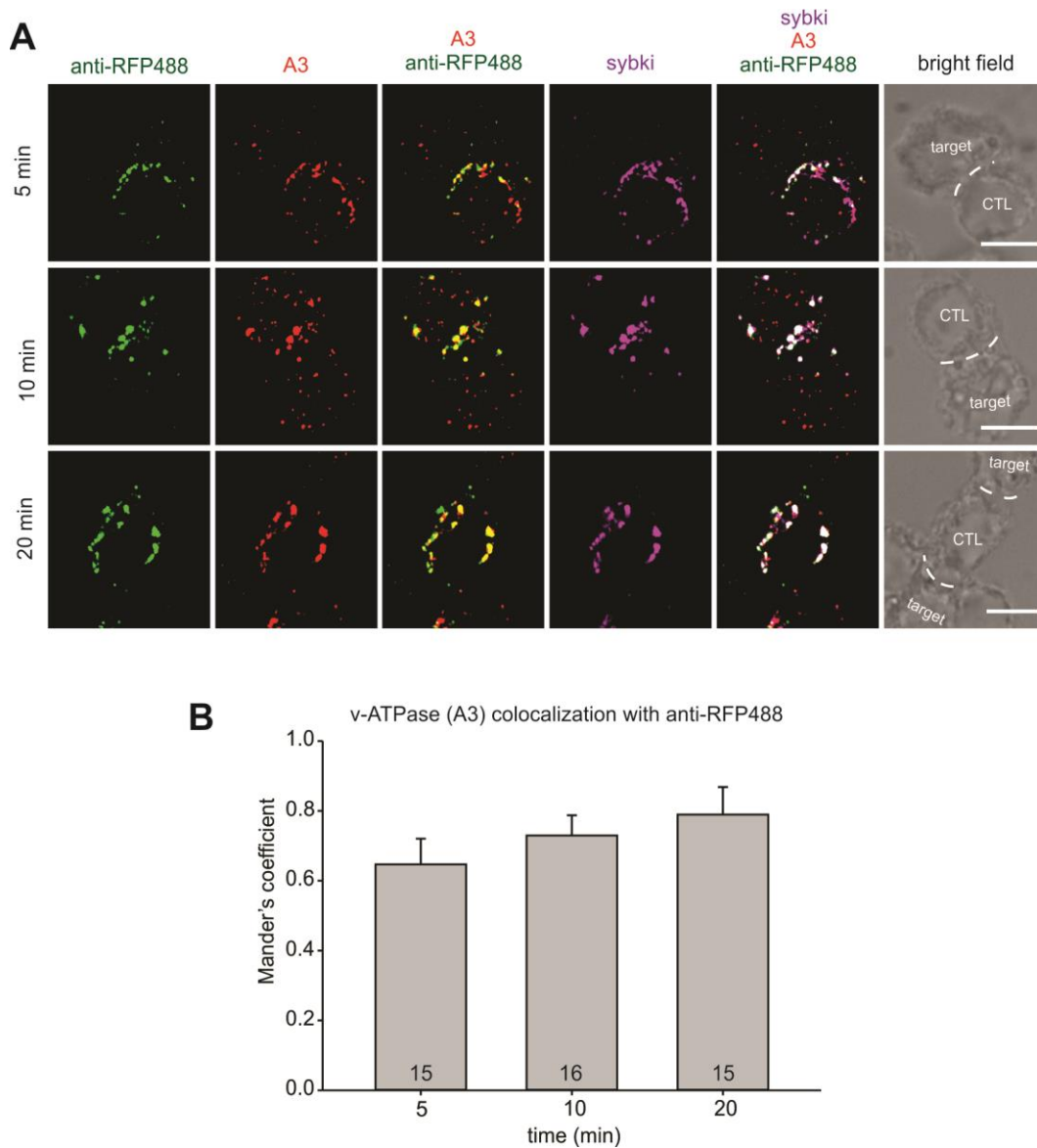


Figure 13. The a3 subunit of the V-ATPase colocalizes with endo-Syb2 vesicles.

A, SIM images of sybki CTLs (magenta) conjugated with P815 target cells in the presence of anti-RFP antibody coupled to Alexa 488 (anti-RFP488, green). Cells were fixed at the indicated time points (5, 10 and 20 mins), permeabilized and labeled with an anti-a3 antibody, then with a secondary antibody coupled to Alexa 647 (red). Colocalization between a3 signal and anti-RFP488 is seen in yellow color in the merged image (third column), and colocalization between all three channels is seen in white color (the next to last column). B, Quantification of Manders' coefficient of colocalization between the a3 subunit of the v-ATPase and anti-RFP488 of the endo-Syb2 vesicles. Scale bar: 5 μ m. Data are representative of two independent experiments. Error bars represent SEM. Numbers in the bar graphs represent the cell number per group.

III.2.4 H⁺ V-ATPase is colocalized with endo-Syb2 vesicles 1-2 min following exposure of Syb2-mRFP at the plasma membrane shown by live imaging

We have shown that endo-Syb2 vesicles colocalized rapidly with H⁺ V-ATPase, prior to fusion with endosomal compartments (section III.3.1), using high resolution imaging of fixed cells. We wanted to investigate, using live imaging whether we would be able to detect the acidification of endo-Syb2 vesicles. The results from this experiment might indicate whether some of the CG membrane components are endocytosed together, which would be important for their maturation into CG. Since an acidic pH is a key feature of CGs, we investigated the time required for the acidification of endo-Syb2 vesicles. For this purpose, anti-RFP antibody, which detects fused Syb2-mRFP, was coupled to two different fluorophores, Alexa405 and pHrodo green which are pH-insensitive (i.e. it is fluorescent in neutral and acidic environments) and pH-sensitive dye, respectively. PHrodo is not fluorescent in neutral environment, but it increases fluorescence with decreasing pH (Miksa et al., 2009). Figure 14A shows live cell imaging of a sybki CTL forming an immunological synapse (IS) with a P815 target cell in the presence of anti-RFP405/pHrodo. Upon CTL contact with the target cell, CGs (endogenously labeled with Syb2-mRFP) are polarized towards the IS (Figure 14A, third row). Immediately upon antibody binding, the Alexa405 signal is visible (Figure 14A, first row, yellow arrows), pHrodo is seen about two minutes later (Figure 14A, second row, yellow arrows). Detection of pHrodo signal indicates that Syb2-mRFP is already endocytosed in a compartment that has an acidic pH. The acidity of this endocytosed vesicle increases further, as seen by the constitutive increase in pHrodo signal (Figure 14A, second row). The merged image for all channels shows the colocalization of the fluorescent signals (Figure 14A, last row). Next, sybki CTLs were allowed to settle on an anti-CD3-coated coverslips to induce IS formation. Fluorescently-labeled anti-RFP antibody was added to the medium, and upon CG fusion, signal from anti-RFP405 was visible first (Figure 14B, first row, yellow arrows), and signal from anti-RFP-pHrodo, an average of one minute later (Figure 14B, second row, yellow arrows). Quantification of the time required for acidification of endo-Syb2 vesicles indicated that the average times for acidification were 125 ± 19.1 seconds for stimulation with target cells and 61 ± 6.2 seconds for stimulation with anti-CD3-coated coverslips. Data are representative of 9 cells from four independent experiments (Figure 14A) and 32 cells from two independent experiments (figure 14B). Variability in the time required for

RESULTS

acidification between the two methods used might be explained by the stimulus strength given to the CTL. Stimulation with anti-CD3-coated coverslips probably induces a stronger stimulation of the CTL than contact with the target cell, thus inducing faster exocytosis and endocytosis.

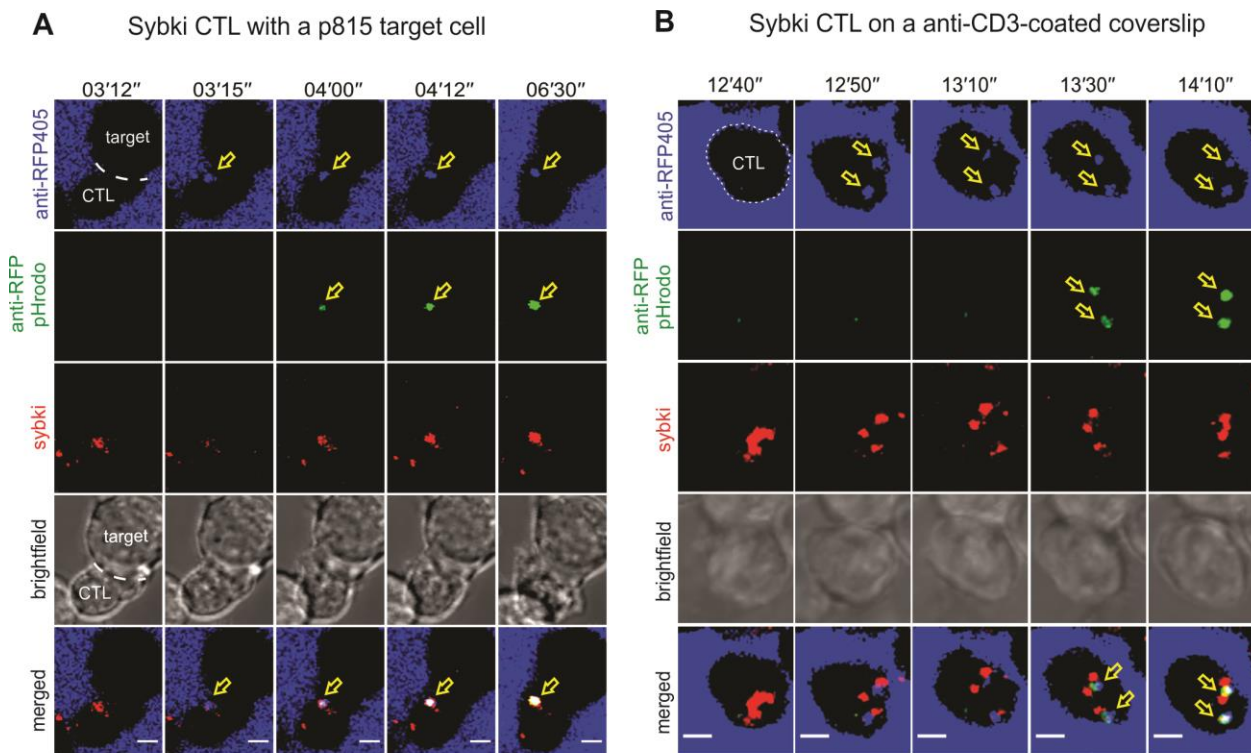


Figure 14. Acidification of endo-Syb2 vesicles in CTLs.

Confocal time lapse imaging of sybki CTLs (red) incubated with P815 target cells (A) or on an anti-CD3-coated coverslips (B) in the presence of anti-RFP antibody coupled to Alexa405 (blue) and pHrodo green (green). Initially only Alexa405 signal is seen upon antibody binding to exposed mRFP (A and B, first row). Only upon acidification of endo-Syb2 vesicles, pHrodo signal appears (A and B, second row). The bright field images show the CTL with the target cell (A) or only CTL (B). The merged images show the colocalization of the anti-RFP405 and pHrodo together and with sybki (A and B, last row). Numbers at the top indicate time scale. Scale bar, 3 μm .

III.3 Trafficking of endo-Syb2 vesicles through the endosomal pathway

We have shown that Syb2 is endocytosed in mouse CTLs along with other proteins in the same vesicle (SNAP-23 and ZAP70), including other CG membrane components (H^+ V-ATPase). In the next step, we were interested in elucidating the pathway of maturation of endo-Syb2 vesicles to CG. To define the main endosomal hubs, different markers labelling each of these were utilized. We used eGFP-Rab5 to label early endosomes, eGFP-Rab7 to label late endosomes (Rink et al., 2005) and eGFP-Rab11 to label recycling endosomes.

III.3.1 Endo-Syb2 vesicles reach early endosomes within 15 min of target cells' addition

The first intracellular organelles that nascent endocytosed vesicles fuse with are early endosomes. Therefore we investigated the colocalization of endo-Syb2 with early endosomes using Rab5 as the organelle marker (Chavrier et al., 1990). Sybki CTLs were transfected with a construct encoding eGFP-Rab5 by electroporation. Transfected cells were conjugated with P815 target cells for 5, 15, 30 and 60 minutes in the presence of anti-RFP647 antibody. Figure 15A shows SIM images of the conjugated cells, with eGFP-Rab5 shown in green, Syb2-mRFP in red and anti-RFP647 antibody corresponding to endo-Syb2 in magenta. The colocalization between all three channels is seen in white color in the merged images (Figure 15A). Quantification of colocalization between endo-Syb2 vesicles (containing anti-RFP647) and the eGFP-Rab5 was calculated using the JACoP plugin from FIJI. The Manders' coefficient obtained by JACoP is plotted and shown as a dot plot (Figure 15B) for the different time points. We were interested to check the fraction of endo-Syb2 that colocalizes with early endosomes, thus we used Manders' coefficient for quantification of this colocalization (Bolte and Cordelieres, 2006). Colocalization started low (0.31 ± 0.02) at 5 minutes of CTL:target cell conjugation but increased to a maximum (0.51 ± 0.02) after 15 min, to decrease again after 30 min (0.37 ± 0.02) and then reach a minimum (0.29 ± 0.02) after 60 min of conjugation (Figure 15B). Statistical analysis shows a significant difference between the Manders' coefficient at 15 min with that at 5 min ($P < 0.001$) and between the values at 15 min and at 30 min ($P < 0.001$). Mander's coefficient value of 0.2 for example, indicates that 20% of the signal from one channel colocalizes with the signal from the other channel (Bolte and Cordelieres, 2006). Therefore, these data show that at least 50% of endo-Syb2 colocalizes with early endosomes after 15 min of CTL:target cell conjugation.

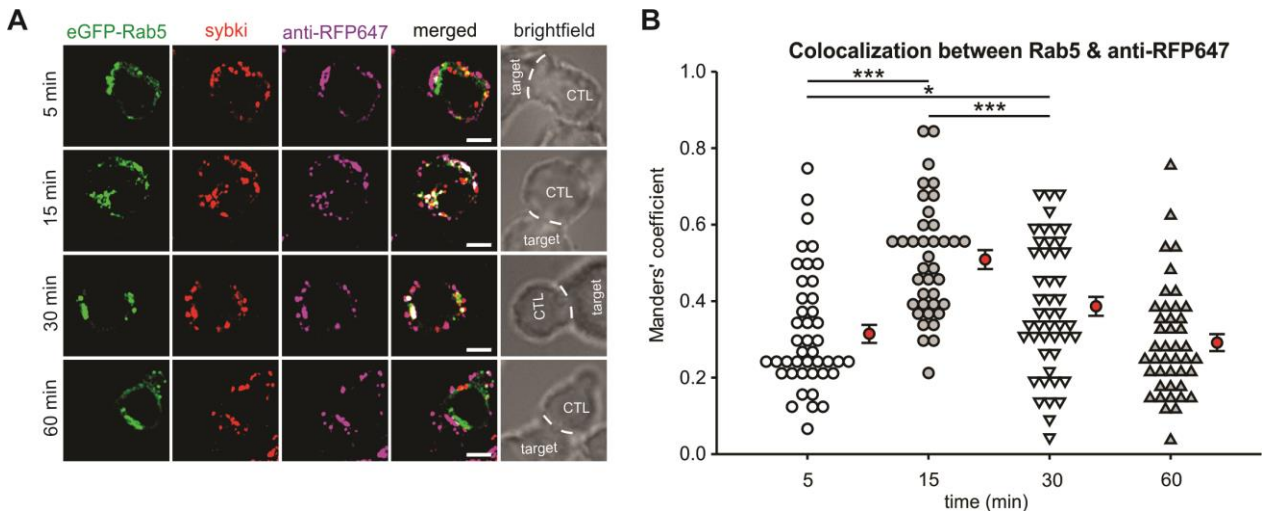


Figure 15. Endo-Syb2 colocalizes with early endosomes 15 min after endocytosis.

A, SIM images of sybki CTLs (red) transfected with eGFP-Rab5 (green) conjugated with P815 target cells in the presence of anti-RFP647 antibody (magenta) and fixed at the indicated time points. The next to last column shows the merged images from all three channels, with white color indicating colocalization between these channels. Scale bar: 5 μ m. B, the graph represents quantification of the Manders' coefficient for colocalization between eGFP-Rab5 and endocytosed vesicles containing anti-RFP647 antibody (endo-Syb2), at the different time points of CTL:target cell conjugation. Data are from three independent experiments. Red circles represent mean \pm SEM for each time point. Asterisks indicate significance in one-tailed Student's t-test; * $P < 0.05$, *** $P < 0.001$. Sybki: Synaptobrevin2-mRFP knock-in.

III.3.2 Endo-Syb2 vesicles show no colocalization with recycling endosomes

Endocytosed proteins that reach the early endosomes are either recycled back to the plasma membrane via recycling endosomes (Sonnichsen et al., 2000), or they further traffic to late endosomes (Schmid et al., 1988). Sybki CTLs were transfected with a construct encoding eGFP-Rab11, which labels recycling endosomes, to test whether endo-Syb2 vesicles fused with the recycling endosomes. After incubation with P815 target cells in the presence of anti-RFP647, CTLs were fixed at 5, 15, 30 and 60 min. Figure 16A shows SIM images of the conjugated cells with eGFP-Rab11 shown in green, Syb2-mRFP in red and endo-Syb2 vesicles (containing anti-RFP647) in magenta. The colocalization between all three channels is seen in white color in the merged image column (Figure 16A). Quantification of colocalization between endo-Syb2 vesicles and the eGFP-Rab11 was calculated using JACoP plugin from FIJI. The Manders' coefficient obtained by JACoP is plotted and shown as a dot plot (Figure 16B) for the different time points. In contrast to the results obtained with eGFP-Rab5, colocalization of endo-Syb2 was minimal with eGFP-Rab11 (0.27 ± 0.02 at 5 min to 0.24 ± 0.03 at 60 min). Statistical analysis showed no significant difference between the Manders' coefficient for any of the time points

RESULTS

shown in the figure. Therefore these data show that the main pathway followed by endo-Syb2 might not include recycling through recycling endosomes.

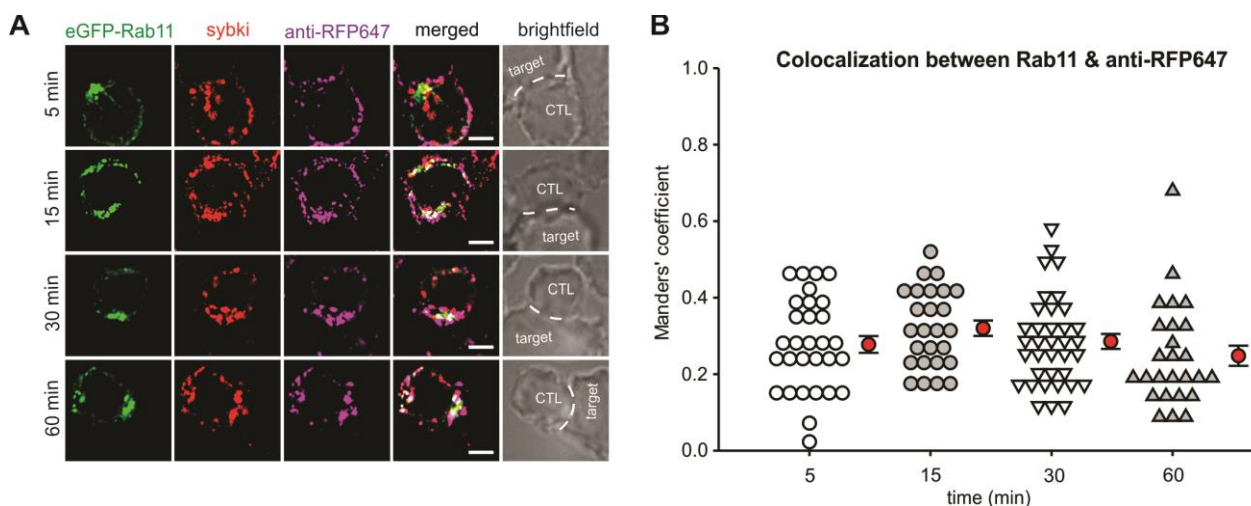


Figure 16. Endo-Syb2 does not traffic through recycling endosomes.

A, SIM images of sybki CTLs (red) transfected with eGFP-Rab11 (green) conjugated with P815 target cells in the presence of anti-RFP647 antibody (magenta) and fixed at the indicated time points. The next to last column shows the merged images from all three channels, with white color indicating colocalization between these channels. Scale bar: 5 μ m. B, the graph represents quantification of the Manders' coefficient for colocalization between eGFP-Rab11 and endocytosed vesicles containing anti-RF647 antibody (endo-Syb2), at the different time points of CTL:target cell conjugation. Data are from two independent experiments. Red circles represent mean \pm SEM for each time point. Sybki: Synaptobrevin2-mRFP knock-in.

III.3.3 Endo-Syb2 vesicles reach late endosomes 30-60 min after CTL:target cell conjugation

Endo-Syb2 vesicles showed minimal colocalization with eGFP-Rab11 indicating that these vesicles do not traffic through the recycling endosomes. To test whether these vesicles traffic through the late endosomes, we transfected sybki CTLs with a construct encoding eGFP-Rab7, as a marker for late endosomes and examined the localization of endo-Syb2 in relation to that of late endosomes. Transfected cells were incubated with P815 target cells in the presence of anti-RFP647 and fixed at 5, 15, 30 and 60 min. Figure 17A shows SIM images of the conjugated cells with eGFP-Rab7 shown in green color, Syb2-mRFP in red color and endo-Syb2 (containing anti-RFP647) in magenta color. The colocalization between all three channels is seen in white color in the merged image column (Figure 17A). Quantification of colocalization between endo-Syb2 and the eGFP-Rab7 was calculated using JACoP plugin from FIJI. The Manders' coefficient obtained by JACoP is shown as a dot plot (Figure 17B) for the different time points. The

RESULTS

colocalization between eGFP-Rab7 and endo-Syb2 started low (0.17 ± 0.02) after 5 min of CTL:target cell conjugation and started to increase progressively after 15 min (0.33 ± 0.02) and 30 min (0.4 ± 0.02) to reach a maximum after 60 min (0.45 ± 0.02) of CTL:target conjugation. Statistical analysis shows significant difference in the Manders' coefficient at 5 min to that at the other time points studied ($P < 0.001$), and between 15 min and 60 min ($P < 0.012$). These results implicate that endo-Syb2 is probably trafficked mainly from the early endosomes to late endosomes and not through recycling endosomes.

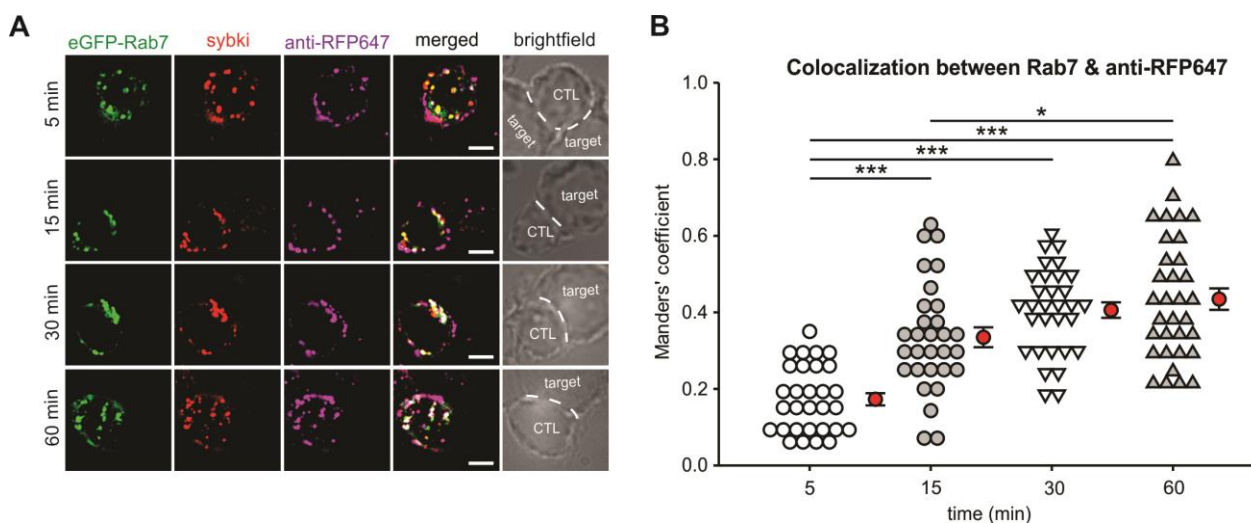


Figure 17. Endo-Syb2 colocalizes with late endosomes 30-60 min after endocytosis.

A, SIM images of sybki CTLs (red) transfected with eGFP-Rab7 (green) conjugated with P815 target cells in the presence of anti-RFP647 antibody (magenta) and fixed at the indicated time points. The next to last column shows the merged images from all three channels, with white color indicating colocalization between these channels. Scale bar: 5 μ m. B, the graph represents quantification of the Manders' coefficient for colocalization between eGFP-Rab7 and endo-Syb2 vesicles containing anti-RFP647 antibody (endo-Syb2), at the different time points of CTL:target cell conjugation. Data are from two independent experiments. Red circles represent mean \pm SEM for each time point. Asterisks indicate significance in one-tailed Student's t-test; * $P < 0.05$, *** $P < 0.001$. Sybki: Synaptobrevin2-mRFP knock-in.

III.4 Acquisition of granzyme B by endo-Syb2 vesicles

The main pathway followed by endo-Syb2 is from early endosomes to late endosomes. However, since cytotoxic proteins such as granzyme B constitute a hallmark of a mature cytotoxic granule, we next investigated the time point at which granzyme B is incorporated into endo-Syb2 vesicles to determine whether this occurs in early or late endosomes. For that purpose, we transfected sybki CTLs with either eGFP-Rab5 or eGFP-Rab7 and then conjugated these cells with P815

target cells in medium containing anti-RFP405 to label endo-Syb2. Cells were fixed at various time points after target cell addition and then washed, permeabilized and stained with an anti-granzyme B antibody coupled to Alexa647.

III.4.1 Endo-Syb2 vesicles do not acquire granzyme B at Rab5-containing early endosomes

In order to address whether endo-Syb2 vesicles regain granzyme B from early endosomes, sybki CTLs were transfected with a construct encoding eGFP-Rab5 (green) to label early endosomes and conjugated with P815 target cells in the presence of anti-RFP antibody coupled to Alexa405 (anti-RFP405, blue) to label endo-Syb2 vesicles (Figure 18A). The figure shows SIM images of CTL:target cell conjugates at the different time points of conjugation labeled with an anti-granzyme B antibody coupled to Alexa647 (red). The images from the anti-RFP405 channel and that of eGFP-Rab5 are shown as a merged image for each time point in the third column (colocalization is shown as cyan) (Figure 18A). This merged image at each time point is again merged with the corresponding granzyme B image to produce the merged image of all three channels shown one before the last column (colocalization is seen in white) (Figure 18A). To find out at which time point is granzyme B reincorporated into the endo-Syb2 vesicles, we did a three-channel colocalization. First, we calculated the number of colocalized pixels between the anti-RFP405 (endo-Syb2) and eGFP-Rab5 by obtaining a corresponding image showing only the colocalized pixels in the foreground (anti-RFP405+eGFP-Rab5) (Figure 18B) (see Materials and Methods). The resulting image was then merged with the corresponding image containing only granzyme B fluorescent pixels in the foreground (Figure 18C) in order to finally obtain an image that contained the colocalized anti-RFP405+eGFP-Rab5 pixels having also granzyme B (anti-RFP405+eGFP-Rab5+granzyme B) (Figure 18C). The graphs (Figure 18B-D) show the quantification of the corresponding pixel number at each of the aforementioned steps at the different time points of CTL:target cell conjugation. Colocalization between eGFP-Rab5 and anti-RFP405 using the above described common pixel analysis method (Figure 18B), showed maximum colocalization after 15 min of CTL:target cell conjugation that decreased again at 30 to 60 min after conjugation. These results further confirm the results obtained by analysis using Manders' coefficient for colocalization (Section III.3.1; Figure 15B). Figure 18C shows the number of colocalized anti-RFP405, eGFP-Rab5 and granzyme B fluorescent pixels from all three channels at the indicated time points of CTL:target cell conjugation. The pixel ratio (pixel

RESULTS

values from figure 18B/pixel values from figure 18C) is shown as a percentage in figure 18D for each time point of conjugation; it indicates the increase of granzyme B accumulation with endo-Syb2 in the early endosomes. Initially the percentage of pixel colocalization is 5% at 5 min and only increases maximally to 10% after 30 min of conjugation. These results imply that endo-Syb2 vesicles do not acquire granzyme B at the early endosomal stage.

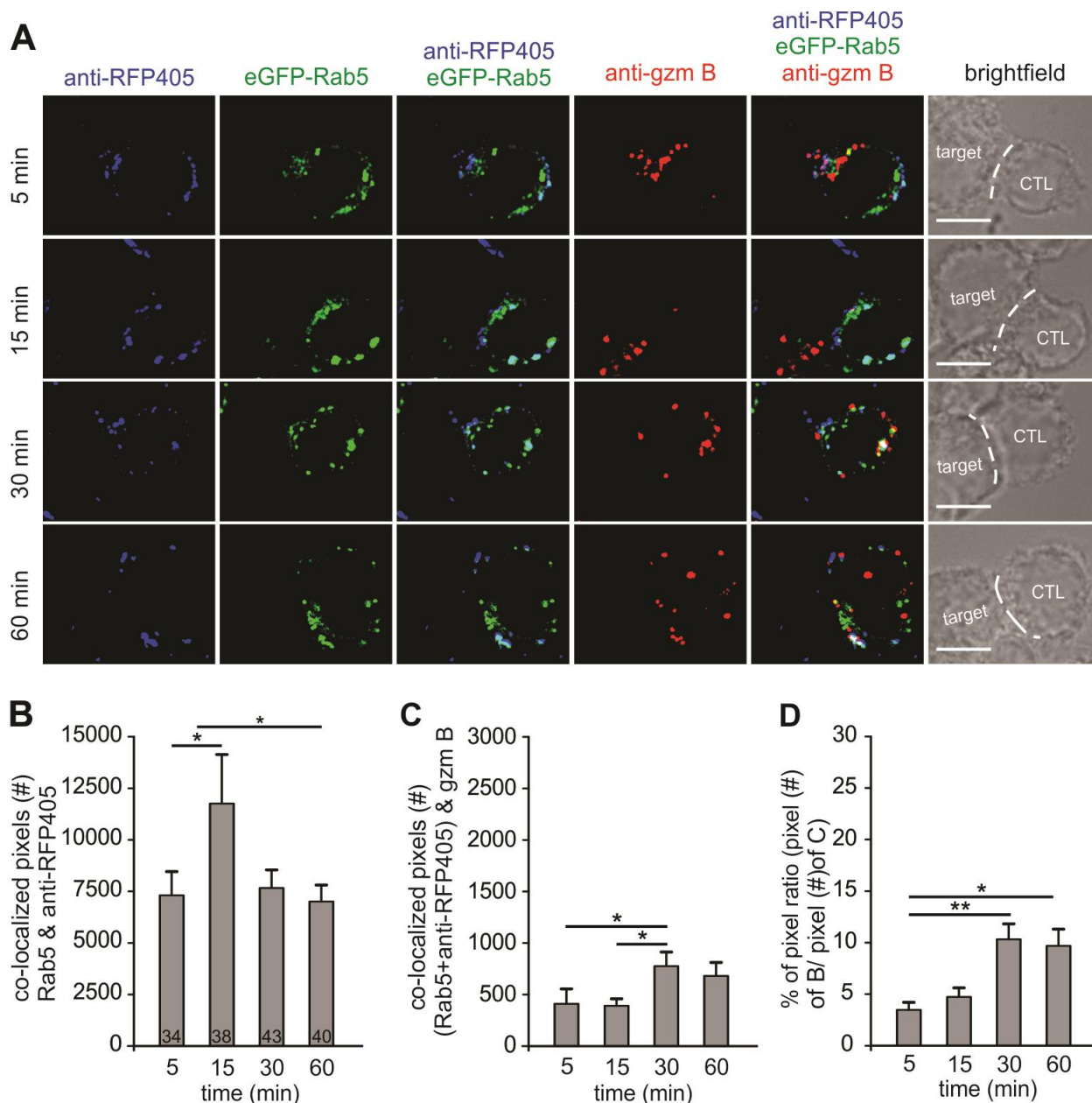


Figure 18. Granzyme B is not acquired by endo-Syb2 vesicles from the Rab5-containing early endosomes.

Sybki CTLs were transfected with eGFP-Rab5 for 12 hrs and then incubated with P815 target cells in the presence of an anti-RFP antibody coupled to Alexa405 (anti-RFP405). Cells were then fixed after the indicated time points. A, SIM images of representative cells for each time point. RFP-405 (blue, 1st column), eGFP-Rab5 (green, 2nd

column), merge of these two channels (cyan, 3rd column), Granzyme B (red, 4th column), merge of all channels (the next to the last column) and the last column with bright field showing CTLs and target cells. B, Shows the quantification of colocalized pixels between eGFP-Rab5 and endo-Syb2 vesicles (anti-RFP405) at the different time points indicated, with maximum colocalization after 15 minutes of CTL: target cell conjugation. C, Quantification of the colocalized pixels between colocalized pixels from (B) and granzyme B. D, Percentage of the ratio of colocalized pixels between all three channels to that of the ones from eGFP-Rab5 and anti-RFP405. Scale bar: 5 μ m. Data are from four independent experiments. Asterisks indicate significance in one-tailed Student's t-test; *P<0.05, **P<0.01, ***P<0.001. Sybki: Synaptobrevin2-mRFP knock-in, gzm B: granzyme B.

III.4.2 Endo-Syb2 vesicles colocalize with granzyme B at the late endosomes 60 min after CTL:target cell conjugation

Because we didn't find much colocalization of (endo-Syb2+eGFP-Rab5) with granzyme B, we thought that the early endosomes are not the site where granzyme B is acquired by endo-Syb2 vesicles. To further address other potential sites at which granzyme B could be acquired, we transfected sybki CTLs with a construct encoding eGFP-Rab7 to label late endosomes. Endo-Syb2 vesicles show maximum colocalization with late endosomes at 60 min after CTL:target cell conjugation (Section III.3.3; Figure 17B).

Figure 19A shows SIM images of sybki CTLs transfected with eGFP-Rab7 (green) and conjugated with P815 target cells in the presence of anti-RFP405 (blue) and fixed after different time points (5, 15, 30 and 60 min). Fixed cells were then stained with anti-granzyme B antibody coupled to Alexa647 (red). The images from the anti-RFP405 channel and that of eGFP-Rab7 are shown as a merged image for each time point in the third column (colocalization is shown as cyan). This merged image at each time point is again merged with the corresponding granzyme B image to produce the merged image of all three channels and is shown in the next to last column (colocalization is seen in white) (Figure 19A). We performed a three-channel colocalization to analyze this set of data as well, to determine whether granzyme B is incorporated into the endo-Syb2 vesicles at the late endosomes and at which time point. First, we calculated the number of colocalized pixels between the anti-RFP405 (endo-Syb2) and eGFP-Rab7 by obtaining a corresponding image showing only the colocalized pixels in the foreground (anti-RFP405+eGFP-Rab7) (Figure 19B) (see Materials and Methods). The resulting image was then merged with the corresponding image containing only granzyme B fluorescent pixels in the foreground in order to finally obtain an image that contained the colocalized anti-RFP405+eGFP-Rab7 pixels having also granzyme B (anti-RFP405+eGFP-Rab7+granzyme B) (Figure 19C). The graphs (Figure 19B-D) show the quantification of the corresponding pixel

RESULTS

number at each of the aforementioned steps at the different time points of CTL:target cell conjugation. Colocalization between eGFP-Rab7 and anti-RFP405 using the above described common pixel analysis method (Figure 19B), showed an increase in colocalization after 30 min of CTL:target cell conjugation to reach a maximum after 60 min conjugation. These results further confirm the results obtained by analysis using Manders' coefficient for colocalization (Section III.3.3; Figure 17B). Figure 19C shows the number of colocalized anti-RFP405+eGFP-Rab7+granzyme B pixels at the indicated time points of CTL:target cell conjugation. The number of colocalizing pixels starts to increase after 30 min of endocytosis to reach a maximum after 60 min, which can be related to the time points where the highest colocalization was seen between anti-RFP405 and eGFP-Rab7. This correlation indicates that granzyme B is incorporated into the endo-Syb2 vesicles at the late endosomes. The pixel ratio (pixel values from figure 19B/ pixel values from figure 19C) is shown as a percentage in figure 19D for each time point of conjugation; it indicates the increase of granzyme B accumulation with endo-Syb2 colocalized with late endosomes. This graph shows that about 30% of granzyme B pixels colocalize with endo-Syb2 in the late endosomes. These results imply that endo-Syb2 vesicles would acquire granzyme B at the late endosomal stage.

RESULTS

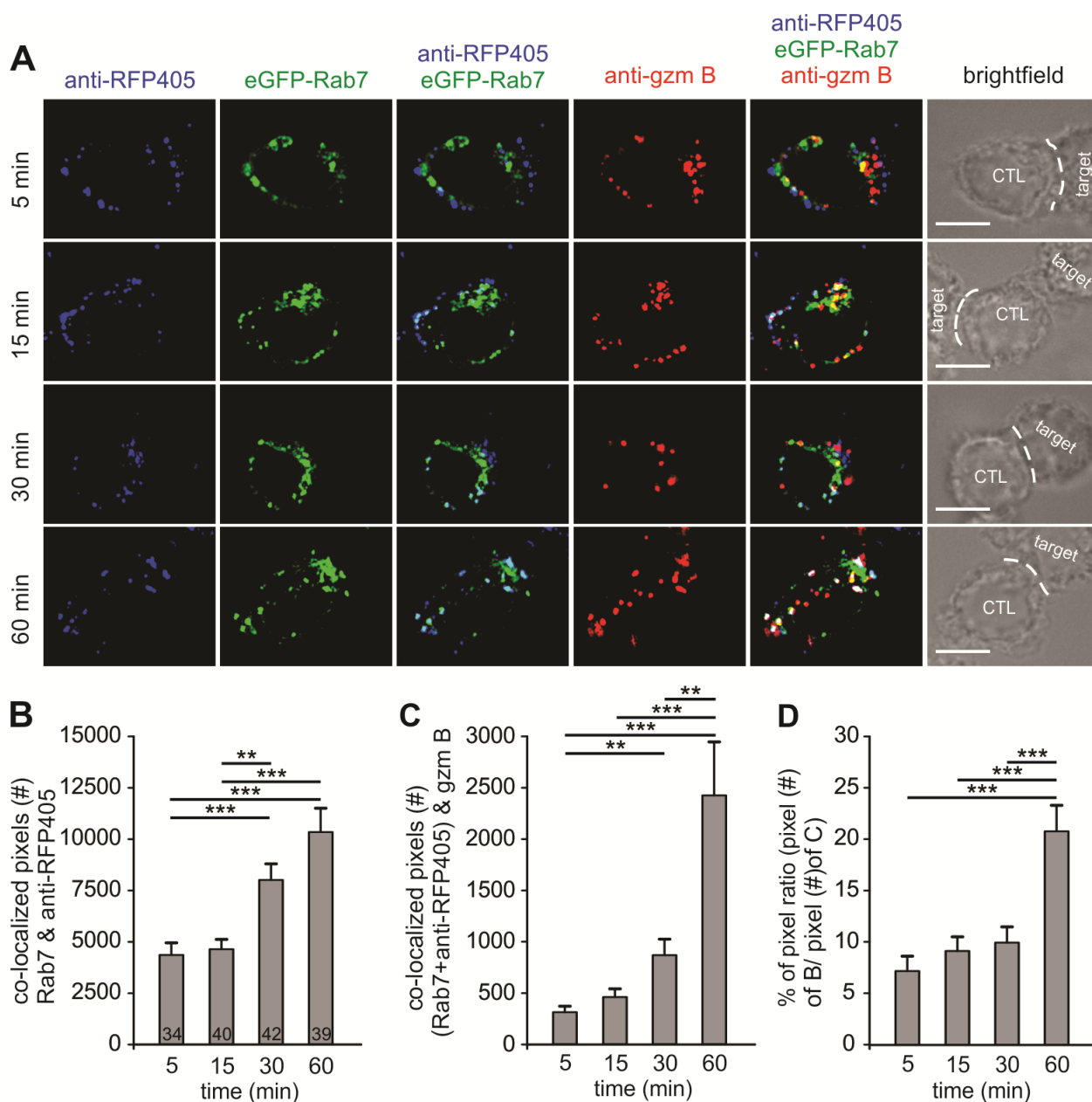


Figure 19. Granzyme B is acquired by endo-Syb2 vesicles from the Rab7-containing late endosomes.

Sybki CTLs were transfected with eGFP-Rab7 for 12 hrs and then incubated with P815 target cells in the presence of anti-RFP antibody coupled to Alexa405 (anti-RFP405). Cells were then fixed after the indicated time points. **A**, SIM images of representative cells for each time point. Anti-RFP405 (blue, 1st column), eGFP-Rab7 (green, 2nd column), merge of these two channels (cyan, 3rd column), Granzyme B (red, 4th column), merge of all channels (the next to the last column) and the last column with bright field showing CTLs and target cells. **B**, Shows the quantification of colocalized pixels between eGFP-Rab7 and endo-Syb2 vesicles (anti-RFP405) at the different time points indicated, with maximum colocalization after 60 minutes of CTL: target cell conjugation. **C**, Quantification of the colocalized pixels between colocalized pixels from (B) and granzyme B. **D**, Percentage of the ratio of colocalized pixels between all three channels to that of the ones from eGFP-Rab7 and anti-RFP405. Data are from four independent experiments. Scale bar: 5 μ m. Asterisks indicate significance in one-tailed Student's t-test; * P <0.05, ** P <0.01, *** P <0.001. Sybki: Synaptobrevin2-mRFP knock-in, gzm B: granzyme B.

IV. Discussion

The data presented here show that synaptobrevin2 (Syb2), the v-SNARE of cytotoxic granules (CGs) of mouse Cytotoxic T lymphocytes (CTLs), interacts with SNAP-23 to drive exocytosis of the CTL's CGs, thus identifying SNAP-23 as a t-SNARE required for CG fusion in these cells. After fusing with the plasma membrane, CG membrane protein Syb2 is endocytosed in a vesicle that is acidified in one to two minutes as shown by live imaging. These endocytosed vesicles colocalize with the $\alpha 3$ subunit of the V-ATPase's V0 domain as early as 5 minutes after CTL:target cell conjugation. Syb2 is endocytosed along with ZAP70 and SNAP-23 into a vesicle which reaches the early endosomes within 15 min of CTL:target cell conjugation. From the early endosomes, Syb2, moves to the late endosomes without entering the recycling endosomes. Syb2 exhibits maximum colocalization with the late endosomes within 60 min of target cell addition. Endo-Syb2 vesicles acquire granzyme B from late endosomes, marking the emergence of fully mature CGs that are ready to undergo a second round of fusion to kill target cells.

IV.1 SNAP-23 is a t-SNARE required for CG fusion in mouse CTLs

Our group has previously shown that Syb2 is the v-SNARE (Matti et al., 2013) and that STX11 is one of the t-SNAREs (Halimani et al., 2014) required for fusion of CGs in mouse and human CTLs, respectively. Fusion of the CGs with the plasma membrane requires a v-SNARE at the CG membrane and two or three t-SNAREs at the plasma membrane (depending on the number of α -helices they contribute to the forming SNARE complex). We then determined what is/are the other t-SNARE/s involved in CG fusion in mouse CTLs. A likely candidate t-SNARE for secretion of CGs in CTLs was SNAP-23, since it widely expressed at the plasma membrane of various types of immune cells and responsible for the secretion of different types of vesicles from mast cells (Paumet et al., 2000), eosinophils ((Logan et al., 2002), and platelets (Chen et al., 2000; Feng et al., 2002). SNAP-23 and syntaxin-4 both t-SNAREs expressed in CTLs are found to polarize to the IS upon conjugation of the CTL with an antigen presenting cell (APC) (Das et al., 2004).

WT CTLs were stimulated with anti-CD3/CD28-coated beads to induce exocytosis. In order to identify whether SNAP-23 is a t-SNARE required for CG fusion in mouse CTLs, an immunoprecipitation (IP) using anti-Syb2 antibody was performed from WT CTL lysates harvested at different time points after stimulation. A band corresponding to SNAP-23 immunoprecipitated with Syb2 after 30 and 60 min of CTL stimulation (Figure 10A).

The discrepancy in the time required for detecting co-immunoprecipitated SNAP-23 with Syb2 (detected after 30 min of bead stimulation) and that of Syb2 endocytosis into the different endocytic compartment (Syb2 already fuses with early endosomes after 15 min of CTL:target cell conjugation) is probably due the stimulation of CTLs in the different experiments. For the IP experiment, CTLs were stimulated with anti-CD3/CD28-coated beads to induce a high number of CTLs in order to produce enough protein to be used simultaneously for the different IP conditions. Target cells (the stimulus used for other experiments) could not be used to stimulate CTLs in this experiment because their presence would have contaminated the lysate used for the IPs. Furthermore, we used sybki CTLs stimulated with anti-CD3/CD28-coated beads, similarly to WT CTLs for the IP experiment, in the presence of anti-RFP647 to detect the amount of fused and endo-Syb2 with such a stimulation. The results of this experiment showed that anti-RFP647 detected fused Syb2 at the plasma membrane mostly after 30 min of bead-stimulation, consistent with the time window shown with the IP experiment for the formation of the SNARE complex (data not shown).

In another independent immunoprecipitation experiment using anti-Syb2 antibody, in which the gel was allowed to run for a longer time to allow for a better separation of the bands (Figure 10B), we detected two bands of SNAP-23 in the input and supernatant lanes corresponding to the phosphorylated and un-phosphorylated forms of SNAP-23. Interestingly, only the un-phosphorylated form of SNAP-23 was co-immunoprecipitated with Syb2 after 30 min of CTL stimulation (Figure 10C). In B cells, SNAP-23 phosphorylation by the specific SNAK kinase, enhances the assembly of SNAP-23 into t-SNARE complexes. Surprisingly, the phosphorylated SNAP-23 resided exclusively in the cytosol and only the un-phosphorylated form of SNAP-23 was incorporated into the t-SNARE complexes. The authors concluded that the increase of SNARE complex assembly upon overexpression of SNAK in Hela cells was due to an increase of the overall expression and stability of de novo synthesized SNAP-23, which alters the kinetics of SNAP-23 binding to the complex (Cabaniols et al., 1999). Thus the results from B cells are

consistent with our conclusion that un-phosphorylated SNAP-23 engages in the SNARE complex.

Finally, we tested whether STX11 co-immunoprecipitated with Syb2 as it has been shown to be the t-SNARE required for CG fusion in human CTLs. However, no band corresponding to STX11 could be detected in the IP fraction with Syb2 (Figure 10A). It may be that our experimental conditions hinder Syb2-STX11 interaction or that there is a different combination of t-SNAREs in mouse CTLs.

IV.2 H⁺ V-ATPase is endocytosed along with Syb2, the v-SNARE of CGs, into early endosomes

CGs are acidic with a pH value near 5.5 (Burkhardt et al., 1990) where the acidic pH is maintained by the action of the vesicular H⁺-adenosine triphosphatase (H⁺ V-ATPase). The V-ATPase is a complex protein composed of two multi-subunit domains V0 and V1. V0 is the transmembrane domain responsible for translocation of protons from the cytosol to the vesicle lumen and V1 is the cytosolic domain with the ATPase activity (Forgac, 2007).

In an attempt to study the V-ATPase function and its role in synaptic vesicle exocytosis, Poëa-Guyon et al. abolished the compartmental proton gradient by using inhibitors or acute photo-inactivation of V0 or V1 domains' subunits (Poea-Guyon et al., 2013). Inhibitors used included bafilomycin, a known pharmacological specific inhibitor of the V-ATPase, and an alkalizing agent, ammonium chloride, which reduces the acidity of different vesicular compartments (Wang and Hiesinger, 2013). The authors found that ammonium chloride but not bafilomycin blocked exocytosis of synaptic vesicles. Treatment with bafilomycin was able to override the inhibitory effect of ammonium chloride on exocytosis. The increased association of the V0-V1 domains upon ammonium chloride treatment and increased free V0 domain with bafilomycin treatment led the authors to conclude that the free V0 domain is required for the vesicles to be exocytosed. In another study, neutrophils pretreated with bafilomycin also showed an increase in surface expression of a2 subunit of the V0 domain that is mainly localized to the primary granules (Gilman-Sachs et al., 2015). The 'a' subunit of V0 domain has four isoforms: a1, a2, a3, and a4 that are expressed differentially in different tissues and on different vesicles at the cellular level. The a3 isoform is expressed in several tissues such as liver, heart, kidney, brain, and spleen and

in osteoclasts where mutations in the gene expressing this isoform lead to osteopetrosis (Matsumoto et al., 2014). Acute photo-inactivation of $\alpha 1$ subunit of the V0 domain decreased secretion from neuronal and chromaffin cells but not when the $\alpha 1$ subunit of the V1 domain was inactivated (Poea-Guyon et al., 2013). The experiments above show that vesicle fusion with the plasma membrane requires the dissociation of the V0-V1 domain of the V-ATPase. The V0 domain of the V-ATPase also plays a role in vacuolar fusion in yeast, as mutations in V0 showed more dramatic effects than those of V1 on vacuolar fusion, which indicates that V0 has roles other than vacuolar acidification (Bayer et al., 2003). Taken together these data show that V0-V1 dissociation is required for vesicle fusion, and that V0 might be involved in vesicle fusion.

The V0 domain of the V-ATPase has been shown to interact with Syb2 on synaptic vesicles even when incorporated into the SNARE complex (Morel et al., 2003). Using an antibody against the $\alpha 3$ subunit of the V0 domain, we saw colocalization between endo-Syb2 vesicles and the $\alpha 3$ subunit (Figure 13A) quantified by the Manders' coefficient for colocalization. Values for Manders' coefficient were 0.65 ± 0.07 after only 5 min and stayed high even after 15 min of CTL:target conjugation (0.73 ± 0.06 after 10 min and 0.78 ± 0.07 after 15 min) (Figure 13B). This data shows that $\alpha 3$ colocalized with endo-Syb2 at 5 and 10 min time points, i.e. before endo-Syb2 fuses with early endosomes (see below, section IV.3). In a following experiment, we showed that endo-Syb2 vesicles are acidified within one to two min of Syb2-mRFP exposure at the plasma membrane, using live imaging with anti-RFP antibodies coupled to Alexa405 and to pH-sensitive pHrodo green dyes. This delay may correspond to the time required for Syb2 to be incorporated into a vesicle along with the V0 subunit, where the V1 would then associate with the membrane-bound V0 domain to establish once again a functional proton pump. In live imaging we observed a gradual increase in the intensity of pHrodo-green signal, indicating a continuous increase of acidity of the endocytosed vesicle (Figure 14). Thus we speculate that the nascent endo-Syb2 vesicles are acidified immediately by the V-ATPase, even before fusion with early endosomes.

IV.2.1 SNAP-23 and ZAP70 are endocytosed along with endo-Syb2 into early endosomes

It has been shown using immunostaining that Syb2 endocytosis is clathrin-mediated and that CALM is a specific adaptor protein for Syb2 endocytosis (Chang et al., 2016). We did an

immunoprecipitation experiment with stimulated CTL lysates using anti-Syb2 antibody to determine whether CALM co-immunoprecipitates with Syb2 (Figure 10B). Although Syb2 can be immunoprecipitated, no band corresponding to CALM could be detected to be co-immunoprecipitated along with Syb2. This might indicate that the interaction between CALM and Syb2 is probably transient or that the conditions tested here for IP are not optimal to favor an interaction between Syb2 and CALM. Using GST fusion of the CALM-ANTH domain and His₆-Syb2 (N-terminus), Koo et al could show that CALM is an adaptor protein for Syb2 (Koo et al., 2011a). Further optimization of our conditions might favor Syb2-CALM interaction and thus allow for co-immunoprecipitation of CALM along with Syb2.

We have shown above that Syb2 is endocytosed in a vesicle that contains at least the V0 domain of the H⁺ V-ATPase within one to two minutes of Syb2 exposure at the plasma membrane, i.e. CG fusion. We wanted to test for other proteins that are endocytosed in the same vesicle as Syb2. For this reason, we used antibodies against SNAP-23 (Figure 11), which we have shown above is a t-SNARE required for CG fusion, and ZAP70 (Figure 12), a signaling protein that acts upstream in the signaling pathway after CTL contact with a target cell, to test whether these proteins were endocytosed with Syb2.

It has been shown that both v- and t-SNAREs can reside on the same vesicle and they can interact with each other on the same membrane. STX11 and SNAP-23 were found to colocalize at the late endosomes and TGN where they probably form a complex at a steady state, although SNAP-23 was mainly localized to the plasma membrane (Valdez et al., 1999). Syntaxin 1 and SNAP-25, the t-SNAREs required for synaptic vesicle (SV) fusion, were found on recycling SVs and account for about 6% of the protein content of purified SVs in comparison to 8.7% for Syb2 (Walch-Solimena et al., 1995). These results are in contradiction with other data indicating that synaptic vesicles maintain their composition during successive rounds of exo- and endocytosis (Valtorta et al., 1988). Our immunostaining data show that SNAP-23 colocalized with vesicles containing Syb2 as early as 5 min and till at least 15 min (probably in early endosomes) of CTL:target cell conjugation, with a Manders' coefficient staying above 0.7 (Figure 11). These data indicate that t-SNAREs of CTLs can be recycled with CG components, including the v-SNARE Syb2. Following CG fusion, t- and v-SNAREs on the plasma membrane might be endocytosed into the same vesicle until they fuse with early/sorting endosomes. Since we show that Syb2 traffics from early to late endosomes, it might be that at later time points (30 or 60

min) Syb2 does not colocalize with SNAP-23. This is expected since the t-SNAREs are likely sorted via recycling endosomes and then delivered to the plasma membrane for subsequent rounds of fusion. Endocytosis of t-SNAREs along with CG components in the same vesicle might also aid in the fusion of the nascent endocytosed vesicles with early endosomes.

A few peptide-MHC complexes are enough to activate T cells, although a similar number of TCR complexes on the surface of T cells will not be sufficient to activate them. It was shown that this small number of peptide-MHC complexes could activate T cells because each complex is able to engage serially with up to 200 TCR molecules (Valitutti et al., 1995). This explains the requirement for the efficient endocytosis of the activated TCR complexes. Constitutively endocytosed TCR-CD3 complexes are recycled back to the plasma membrane (Minami et al., 1987), however TCR-antigen ligation induces the disassembly of the CD3 ζ -chain from the TCR-CD3 complex (Liu et al., 2000), which is down regulated (Dietrich et al., 1994) whereas the ζ -chain is targeted for degradation (Dumont et al., 2002). The ζ -chain of the TCR-CD3 complex follows a different metabolic pathway than the rest of the TCR-CD3 complex with different turnover times; the half-life for the ζ -chain is 4 hrs (Ono et al., 1995) and 20 hrs for the rest of the complex (Alcover and Alarcon, 2000; Dumont et al., 2002). ZAP70, a tyrosine kinase that binds to and phosphorylates residues of the CD3 ζ -chain is involved in the regulation of activated TCR-CD3 complexes and in down modulation and degradation of the ζ -chain (Dumont et al., 2002; Luton et al., 1994). This means that ZAP70 can be endocytosed along with ζ -chain, independently of the TCR-CD3 complex thereby supporting our data in which ZAP70 is endocytosed in the same nascent vesicle as endo-Syb2. Quantification of colocalization between ZAP70 and endo-Syb2 showed that both proteins were internalized in the same vesicle at least until after 15 min after target cell addition (Figure 12) (until they reach the early endosomes, see below).

IV.3 Syb2 reaches the early endosomes within 15 min after addition of target cells

Endocytosis has been widely studied for many different proteins utilizing different pathways of endocytosis. Generally, endocytosis occurs to regenerate membrane proteins or to endocytose receptor-bound ligands to increase or attenuate the signaling response depending on the

endocytosed receptor. The general pathway taken by proteins destined to be recycled e.g. the transferrin receptor (Watts, 1985) is through vesicles that fuse with the early endosomes and then from the early endosomes to the plasma membrane through recycling endosomes. Other proteins destined for degradation such as epidermal growth factor receptor (EGF-R) (Beguinot et al., 1984) are endocytosed through vesicles that fuse with the early endosomes and then are transported to the degradative lysosomes through late endosomes.

We have shown that different proteins are endocytosed along with Syb2 in the same vesicle, including other components of mature CGs (V-ATPase). In order to determine the pathway taken by endo-Syb2 through the different endocytic compartments, we transfected sybki CTLs with different markers of early, recycling and late endosomes, to label each of these endosomes, and examined their colocalization with endo-Syb2 (labeled with anti-RFP647). Anti-RFP647 was added to the medium containing CTL:target cell conjugates and cells were fixed at different times after target cell addition. We found that Syb2 arrives at the early endosomes 15 min after target cell addition. We observed maximum colocalization with eGFP-Rab5, our marker for early endosomes at this time. Colocalization between endo-Syb2 and eGFP-Rab5 was low after 5 min of CTL:target cell conjugation but reached a maximum after 15 min of target cell addition, and then it decreased at the 30 and 60 min time points (Figure 15). The early endosomes are known as sorting endosomes because they receive incoming cargo from the plasma membrane, which are then sorted to their destinations (Maxfield and McGraw, 2004). We show that it requires about 15 min of CTL:target cell contact for endo-Syb2 to reach the early endosomes.

Syb2 along with its interacting t-SNAREs (SNAP-25 and syntaxin) undergo both slow (10-60 seconds) and rapid (1-3 seconds) endocytosis at the calyx of held nerve terminus (Xu et al., 2013). This neuronal synapse contains hundreds of synaptic vesicles that need to be replenished rapidly to maintain the high rate of synaptic vesicle fusion found at this synapse. The much slower endocytosis we have observed likely reflects the small numbers and slow rates of release of CGs in CTLs.

IV.4 Endo-Syb2 traffics through early endosomes and late endosomes but not recycling endosomes

Cargo trafficked from the plasma membrane to the early endosomes is either recycled back to the plasma membrane via recycling endosomes (Rab11 positive), or trafficked further in the endosomal pathway to reach the late endosomes (Rab7 positive) (Rink et al., 2005). We transfected sybki CTLs with markers for recycling and late endosomes, then quantified the colocalization between endo-Syb2 (anti-RFP647) and either eGFP-Rab11 or eGFP-Rab7 using Manders' coefficient for colocalization. Our results demonstrated weak colocalization between endo-Syb2 and eGFP-Rab11 at all time points of CTL:target cell conjugation (5, 15, 30 and 60 min) (Figure 16). However, endo-Syb2 was colocalized with eGFP-Rab7 after 30 min, and colocalization was maximal at 60 min of CTL:target cell conjugation (Figure 17).

These data show that Syb2 traffics from early endosomes to late endosomes, but not to recycling endosomes. Endocytosis of most proteins studied in immune cells follows the recycling endosomal pathway. Peptide-loaded MHC-II receptors (pMHC-II) fuse with early endosomes upon internalization where they are probably reloaded with new peptides and then recycled to present their new cargo at the plasma membrane (Walseng et al., 2008). Constitutively endocytosed CD3-TCR complexes are also transported mainly through the recycling endosomes (Minami et al., 1987). Lamp-1 an important constituent of CGs, that also constitutes about 50% of the lysosomal membrane proteins, recycles in activated CTLs in an exo-endocytic cycle starting at the IS (Liu et al., 2009). Proteins important for the fusion of CG, like the priming factor munc13-4 have also been shown to be recycled after CG fusion at the IS to aid in the serial killing of the CTL or NK cells (Capuano et al., 2012). Therefore, our findings indicate a pathway that is not widely used by recycling proteins of lymphocytes. Recycling endosomes fuse with the plasma membrane to deliver plasma membrane resident proteins or proteins that need to function at the plasma membrane (Marshall et al., 2015). Since Syb2 is a CG membrane resident protein it should follow a different path. CGs, also known as secretory lysosomes might mature from late endosomes or multivesicular bodies (MVBs), as do conventional lysosomes. Electron microscope images have in fact demonstrated MVBs and late endosomes to have varying electron dense core, representing different maturation stages with CGs having the most dense core.

Although, non-CG resident proteins are endocytosed along with Syb2 in the same vesicle at least till early/sorting endosomes, we tested another CG membrane protein, the V-ATPase (probably only V0 domain), and found it to be endocytosed along with Syb2 in the same vesicle at least until it reaches the early endosomes. It would be interesting to see if the colocalization between endo-Syb2 and non-resident CG proteins decreases within 60 minutes of target cell addition where most of the endo-Syb2 is in the late endosomes (section III.3.3).

IV.5 Endo-Syb2 vesicles acquire granzyme B at the late endosomes to become a fully mature vesicle

Fully mature CGs contain Syb2 as a v-SNARE (Matti et al., 2013) and contain the cytotoxic proteins perforin and granzymes among other proteins that give the CGs their characteristic dense core (Matti et al., 2013). Our data showed that endo-Syb2 vesicles fuse with the early endosomes after 15 min of target cell addition and with late endosomes after 30-60 min showing maximum colocalization within 60 min. We followed the maturation of endo-Syb2 after endocytosis and investigated when and where granzyme B is incorporated. Our data show that Syb2 proceeds from the early endosomes to late endosomes and not through recycling endosomes, we tested whether endo-Syb2 would colocalize with granzyme B either in early or late endosomes. Data analysis was done by calculating the colocalization between three proteins namely endo-Syb2, granzyme B and Rab5/7. The number of endo-Syb2 pixels that colocalized with Rab5 or Rab7 fluorescent pixels and also contained granzyme B fluorescent pixels was calculated for various time points (Figures 17 and 18, respectively). We found that Syb2 colocalizes with granzyme B at the late endosomal stage and not at the early endosomal stage, where it shows maximum colocalization with granzyme B after 60 min of target cell addition, the same time that is required for Syb2 to colocalize maximally with late endosomes.

Newly synthesized granzyme B is transported from the trans-Golgi network (TGN) to the late endosomes via mannose-6-phosphate receptor (M6PR) (Griffiths and Isaaz, 1993). CGs discharge their entire content of granzyme B upon fusion, indicating that these vesicles need to be refilled with granzyme B to be competent for killing (Chang et al., 2016). From the current experiments, we see that Syb2 associates again with granzyme B at the late endosomes, which is likely the final maturation. It has been suggested that granzyme B-containing vesicles fuse with

Rab11/Rab27/Munc13-4 positive vesicles before they fuse with the plasma membrane (Menager et al., 2007). In Our experiments, Rab27 is present on newly synthesized CGs even in unconjugated CTLs, and is present on CGs that have not polarized to the IS in conjugated CTLs (data not shown). For NK cells, Rab11-positive recycling endosomes (REs) did not associate with CGs at the NK cell synapse and the inactivation of REs did not affect the release of preformed mature NK cell granules, but it is suggested that REs might be involved in earlier maturation steps of CG formation (Reefman et al., 2010). The authors of this paper also showed that REs were functionally required for the surface delivery and release of cytokines (TNF α and INF γ) (Reefman et al., 2010).

Proteins destined for degradation are transported from the late endosomes to lysosomes (Huotari and Helenius, 2011). Huotari et al referred to the lysosomal compartment where degradation of endocytosed proteins takes place as the endolysosome, because these organelles are the result of fusion between late endosomes and lysosomes. However, several proteins including M6PR and some SNARE proteins do not necessarily follow this pathway and might escape degradation in the endolysosome, probably by fusing with the lysosomal compartment that has the dense core with all proteins necessary for maturation of CGs or by escaping lysosomal degradation via vesicular trafficking (Huotari and Helenius, 2011). For example, Rab9 is involved in the recycling of M6PRs from the late endosomes to the TGN through interacting with its effector TIP47 (Carroll et al., 2001). Consistent with the maturation of endo-Syb2 vesicles by acquiring granzyme B at the late endosomes within 60 min of target cell addition, these vesicles were also shown to polarize to a second IS formed by the CTL, with the same time range, indicating that these vesicles are again ready to fuse and kill their target (Chang et al., 2016). We show that Syb2 doesn't undergo the classical trafficking from late endosomes to endolysosomes to be degraded, but is rather further trafficked from the late endosomes either directly into a fully mature CG or might acquire further lysosomal proteins from the lysosomal dense core to be capable of another round of fusion.

IV.6 Model for Syb2 endocytosis

Activation of CTLs for killing of target cells is initiated by the recognition of foreign peptides presented on MHC-I molecule on the surface of the target cell (pMHC-I) by the T cell receptor (TCR). TCR-pMHC-I interaction leads to the activation of the TCR-CD3 complex and recruitment of different kinases that phosphorylate residues important for activating other proteins involved in signaling pathway activation. One such kinase is the protein tyrosine kinase ZAP70. It binds to the ζ -chain of the CD3 receptor, initiating the signaling cascade, which is followed by recruitment of the cytotoxic granules (CGs) to the newly formed IS. Fully mature CGs containing cytotoxic proteins are acidic with pH around 4.5-5.5 maintained by the function of the V-ATPase. Polarized CGs ready for fusion have their V1 domain dissociated from the V-ATPase complex, leaving the V0 domain integrated in the CG membrane where it might interact with the forming SNARE complex upon CG fusion. After CG fusion, the CG membrane proteins diffuse in the plasma membrane. NSF disassembles the SNARE complex into the single proteins, which appear to remain in close proximity at the plasma membrane to be endocytosed together in one vesicle as we have seen for Syb2 and SNAP-23. Also the ζ -chain of the TCR-CD3 complex, along with the bound ZAP70, dissociates from the complex and is probably endocytosed along with Syb2 in the same vesicle. From previous studies it was shown that V0 of the V-ATPase is free from V1 upon synaptic vesicle fusion. We suggest that this is the case also for CGs and the V0 domain of the V-ATPase is endocytosed along with Syb2 in the same vesicle. After one to two minutes of Syb2 exposure at the plasma membrane these components are endocytosed into one vesicle as the V1 then associates with the V0 domain to form a functional V-ATPase that starts to gradually increase the acidity of the endocytic vesicle. Within 15 min this endocytic vesicle fuses with the early endosomes where some of its components might then diffuse with the early endosomal membrane, taking a different endocytic pathway than Syb2. At least one other CG membrane protein, the V-ATPase, remains in the same endocytic vesicle as Syb2. After 30 to 60 min endo-Syb2 vesicles arrive at the late endosomes where they acquire granzyme B. The CGs then acquire LAMP proteins and other proteins required for killing activity, most likely by fusing with lysosomes (CGs are also known as secretory lysosomes), or with the late endosomes, where they then bud out forming mature CGs. These mature CGs are then capable of another round of fusion with the plasma membrane and capable of killing another target cell (Figure 20).

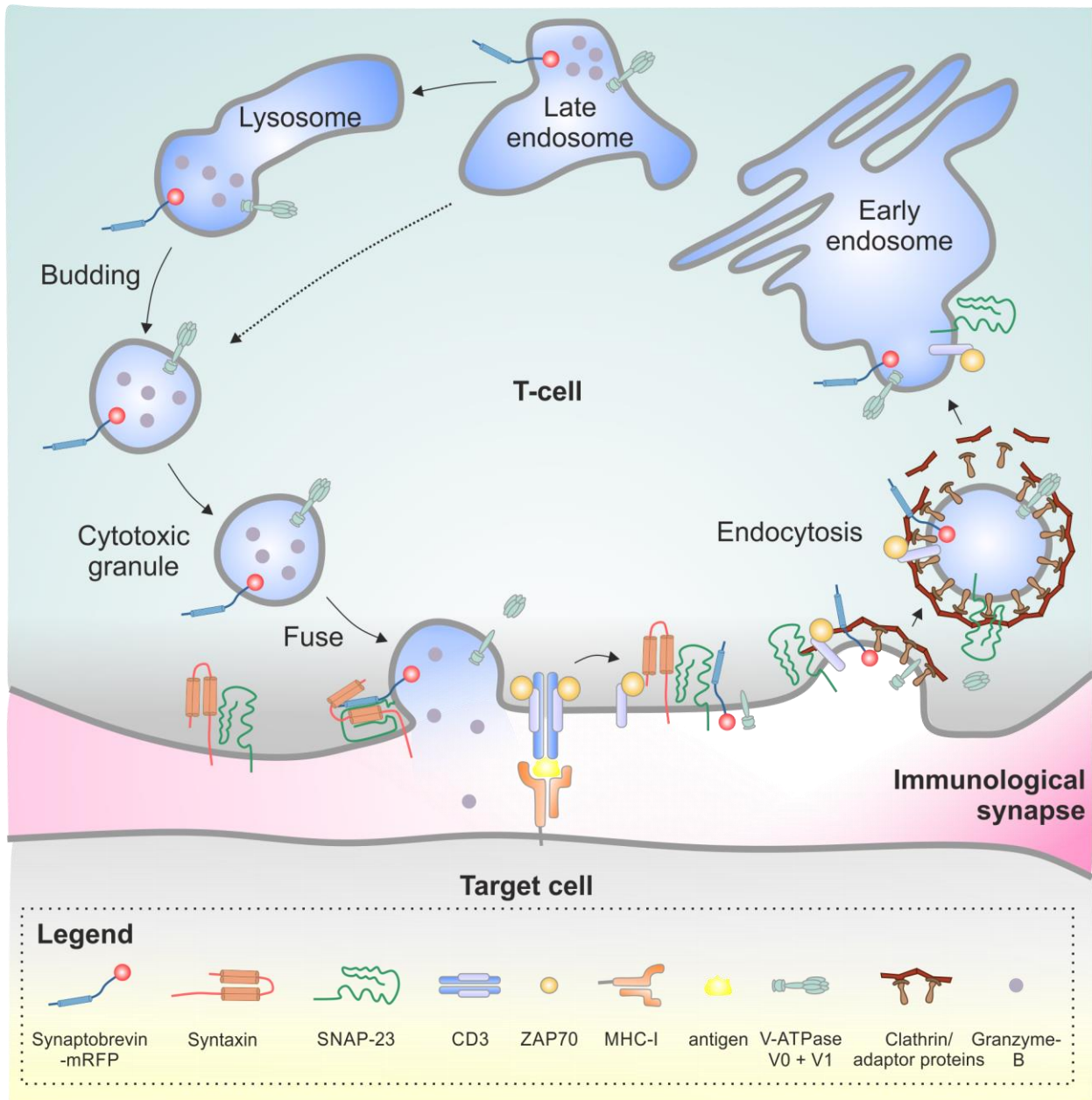


Figure 20. Model for Syb2 endocytosis through the endosomal pathway.

CG fusion is effected by the formation of the SNARE complex comprised of the v-SNARE, Syb2 and the t-SNAREs, SNAP-23 and syntaxin. CG exocytosis leads to the diffusion of Syb2 with the plasma membrane. Syb2 is then endocytosed with the V0 domain of the V-ATPase along with other proteins in the same vesicle, including ZAP70 and SNAP-23. Directly after endocytosis the V1 domain associates with V0 domain of the V-ATPase to form a functional proton pump that acidifies the endocytic vesicle. The latter then arrives 15 min later at the early endosomes. From the early endosomes, Syb2 is further trafficked along with the V-ATPase to reach late endosomes in 30 to 60 min after endocytosis. At the late endosomes, Syb2 associates with granzyme B into one vesicle and might acquire lysosomal proteins either at late endosomes or by further fusing with lysosomes. This is considered to be the final maturation step of the CG that is then capable of another round of fusion.

V. Outlook

We have elucidated the pathway for maturation of a CG membrane component, Syb2, until it is incorporated into a mature CG ready for a second round of fusion. Replenishment of mature CGs is critical for the serial killing function of CTLs, thus any disturbance in CG maturation from its endocytosed components would lead to serious malfunctioning of the CTLs. Identifying the mechanism of Syb2 (a main component of CGs) endocytosis, gives us more insight into the deregulation that might occur along the way of their maturation.

To better understand Syb2 interactions during CG fusion, further experiments are required to identify other interacting t-SNAREs, whether it's STX11 or other syntaxin that is required for CG fusion in mouse CTLs. Also it would be interesting to follow up whether SNAP-23 is recycled to the plasma membrane directly from early endosomes via recycling endosomes, which would indicate that it might be endocytosed with Syb2 in the same vesicle because it is required for the fusion of this vesicle with early endosomes; after fusion with early endosomes, SNAP-23 would be incorporated into recycling endosomes to be recycled again to the plasma membrane. A very interesting experiment would be to check how and when do mature endo-Syb2 vesicles fuse with the plasma membrane. This experiment might be done using TIRF microscopy to check for the fusion of endo-Syb2 vesicles, or using live cell imaging with target cells and using for example, a pH-dependent fluorophore coupled to anti-RFP antibody that can identify, initially endocytosed vesicles, and then mature endo-Syb2 vesicles that undergo fusion and lose their fluorescence due to change in their pH upon fusion.

VI. Summary

Cytotoxic T lymphocytes (CTLs) kill target cells by releasing the content of their cytotoxic granules (CGs). CTLs are known as serial killers due to their ability to kill multiple target cells. Serial killing requires that CTLs replenish their CGs to be available for a new round of killing. Newly produced CGs could be formed by de novo synthesis or by recycling of their components to ensure fast replenishment of mature CGs. To better understand the mechanism of recycling of CG components, we studied the endocytosis pathway of synaptobrevin2 (Syb2), the v-SNARE present on CGs of murine CTLs. In order to specifically follow up Syb2 we used CTLs from Syb2-mRFP knock-in (sybki) mice and utilized anti-RFP antibody to track Syb2-mRFP (Shortly, Syb2) after CG fusion and Syb2 exposure at the plasma membrane.

We started our study from the point of CG fusion with the plasma membrane. Using co-immunoprecipitation, we found that Syb2 interacts with synaptosomal-associated protein-23 (SNAP-23) during SNARE complex formation to initiate fusion of CGs with the plasma membrane, indicating that SNAP-23 is a t-SNARE required for CG fusion. After exposure of Syb2 at the plasma membrane upon CG fusion, the mRFP fused to Syb2 faces to the extracellular medium. Utilizing fluorescently-labeled anti-RFP antibody allows for tracking the endocytic pathway followed by Syb2. We identified some proteins that were endocytosed with Syb2 in the same vesicle, at least until it fuses with early endosomes. Proteins endocytosed with Syb2 include the t-SNARE SNAP-23, zeta-chain associated 70 kDa tyrosine phosphoprotein (ZAP70) and a CG membrane protein the H⁺ V-ATPase. These results were shown using high resolution imaging of fixed cells at different time points. Endocytosis of the V-ATPase with Syb2 in the same vesicle was further verified using live cell imaging, where the acidification of endocytosed Syb2-containing (endo-Syb2) vesicles occurred within one to two minutes (min) of Syb2 exposure at the plasma membrane. Endo-Syb2 arrives at the early endosomes within 15 min of target cell addition; shown by its colocalization with eGFP-Rab5, the early endosomal marker. From the early endosomes, endo-Syb2 further traffics to late endosomes within 60 min of target cell addition but not through recycling endosomes, also shown by its colocalization with eGFP-Rab7 but not with eGFP-Rab11, the markers for late and recycling endosomes, respectively. In order to investigate whether endo-Syb2 vesicles would undergo maturation to

become fully mature CGs, we tested whether they would regain granzyme B, the marker of mature CGs, when and where. We found that endo-Syb2 vesicles colocalized with granzyme B at the late endosomes within 60 min of target cell addition, at the time where endo-Syb2 shows maximum colocalization with late endosomes.

Our study identifies SNAP-23 as a t-SNARE interacting with the v-SNARE Syb2 to initiate CG fusion. It further shows that Syb2 is endocytosed along with other components of CGs where this might be important for the replenishment of fully mature CGs containing granzyme B and ready for another round of target cell killing, a critical aspect of CTL function.

Literature

- Abbas, A. K., Lichtman, A. H., Pillai, S., (2015). Cellular and molecular immunology. 8th Edition, Saunders ELSEVIER.
- Abbe, E. (1873). Beiträge zur Theorie des Mikroskops und der mikroskopischen Wahrnehmung. *Arch Mikrosk Anat* 9, 413-446.
- Ait-Slimane, T., Galmes, R., Trugnan, G., and Maurice, M. (2009). Basolateral internalization of GPI-anchored proteins occurs via a clathrin-independent flotillin-dependent pathway in polarized hepatic cells. *Mol Biol Cell* 20, 3792-3800.
- Alcover, A., and Alarcon, B. (2000). Internalization and intracellular fate of TCR-CD3 complexes. *Crit Rev Immunol* 20, 325-346.
- Anderson, R.G., Brown, M.S., Beisiegel, U., and Goldstein, J.L. (1982). Surface distribution and recycling of the low density lipoprotein receptor as visualized with antireceptor antibodies. *J Cell Biol* 93, 523-531.
- Archer, B.T., 3rd, Ozcelik, T., Jahn, R., Francke, U., and Sudhof, T.C. (1990). Structures and chromosomal localizations of two human genes encoding synaptobrevins 1 and 2. *The Journal of biological chemistry* 265, 17267-17273.
- Baetz, K., Isaaz, S., and Griffiths, G.M. (1995). Loss of cytotoxic T lymphocyte function in Chediak-Higashi syndrome arises from a secretory defect that prevents lytic granule exocytosis. *J Immunol* 154, 6122-6131.
- Balaji, K.N., Schaschke, N., Machleidt, W., Catalfamo, M., and Henkart, P.A. (2002). Surface cathepsin B protects cytotoxic lymphocytes from self-destruction after degranulation. *J Exp Med* 196, 493-503.
- Barbosa, M.D., Nguyen, Q.A., Tchernev, V.T., Ashley, J.A., Detter, J.C., Blaydes, S.M., Brandt, S.J., Chotai, D., Hodgman, C., Solari, R.C., *et al.* (1996). Identification of the homologous beige and Chediak-Higashi syndrome genes. *Nature* 382, 262-265.
- Basu, S.K., Goldstein, J.L., Anderson, R.G., and Brown, M.S. (1981). Monensin interrupts the recycling of low density lipoprotein receptors in human fibroblasts. *Cell* 24, 493-502.
- Baumert, M., Maycox, P.R., Navone, F., De Camilli, P., and Jahn, R. (1989). Synaptobrevin: an integral membrane protein of 18,000 daltons present in small synaptic vesicles of rat brain. *EMBO J* 8, 379-384.
- Bayer, M.J., Reese, C., Buhler, S., Peters, C., and Mayer, A. (2003). Vacuole membrane fusion: V0 functions after trans-SNARE pairing and is coupled to the Ca²⁺-releasing channel. *J Cell Biol* 162, 211-222.
- Beal, A.M., Anikeeva, N., Varma, R., Cameron, T.O., Vasiliver-Shamis, G., Norris, P.J., Dustin, M.L., and Sykulev, Y. (2009). Kinetics of early T cell receptor signaling regulate the pathway of lytic granule delivery to the secretory domain. *Immunity* 31, 632-642.
- Becherer, U., and Rettig, J. (2006). Vesicle pools, docking, priming, and release. *Cell Tissue Res* 326, 393-407.
- Beguinet, L., Lyall, R.M., Willingham, M.C., and Pastan, I. (1984). Down-regulation of the epidermal growth factor receptor in KB cells is due to receptor internalization and subsequent degradation in lysosomes. *Proc Natl Acad Sci U S A* 81, 2384-2388.

- Betts, M.R., Brenchley, J.M., Price, D.A., De Rosa, S.C., Douek, D.C., Roederer, M., and Koup, R.A. (2003). Sensitive and viable identification of antigen-specific CD8⁺ T cells by a flow cytometric assay for degranulation. *J Immunol Methods* 281, 65-78.
- Beyenbach, K.W., and Wieczorek, H. (2006). The V-type H⁺ ATPase: molecular structure and function, physiological roles and regulation. *J Exp Biol* 209, 577-589.
- Blasi, J., Chapman, E.R., Link, E., Binz, T., Yamasaki, S., De Camilli, P., Sudhof, T.C., Niemann, H., and Jahn, R. (1993a). Botulinum neurotoxin A selectively cleaves the synaptic protein SNAP-25. *Nature* 365, 160-163.
- Blasi, J., Chapman, E.R., Yamasaki, S., Binz, T., Niemann, H., and Jahn, R. (1993b). Botulinum neurotoxin C1 blocks neurotransmitter release by means of cleaving HPC-1/syntaxin. *EMBO J* 12, 4821-4828.
- Blott, E.J., and Griffiths, G.M. (2002). Secretory lysosomes. *Nat Rev Mol Cell Biol* 3, 122-131.
- Bolte, S., and Cordelières, F.P. (2006). A guided tour into subcellular colocalization analysis in light microscopy. *J Microsc* 224, 213-232.
- Boucrot, E., Ferreira, A.P., Almeida-Souza, L., Debard, S., Vallis, Y., Howard, G., Bertot, L., Sauvonnet, N., and McMahon, H.T. (2015). Endophilin marks and controls a clathrin-independent endocytic pathway. *Nature* 517, 460-465.
- Brennan, A.J., Chia, J., Browne, K.A., Ciccone, A., Ellis, S., Lopez, J.A., Susanto, O., Verschoor, S., Yagita, H., Whisstock, J.C., *et al.* (2011). Protection from endogenous perforin: glycans and the C terminus regulate exocytic trafficking in cytotoxic lymphocytes. *Immunity* 34, 879-892.
- Brose, N., Rosenmund, C., and Rettig, J. (2000). Regulation of transmitter release by Unc-13 and its homologues. *Curr Opin Neurobiol* 10, 303-311.
- Brumell, J.H., Volchuk, A., Sengelov, H., Borregaard, N., Cieutat, A.M., Bainton, D.F., Grinstein, S., and Klip, A. (1995). Subcellular distribution of docking/fusion proteins in neutrophils, secretory cells with multiple exocytic compartments. *J Immunol* 155, 5750-5759.
- Bucci, C., Parton, R.G., Mather, I.H., Stunnenberg, H., Simons, K., Hoflack, B., and Zerial, M. (1992). The small GTPase rab5 functions as a regulatory factor in the early endocytic pathway. *Cell* 70, 715-728.
- Burkhardt, J.K., Hester, S., Lapham, C.K., and Argon, Y. (1990). The lytic granules of natural killer cells are dual-function organelles combining secretory and pre-lysosomal compartments. *J Cell Biol* 111, 2327-2340.
- Cabaniols, J.P., Ravichandran, V., and Roche, P.A. (1999). Phosphorylation of SNAP-23 by the novel kinase SNAK regulates t-SNARE complex assembly. *Mol Biol Cell* 10, 4033-4041.
- Campi, G., Varma, R., and Dustin, M.L. (2005). Actin and agonist MHC-peptide complex-dependent T cell receptor microclusters as scaffolds for signaling. *J Exp Med* 202, 1031-1036.
- Capuano, C., Paolini, R., Molfetta, R., Frati, L., Santoni, A., and Galandrini, R. (2012). PIP2-dependent regulation of Munc13-4 endocytic recycling: impact on the cytolitic secretory pathway. *Blood* 119, 2252-2262.
- Carroll, K.S., Hanna, J., Simon, I., Krise, J., Barbero, P., and Pfeffer, S.R. (2001). Role of Rab9 GTPase in facilitating receptor recruitment by TIP47. *Science* 292, 1373-1376.
- Chang, H.F., Bzeih, H., Schirra, C., Chitirala, P., Halimani, M., Cordat, E., Krause, E., Rettig, J., and Pattu, V. (2016). Endocytosis of Cytotoxic Granules Is Essential for Multiple Killing of Target Cells by T Lymphocytes. *J Immunol* 197, 2473-2484.
- Chavrier, P., Parton, R.G., Hauri, H.P., Simons, K., and Zerial, M. (1990). Localization of low molecular weight GTP binding proteins to exocytic and endocytic compartments. *Cell* 62, 317-329.

- Chen, D., Guo, J., Miki, T., Tachibana, M., and Gahl, W.A. (1997). Molecular cloning and characterization of rab27a and rab27b, novel human rab proteins shared by melanocytes and platelets. *Biochem Mol Med* 60, 27-37.
- Chen, D., Lemons, P.P., Schraw, T., and Whiteheart, S.W. (2000). Molecular mechanisms of platelet exocytosis: role of SNAP-23 and syntaxin 2 and 4 in lysosome release. *Blood* 96, 1782-1788.
- Choudhuri, K., Wiseman, D., Brown, M.H., Gould, K., and van der Merwe, P.A. (2005). T-cell receptor triggering is critically dependent on the dimensions of its peptide-MHC ligand. *Nature* 436, 578-582.
- Christoforidis, S., McBride, H.M., Burgoyne, R.D., and Zerial, M. (1999). The Rab5 effector EEA1 is a core component of endosome docking. *Nature* 397, 621-625.
- Collins, B.M., McCoy, A.J., Kent, H.M., Evans, P.R., and Owen, D.J. (2002). Molecular architecture and functional model of the endocytic AP2 complex. *Cell* 109, 523-535.
- Cote, M., Menager, M.M., Burgess, A., Mahlaoui, N., Picard, C., Schaffner, C., Al-Manjomi, F., Al-Harbi, M., Alangari, A., Le Deist, F., *et al.* (2009). Munc18-2 deficiency causes familial hemophagocytic lymphohistiocytosis type 5 and impairs cytotoxic granule exocytosis in patient NK cells. *J Clin Invest* 119, 3765-3773.
- Cremona, O., Di Paolo, G., Wenk, M.R., Luthi, A., Kim, W.T., Takei, K., Daniell, L., Nemoto, Y., Shears, S.B., Flavell, R.A., *et al.* (1999). Essential role of phosphoinositide metabolism in synaptic vesicle recycling. *Cell* 99, 179-188.
- D'Angelo, M.E., Bird, P.I., Peters, C., Reinheckel, T., Trapani, J.A., and Sutton, V.R. (2010). Cathepsin H is an additional convertase of pro-granzyme B. *The Journal of biological chemistry* 285, 20514-20519.
- Damke, H., Baba, T., van der Blik, A.M., and Schmid, S.L. (1995). Clathrin-independent pinocytosis is induced in cells overexpressing a temperature-sensitive mutant of dynamin. *J Cell Biol* 131, 69-80.
- Das, V., Nal, B., Dujeancourt, A., Thoulouze, M.I., Galli, T., Roux, P., Dautry-Varsat, A., and Alcover, A. (2004). Activation-induced polarized recycling targets T cell antigen receptors to the immunological synapse; involvement of SNARE complexes. *Immunity* 20, 577-588.
- de Saint Basile, G., Menasche, G., and Fischer, A. (2010). Molecular mechanisms of biogenesis and exocytosis of cytotoxic granules. *Nat Rev Immunol* 10, 568-579.
- Delprato, A., Merithew, E., and Lambright, D.G. (2004). Structure, exchange determinants, and family-wide rab specificity of the tandem helical bundle and Vps9 domains of Rabex-5. *Cell* 118, 607-617.
- Dempsey, P.W., Vaidya, S.A., and Cheng, G. (2003). The art of war: Innate and adaptive immune responses. *Cell Mol Life Sci* 60, 2604-2621.
- Dhein, J., Walczak, H., Baumler, C., Debatin, K.M., and Krammer, P.H. (1995). Autocrine T-cell suicide mediated by APO-1/(Fas/CD95). *Nature* 373, 438-441.
- Dietrich, J., Hou, X., Wegener, A.M., and Geisler, C. (1994). CD3 gamma contains a phosphoserine-dependent di-leucine motif involved in down-regulation of the T cell receptor. *EMBO J* 13, 2156-2166.
- Dulubova, I., Sugita, S., Hill, S., Hosaka, M., Fernandez, I., Sudhof, T.C., and Rizo, J. (1999). A conformational switch in syntaxin during exocytosis: role of munc18. *EMBO J* 18, 4372-4382.
- Dumont, C., Blanchard, N., Di Bartolo, V., Lezot, N., Dufour, E., Jauliac, S., and Hivroz, C. (2002). TCR/CD3 down-modulation and zeta degradation are regulated by ZAP-70. *J Immunol* 169, 1705-1712.

- Dustin, M.L., and Springer, T.A. (1989). T-cell receptor cross-linking transiently stimulates adhesiveness through LFA-1. *Nature* *341*, 619-624.
- Fasshauer, D., Otto, H., Eliason, W.K., Jahn, R., and Brunger, A.T. (1997). Structural changes are associated with soluble N-ethylmaleimide-sensitive fusion protein attachment protein receptor complex formation. *The Journal of biological chemistry* *272*, 28036-28041.
- Fasshauer, D., Sutton, R.B., Brunger, A.T., and Jahn, R. (1998). Conserved structural features of the synaptic fusion complex: SNARE proteins reclassified as Q- and R-SNAREs. *Proc Natl Acad Sci U S A* *95*, 15781-15786.
- Fehlmann, M., Carpentier, J.L., Van Obberghen, E., Freychet, P., Thamm, P., Saunders, D., Brandenburg, D., and Orci, L. (1982). Internalized insulin receptors are recycled to the cell surface in rat hepatocytes. *Proc Natl Acad Sci U S A* *79*, 5921-5925.
- Feldmann, J., Callebaut, I., Raposo, G., Certain, S., Bacq, D., Dumont, C., Lambert, N., Ouachee-Chardin, M., Chedeville, G., Tamary, H., *et al.* (2003). Munc13-4 is essential for cytolytic granules fusion and is mutated in a form of familial hemophagocytic lymphohistiocytosis (FHL3). *Cell* *115*, 461-473.
- Feng, D., Crane, K., Rozenvayn, N., Dvorak, A.M., and Flaumenhaft, R. (2002). Subcellular distribution of 3 functional platelet SNARE proteins: human cellubrevin, SNAP-23, and syntaxin 2. *Blood* *99*, 4006-4014.
- Ferguson, S.M., Raimondi, A., Paradise, S., Shen, H., Mesaki, K., Ferguson, A., Destaing, O., Ko, G., Takasaki, J., Cremona, O., *et al.* (2009). Coordinated actions of actin and BAR proteins upstream of dynamin at endocytic clathrin-coated pits. *Dev Cell* *17*, 811-822.
- Forgac, M. (1998). Structure, function and regulation of the vacuolar (H⁺)-ATPases. *FEBS Lett* *440*, 258-263.
- Forgac, M. (2007). Vacuolar ATPases: rotary proton pumps in physiology and pathophysiology. *Nat Rev Mol Cell Biol* *8*, 917-929.
- Fotin, A., Cheng, Y., Sliz, P., Grigorieff, N., Harrison, S.C., Kirchhausen, T., and Walz, T. (2004). Molecular model for a complete clathrin lattice from electron cryomicroscopy. *Nature* *432*, 573-579.
- Fraser, S.A., Karimi, R., Michalak, M., and Hudig, D. (2000). Perforin lytic activity is controlled by calreticulin. *J Immunol* *164*, 4150-4155.
- Freiberg, B.A., Kupfer, H., Maslanik, W., Delli, J., Kappler, J., Zaller, D.M., and Kupfer, A. (2002). Staging and resetting T cell activation in SMACs. *Nat Immunol* *3*, 911-917.
- Fukuda, M. (1991). Lysosomal membrane glycoproteins. Structure, biosynthesis, and intracellular trafficking. *The Journal of biological chemistry* *266*, 21327-21330.
- Gaidarov, I., and Keen, J.H. (1999). Phosphoinositide-AP-2 interactions required for targeting to plasma membrane clathrin-coated pits. *J Cell Biol* *146*, 755-764.
- Gasteiger, G., and Rudensky, A.Y. (2014). Interactions between innate and adaptive lymphocytes. *Nat Rev Immunol* *14*, 631-639.
- Geiger, B., Rosen, D., and Berke, G. (1982). Spatial relationships of microtubule-organizing centers and the contact area of cytotoxic T lymphocytes and target cells. *J Cell Biol* *95*, 137-143.
- Gilman-Sachs, A., Tikoo, A., Akman-Anderson, L., Jaiswal, M., Ntrivalas, E., and Beaman, K. (2015). Expression and role of $\alpha 2$ vacuolar-ATPase ($\alpha 2V$) in trafficking of human neutrophil granules and exocytosis. *J Leukoc Biol* *97*, 1121-1131.
- Glebov, O.O., Bright, N.A., and Nichols, B.J. (2006). Flotillin-1 defines a clathrin-independent endocytic pathway in mammalian cells. *Nat Cell Biol* *8*, 46-54.

- Grakoui, A., Bromley, S.K., Sumen, C., Davis, M.M., Shaw, A.S., Allen, P.M., and Dustin, M.L. (1999). The immunological synapse: a molecular machine controlling T cell activation. *Science* 285, 221-227.
- Granseth, B., Odermatt, B., Royle, S.J., and Lagnado, L. (2006). Clathrin-mediated endocytosis is the dominant mechanism of vesicle retrieval at hippocampal synapses. *Neuron* 51, 773-786.
- Griffiths, G.M., and Isaaz, S. (1993). Granzymes A and B are targeted to the lytic granules of lymphocytes by the mannose-6-phosphate receptor. *J Cell Biol* 120, 885-896.
- Gruenberg, J. (2001). The endocytic pathway: a mosaic of domains. *Nat Rev Mol Cell Biol* 2, 721-730.
- Guha, A., Sriram, V., Krishnan, K.S., and Mayor, S. (2003). Shibire mutations reveal distinct dynamin-independent and -dependent endocytic pathways in primary cultures of *Drosophila* hemocytes. *J Cell Sci* 116, 3373-3386.
- Guo, Z., Turner, C., and Castle, D. (1998). Relocation of the t-SNARE SNAP-23 from lamellipodia-like cell surface projections regulates compound exocytosis in mast cells. *Cell* 94, 537-548.
- Gustafsson, M.G. (2005). Nonlinear structured-illumination microscopy: wide-field fluorescence imaging with theoretically unlimited resolution. *Proc Natl Acad Sci U S A* 102, 13081-13086.
- Haas, A.K., Yoshimura, S., Stephens, D.J., Preisinger, C., Fuchs, E., and Barr, F.A. (2007). Analysis of GTPase-activating proteins: Rab1 and Rab43 are key Rabs required to maintain a functional Golgi complex in human cells. *J Cell Sci* 120, 2997-3010.
- Hales, C.M., Vaerman, J.P., and Goldenring, J.R. (2002). Rab11 family interacting protein 2 associates with Myosin Vb and regulates plasma membrane recycling. *The Journal of biological chemistry* 277, 50415-50421.
- Halimani, M., Pattu, V., Marshall, M.R., Chang, H.F., Matti, U., Jung, M., Becherer, U., Krause, E., Hoth, M., Schwarz, E.C., *et al.* (2014). Syntaxin11 serves as a t-SNARE for the fusion of lytic granules in human cytotoxic T lymphocytes. *Eur J Immunol* 44, 573-584.
- Han, X., Wang, C.T., Bai, J., Chapman, E.R., and Jackson, M.B. (2004). Transmembrane segments of syntaxin line the fusion pore of Ca²⁺-triggered exocytosis. *Science* 304, 289-292.
- Hanson, P.I., Roth, R., Morisaki, H., Jahn, R., and Heuser, J.E. (1997). Structure and conformational changes in NSF and its membrane receptor complexes visualized by quick-freeze/deep-etch electron microscopy. *Cell* 90, 523-535.
- Henne, W.M., Boucrot, E., Meinecke, M., Evergren, E., Vallis, Y., Mittal, R., and McMahon, H.T. (2010). FCHo proteins are nucleators of clathrin-mediated endocytosis. *Science* 328, 1281-1284.
- Hopkins, C.R., and Trowbridge, I.S. (1983). Internalization and processing of transferrin and the transferrin receptor in human carcinoma A431 cells. *J Cell Biol* 97, 508-521.
- Huotari, J., and Helenius, A. (2011). Endosome maturation. *EMBO J* 30, 3481-3500.
- Jahn, R., and Scheller, R.H. (2006). SNAREs--engines for membrane fusion. *Nat Rev Mol Cell Biol* 7, 631-643.
- Jenkins, M.R., and Griffiths, G.M. (2010). The synapse and cytolytic machinery of cytotoxic T cells. *Curr Opin Immunol* 22, 308-313.
- Jordens, I., Fernandez-Borja, M., Marsman, M., Dusseljee, S., Janssen, L., Calafat, J., Janssen, H., Wubbolts, R., and Neefjes, J. (2001). The Rab7 effector protein RILP controls lysosomal transport by inducing the recruitment of dynein-dynactin motors. *Curr Biol* 11, 1680-1685.
- Keen, J.H. (1987). Clathrin assembly proteins: affinity purification and a model for coat assembly. *J Cell Biol* 105, 1989-1998.

LITERATURE

- Kirchhausen, T., Nathanson, K.L., Matsui, W., Vaisberg, A., Chow, E.P., Burne, C., Keen, J.H., and Davis, A.E. (1989). Structural and functional division into two domains of the large (100- to 115-kDa) chains of the clathrin-associated protein complex AP-2. *Proc Natl Acad Sci U S A* *86*, 2612-2616.
- Kononenko, N.L., and Haucke, V. (2015). Molecular mechanisms of presynaptic membrane retrieval and synaptic vesicle reformation. *Neuron* *85*, 484-496.
- Koo, S.J., Kochlamazashvili, G., Rost, B., Puchkov, D., Gimber, N., Lehmann, M., Tadeus, G., Schmoranzner, J., Rosenmund, C., Haucke, V., *et al.* (2015). Vesicular Synaptobrevin/VAMP2 Levels Guarded by AP180 Control Efficient Neurotransmission. *Neuron* *88*, 330-344.
- Koo, S.J., Markovic, S., Puchkov, D., Mahrenholz, C.C., Beceren-Braun, F., Maritzen, T., Dervede, J., Volkmer, R., Oschkinat, H., and Haucke, V. (2011a). SNARE motif-mediated sorting of synaptobrevin by the endocytic adaptors clathrin assembly lymphoid myeloid leukemia (CALM) and AP180 at synapses. *Proc Natl Acad Sci U S A* *108*, 13540-13545.
- Koo, S.J., Puchkov, D., and Haucke, V. (2011b). AP180 and CALM: Dedicated endocytic adaptors for the retrieval of synaptobrevin 2 at synapses. *Cell Logist* *1*, 168-172.
- Kumari, S., and Mayor, S. (2008). ARF1 is directly involved in dynamin-independent endocytosis. *Nat Cell Biol* *10*, 30-41.
- Kupfer, A., and Singer, S.J. (1989). The specific interaction of helper T cells and antigen-presenting B cells. IV. Membrane and cytoskeletal reorganizations in the bound T cell as a function of antigen dose. *J Exp Med* *170*, 1697-1713.
- Lafourcade, C., Sobo, K., Kieffer-Jaquinod, S., Garin, J., and van der Goot, F.G. (2008). Regulation of the V-ATPase along the endocytic pathway occurs through reversible subunit association and membrane localization. *PLoS One* *3*, e2758.
- Lamaze, C., Dujancourt, A., Baba, T., Lo, C.G., Benmerah, A., and Dautry-Varsat, A. (2001). Interleukin 2 receptors and detergent-resistant membrane domains define a clathrin-independent endocytic pathway. *Mol Cell* *7*, 661-671.
- Le Borgne, R., Bardin, A., and Schweisguth, F. (2005). The roles of receptor and ligand endocytosis in regulating Notch signaling. *Development* *132*, 1751-1762.
- Le Roy, C., and Wrana, J.L. (2005). Clathrin- and non-clathrin-mediated endocytic regulation of cell signalling. *Nat Rev Mol Cell Biol* *6*, 112-126.
- Lin, R.C., and Scheller, R.H. (1997). Structural organization of the synaptic exocytosis core complex. *Neuron* *19*, 1087-1094.
- Link, E., Edelmann, L., Chou, J.H., Binz, T., Yamasaki, S., Eisel, U., Baumert, M., Sudhof, T.C., Niemann, H., and Jahn, R. (1992). Tetanus toxin action: inhibition of neurotransmitter release linked to synaptobrevin proteolysis. *Biochem Biophys Res Commun* *189*, 1017-1023.
- Liu, D., Bryceson, Y.T., Meckel, T., Vasiliver-Shamis, G., Dustin, M.L., and Long, E.O. (2009). Integrin-dependent organization and bidirectional vesicular traffic at cytotoxic immune synapses. *Immunity* *31*, 99-109.
- Liu, H., Rhodes, M., Wiest, D.L., and Vignali, D.A. (2000). On the dynamics of TCR:CD3 complex cell surface expression and downmodulation. *Immunity* *13*, 665-675.
- Llorente, A., Rapak, A., Schmid, S.L., van Deurs, B., and Sandvig, K. (1998). Expression of mutant dynamin inhibits toxicity and transport of endocytosed ricin to the Golgi apparatus. *J Cell Biol* *140*, 553-563.
- Logan, M.R., Lacy, P., Bablitz, B., and Moqbel, R. (2002). Expression of eosinophil target SNAREs as potential cognate receptors for vesicle-associated membrane protein-2 in exocytosis. *J Allergy Clin Immunol* *109*, 299-306.

- Luton, F., Buferne, M., Davoust, J., Schmitt-Verhulst, A.M., and Boyer, C. (1994). Evidence for protein tyrosine kinase involvement in ligand-induced TCR/CD3 internalization and surface redistribution. *J Immunol* *153*, 63-72.
- Macia, E., Ehrlich, M., Massol, R., Boucrot, E., Brunner, C., and Kirchhausen, T. (2006). Dynasore, a cell-permeable inhibitor of dynamin. *Dev Cell* *10*, 839-850.
- Marks, B., Stowell, M.H., Vallis, Y., Mills, I.G., Gibson, A., Hopkins, C.R., and McMahon, H.T. (2001). GTPase activity of dynamin and resulting conformation change are essential for endocytosis. *Nature* *410*, 231-235.
- Marshall, M.R., Pattu, V., Halimani, M., Maier-Peuschel, M., Muller, M.L., Becherer, U., Hong, W., Hoth, M., Tschernig, T., Bryceson, Y.T., *et al.* (2015). VAMP8-dependent fusion of recycling endosomes with the plasma membrane facilitates T lymphocyte cytotoxicity. *J Cell Biol* *210*, 135-151.
- Masson, D., Peters, P.J., Geuze, H.J., Borst, J., and Tschopp, J. (1990). Interaction of chondroitin sulfate with perforin and granzymes of cytolytic T-cells is dependent on pH. *Biochemistry* *29*, 11229-11235.
- Masson, D., and Tschopp, J. (1987). A family of serine esterases in lytic granules of cytolytic T lymphocytes. *Cell* *49*, 679-685.
- Matsumoto, N., Daido, S., Sun-Wada, G.H., Wada, Y., Futai, M., and Nakanishi-Matsui, M. (2014). Diversity of proton pumps in osteoclasts: V-ATPase with $\alpha 3$ and $\alpha 2$ isoforms is a major form in osteoclasts. *Biochim Biophys Acta* *1837*, 744-749.
- Matti, U., Pattu, V., Halimani, M., Schirra, C., Krause, E., Liu, Y., Weins, L., Chang, H.F., Guzman, R., Olausson, J., *et al.* (2013). Synaptobrevin2 is the v-SNARE required for cytotoxic T-lymphocyte lytic granule fusion. *Nat Commun* *4*, 1439.
- Maxfield, F.R., and McGraw, T.E. (2004). Endocytic recycling. *Nat Rev Mol Cell Biol* *5*, 121-132.
- Mayor, S., Presley, J.F., and Maxfield, F.R. (1993). Sorting of membrane components from endosomes and subsequent recycling to the cell surface occurs by a bulk flow process. *J Cell Biol* *121*, 1257-1269.
- McMahon, H.T., and Boucrot, E. (2011). Molecular mechanism and physiological functions of clathrin-mediated endocytosis. *Nat Rev Mol Cell Biol* *12*, 517-533.
- Medzhitov, R., and Janeway, C., Jr. (2000). Innate immunity. *N Engl J Med* *343*, 338-344.
- Mellman, I. (1996). Endocytosis and molecular sorting. *Annu Rev Cell Dev Biol* *12*, 575-625.
- Menager, M.M., Menasche, G., Romao, M., Knapnougel, P., Ho, C.H., Garfa, M., Raposo, G., Feldmann, J., Fischer, A., and de Saint Basile, G. (2007). Secretory cytotoxic granule maturation and exocytosis require the effector protein hMunc13-4. *Nat Immunol* *8*, 257-267.
- Menasche, G., Pastural, E., Feldmann, J., Certain, S., Ersoy, F., Dupuis, S., Wulffraat, N., Bianchi, D., Fischer, A., Le Deist, F., *et al.* (2000). Mutations in RAB27A cause Griscelli syndrome associated with haemophagocytic syndrome. *Nat Genet* *25*, 173-176.
- Miksa, M., Komura, H., Wu, R., Shah, K.G., and Wang, P. (2009). A novel method to determine the engulfment of apoptotic cells by macrophages using pHrodo succinimidyl ester. *J Immunol Methods* *342*, 71-77.
- Minami, Y., Samelson, L.E., and Klausner, R.D. (1987). Internalization and cycling of the T cell antigen receptor. Role of protein kinase C. *The Journal of biological chemistry* *262*, 13342-13347.
- Mollinedo, F., Calafat, J., Janssen, H., Martin-Martin, B., Canchado, J., Nabokina, S.M., and Gajate, C. (2006). Combinatorial SNARE complexes modulate the secretion of cytoplasmic granules in human neutrophils. *J Immunol* *177*, 2831-2841.

- Monks, C.R., Freiberg, B.A., Kupfer, H., Sciaky, N., and Kupfer, A. (1998). Three-dimensional segregation of supramolecular activation clusters in T cells. *Nature* 395, 82-86.
- Morel, N., Dedieu, J.C., and Philippe, J.M. (2003). Specific sorting of the $\alpha 1$ isoform of the V-H+ATPase a subunit to nerve terminals where it associates with both synaptic vesicles and the presynaptic plasma membrane. *J Cell Sci* 116, 4751-4762.
- Mosesson, Y., Mills, G.B., and Yarden, Y. (2008). Derailed endocytosis: an emerging feature of cancer. *Nat Rev Cancer* 8, 835-850.
- Nabi, I.R., and Le, P.U. (2003). Caveolae/raft-dependent endocytosis. *J Cell Biol* 161, 673-677.
- Neef, M., Wieffer, M., de Jong, A.S., Negroiu, G., Metz, C.H., van Loon, A., Griffith, J., Krijgsveld, J., Wulffraat, N., Koch, H., *et al.* (2005). Munc13-4 is an effector of rab27a and controls secretion of lysosomes in hematopoietic cells. *Mol Biol Cell* 16, 731-741.
- Ohno, H., Stewart, J., Fournier, M.C., Bosshart, H., Rhee, I., Miyatake, S., Saito, T., Gallusser, A., Kirchhausen, T., and Bonifacino, J.S. (1995). Interaction of tyrosine-based sorting signals with clathrin-associated proteins. *Science* 269, 1872-1875.
- Ono, S., Ohno, H., and Saito, T. (1995). Rapid turnover of the CD3 zeta chain independent of the TCR-CD3 complex in normal T cells. *Immunity* 2, 639-644.
- Owen, D.J., Vallis, Y., Pearse, B.M., McMahon, H.T., and Evans, P.R. (2000). The structure and function of the beta 2-adaptin appendage domain. *EMBO J* 19, 4216-4227.
- Pagan, J.K., Wylie, F.G., Joseph, S., Widberg, C., Bryant, N.J., James, D.E., and Stow, J.L. (2003). The t-SNARE syntaxin 4 is regulated during macrophage activation to function in membrane traffic and cytokine secretion. *Curr Biol* 13, 156-160.
- Parton, R.G., and Simons, K. (2007). The multiple faces of caveolae. *Nat Rev Mol Cell Biol* 8, 185-194.
- Paumet, F., Le Mao, J., Martin, S., Galli, T., David, B., Blank, U., and Roa, M. (2000). Soluble NSF attachment protein receptors (SNAREs) in RBL-2H3 mast cells: functional role of syntaxin 4 in exocytosis and identification of a vesicle-associated membrane protein 8-containing secretory compartment. *J Immunol* 164, 5850-5857.
- Pearse, B.M. (1975). Coated vesicles from pig brain: purification and biochemical characterization. *J Mol Biol* 97, 93-98.
- Pearse, B.M., and Robinson, M.S. (1984). Purification and properties of 100-kd proteins from coated vesicles and their reconstitution with clathrin. *EMBO J* 3, 1951-1957.
- Peters, P.J., Borst, J., Oorschot, V., Fukuda, M., Krahenbuhl, O., Tschopp, J., Slot, J.W., and Geuze, H.J. (1991). Cytotoxic T lymphocyte granules are secretory lysosomes, containing both perforin and granzymes. *J Exp Med* 173, 1099-1109.
- Peters, P.J., Geuze, H.J., Van der Donk, H.A., Slot, J.W., Griffith, J.M., Stam, N.J., Clevers, H.C., and Borst, J. (1989). Molecules relevant for T cell-target cell interaction are present in cytolytic granules of human T lymphocytes. *Eur J Immunol* 19, 1469-1475.
- Pfeffer, S., and Aivazian, D. (2004). Targeting Rab GTPases to distinct membrane compartments. *Nat Rev Mol Cell Biol* 5, 886-896.
- Pitzurra, L., Rossetto, O., Chimienti, A.R., Blasi, E., and Bistoni, F. (1996). Tetanus toxin-sensitive VAMP-related proteins are present in murine macrophages. *Cell Immunol* 169, 113-116.
- Podack, E.R., and Hengartner, H. (1989). Structure of perforin and its role in cytolysis. *Year Immunol* 6, 245-261.
- Poea-Guyon, S., Ammar, M.R., Erard, M., Amar, M., Moreau, A.W., Fossier, P., Gleize, V., Vitale, N., and Morel, N. (2013). The V-ATPase membrane domain is a sensor of granular pH that controls the exocytotic machinery. *J Cell Biol* 203, 283-298.

- Potter, T.A., Grebe, K., Freiberg, B., and Kupfer, A. (2001). Formation of supramolecular activation clusters on fresh ex vivo CD8+ T cells after engagement of the T cell antigen receptor and CD8 by antigen-presenting cells. *Proc Natl Acad Sci U S A* 98, 12624-12629.
- Radhakrishna, H., and Donaldson, J.G. (1997). ADP-ribosylation factor 6 regulates a novel plasma membrane recycling pathway. *J Cell Biol* 139, 49-61.
- Raiborg, C., Bache, K.G., Gillooly, D.J., Madhus, I.H., Stang, E., and Stenmark, H. (2002). Hrs sorts ubiquitinated proteins into clathrin-coated microdomains of early endosomes. *Nat Cell Biol* 4, 394-398.
- Rapoport, I., Chen, Y.C., Cupers, P., Shoelson, S.E., and Kirchhausen, T. (1998). Dileucine-based sorting signals bind to the beta chain of AP-1 at a site distinct and regulated differently from the tyrosine-based motif-binding site. *EMBO J* 17, 2148-2155.
- Reefman, E., Kay, J.G., Wood, S.M., Offenhauser, C., Brown, D.L., Roy, S., Stanley, A.C., Low, P.C., Manderson, A.P., and Stow, J.L. (2010). Cytokine secretion is distinct from secretion of cytotoxic granules in NK cells. *J Immunol* 184, 4852-4862.
- Rink, J., Ghigo, E., Kalaidzidis, Y., and Zerial, M. (2005). Rab conversion as a mechanism of progression from early to late endosomes. *Cell* 122, 735-749.
- Ritter, A.T., Asano, Y., Stinchcombe, J.C., Dieckmann, N.M., Chen, B.C., Gawden-Bone, C., van Engelenburg, S., Legant, W., Gao, L., Davidson, M.W., *et al.* (2015). Actin depletion initiates events leading to granule secretion at the immunological synapse. *Immunity* 42, 864-876.
- Rizo, J., and Sudhof, T.C. (2002). Snares and Munc18 in synaptic vesicle fusion. *Nat Rev Neurosci* 3, 641-653.
- Rohde, G., Wenzel, D., and Haucke, V. (2002). A phosphatidylinositol (4,5)-bisphosphate binding site within mu2-adaptin regulates clathrin-mediated endocytosis. *J Cell Biol* 158, 209-214.
- Rothstein, T.L., Mage, M., Jones, G., and McHugh, L.L. (1978). Cytotoxic T lymphocyte sequential killing of immobilized allogeneic tumor target cells measured by time-lapse microcinematography. *J Immunol* 121, 1652-1656.
- Ryser, J.E., Rungger-Brandle, E., Chaponnier, C., Gabbiani, G., and Vassalli, P. (1982). The area of attachment of cytotoxic T lymphocytes to their target cells shows high motility and polarization of actin, but not myosin. *J Immunol* 128, 1159-1162.
- Sassa, T., Harada, S., Ogawa, H., Rand, J.B., Maruyama, I.N., and Hosono, R. (1999). Regulation of the UNC-18-Caenorhabditis elegans syntaxin complex by UNC-13. *J Neurosci* 19, 4772-4777.
- Schiavo, G., Benfenati, F., Poulain, B., Rossetto, O., Polverino de Laureto, P., DasGupta, B.R., and Montecucco, C. (1992). Tetanus and botulinum-B neurotoxins block neurotransmitter release by proteolytic cleavage of synaptobrevin. *Nature* 359, 832-835.
- Schlossman, D.M., Schmid, S.L., Braell, W.A., and Rothman, J.E. (1984). An enzyme that removes clathrin coats: purification of an uncoating ATPase. *J Cell Biol* 99, 723-733.
- Schmid, S.L., Fuchs, R., Male, P., and Mellman, I. (1988). Two distinct subpopulations of endosomes involved in membrane recycling and transport to lysosomes. *Cell* 52, 73-83.
- Shi, L., Mai, S., Israels, S., Browne, K., Trapani, J.A., and Greenberg, A.H. (1997). Granzyme B (GraB) autonomously crosses the cell membrane and perforin initiates apoptosis and GraB nuclear localization. *J Exp Med* 185, 855-866.
- Shirakawa, R., Higashi, T., Tabuchi, A., Yoshioka, A., Nishioka, H., Fukuda, M., Kita, T., and Horiuchi, H. (2004). Munc13-4 is a GTP-Rab27-binding protein regulating dense core granule secretion in platelets. *The Journal of biological chemistry* 279, 10730-10737.

- Shirataki, H., Kaibuchi, K., Sakoda, T., Kishida, S., Yamaguchi, T., Wada, K., Miyazaki, M., and Takai, Y. (1993). Rabphilin-3A, a putative target protein for smg p25A/rab3A p25 small GTP-binding protein related to synaptotagmin. *Mol Cell Biol* 13, 2061-2068.
- Shukla, A., Berglund, L., Nielsen, L.P., Nielsen, S., Hoffmann, H.J., and Dahl, R. (2000). Regulated exocytosis in immune function: are SNARE-proteins involved? *Respir Med* 94, 10-17.
- Sieni, E., Cetica, V., Hackmann, Y., Coniglio, M.L., Da Ros, M., Ciambotti, B., Pende, D., Griffiths, G., and Arico, M. (2014). Familial hemophagocytic lymphohistiocytosis: when rare diseases shed light on immune system functioning. *Front Immunol* 5, 167.
- Simons, K., and Ikonen, E. (1997). Functional rafts in cell membranes. *Nature* 387, 569-572.
- Sollner, T., Bennett, M.K., Whiteheart, S.W., Scheller, R.H., and Rothman, J.E. (1993a). A protein assembly-disassembly pathway in vitro that may correspond to sequential steps of synaptic vesicle docking, activation, and fusion. *Cell* 75, 409-418.
- Sollner, T., Whiteheart, S.W., Brunner, M., Erdjument-Bromage, H., Geromanos, S., Tempst, P., and Rothman, J.E. (1993b). SNAP receptors implicated in vesicle targeting and fusion. *Nature* 362, 318-324.
- Sonnichsen, B., De Renzis, S., Nielsen, E., Rietdorf, J., and Zerial, M. (2000). Distinct membrane domains on endosomes in the recycling pathway visualized by multicolor imaging of Rab4, Rab5, and Rab11. *J Cell Biol* 149, 901-914.
- Sorensen, J.B., Wiederhold, K., Muller, E.M., Milosevic, I., Nagy, G., de Groot, B.L., Grubmuller, H., and Fasshauer, D. (2006). Sequential N- to C-terminal SNARE complex assembly drives priming and fusion of secretory vesicles. *EMBO J* 25, 955-966.
- Stein, B.S., and Sussman, H.H. (1986). Demonstration of two distinct transferrin receptor recycling pathways and transferrin-independent receptor internalization in K562 cells. *The Journal of biological chemistry* 261, 10319-10331.
- Stepp, S.E., Dufourcq-Lagelouse, R., Le Deist, F., Bhawan, S., Certain, S., Mathew, P.A., Henter, J.I., Bennett, M., Fischer, A., de Saint Basile, G., *et al.* (1999). Perforin gene defects in familial hemophagocytic lymphohistiocytosis. *Science* 286, 1957-1959.
- Stimpson, H.E., Toret, C.P., Cheng, A.T., Pauly, B.S., and Drubin, D.G. (2009). Early-arriving Syp1p and Ede1p function in endocytic site placement and formation in budding yeast. *Mol Biol Cell* 20, 4640-4651.
- Stinchcombe, J.C., Barral, D.C., Mules, E.H., Booth, S., Hume, A.N., Machesky, L.M., Seabra, M.C., and Griffiths, G.M. (2001a). Rab27a is required for regulated secretion in cytotoxic T lymphocytes. *J Cell Biol* 152, 825-834.
- Stinchcombe, J.C., Bossi, G., Booth, S., and Griffiths, G.M. (2001b). The immunological synapse of CTL contains a secretory domain and membrane bridges. *Immunity* 15, 751-761.
- Stinchcombe, J.C., Majorovits, E., Bossi, G., Fuller, S., and Griffiths, G.M. (2006). Centrosome polarization delivers secretory granules to the immunological synapse. *Nature* 443, 462-465.
- Sutton, R.B., Fasshauer, D., Jahn, R., and Brunger, A.T. (1998). Crystal structure of a SNARE complex involved in synaptic exocytosis at 2.4 Å resolution. *Nature* 395, 347-353.
- Sweitzer, S.M., and Hinshaw, J.E. (1998). Dynamin undergoes a GTP-dependent conformational change causing vesiculation. *Cell* 93, 1021-1029.
- Takamori, S., Holt, M., Stenius, K., Lemke, E.A., Grønborg, M., Riedel, D., Urlaub, H., Schenck, S., Brügger, B., Ringler, P., *et al.* (2006). Molecular anatomy of a trafficking organelle. *Cell* 127, 831-846.
- Tomas, A., Futter, C.E., and Eden, E.R. (2014). EGF receptor trafficking: consequences for signaling and cancer. *Trends Cell Biol* 24, 26-34.

- Trombetta, E.S., Ebersold, M., Garrett, W., Pypaert, M., and Mellman, I. (2003). Activation of lysosomal function during dendritic cell maturation. *Science* 299, 1400-1403.
- Uellner, R., Zvelebil, M.J., Hopkins, J., Jones, J., MacDougall, L.K., Morgan, B.P., Podack, E., Waterfield, M.D., and Griffiths, G.M. (1997). Perforin is activated by a proteolytic cleavage during biosynthesis which reveals a phospholipid-binding C2 domain. *EMBO J* 16, 7287-7296.
- Umeda, A., Meyerholz, A., and Ungewickell, E. (2000). Identification of the universal cofactor (auxilin 2) in clathrin coat dissociation. *Eur J Cell Biol* 79, 336-342.
- Ungewickell, E., Ungewickell, H., Holstein, S.E., Lindner, R., Prasad, K., Barouch, W., Martin, B., Greene, L.E., and Eisenberg, E. (1995). Role of auxilin in uncoating clathrin-coated vesicles. *Nature* 378, 632-635.
- Valdez, A.C., Cabaniols, J.P., Brown, M.J., and Roche, P.A. (1999). Syntaxin 11 is associated with SNAP-23 on late endosomes and the trans-Golgi network. *J Cell Sci* 112 (Pt 6), 845-854.
- Valitutti, S., Muller, S., Cella, M., Padovan, E., and Lanzavecchia, A. (1995). Serial triggering of many T-cell receptors by a few peptide-MHC complexes. *Nature* 375, 148-151.
- Valtorta, F., Jahn, R., Fesce, R., Greengard, P., and Ceccarelli, B. (1988). Synaptophysin (p38) at the frog neuromuscular junction: its incorporation into the axolemma and recycling after intense quantal secretion. *J Cell Biol* 107, 2717-2727.
- Varma, R., Campi, G., Yokosuka, T., Saito, T., and Dustin, M.L. (2006). T cell receptor-proximal signals are sustained in peripheral microclusters and terminated in the central supramolecular activation cluster. *Immunity* 25, 117-127.
- Varoqueaux, F., Sigler, A., Rhee, J.S., Brose, N., Enk, C., Reim, K., and Rosenmund, C. (2002). Total arrest of spontaneous and evoked synaptic transmission but normal synaptogenesis in the absence of Munc13-mediated vesicle priming. *Proc Natl Acad Sci U S A* 99, 9037-9042.
- Verhage, M., Maia, A.S., Plomp, J.J., Brussaard, A.B., Heeroma, J.H., Vermeer, H., Toonen, R.F., Hammer, R.E., van den Berg, T.K., Missler, M., *et al.* (2000). Synaptic assembly of the brain in the absence of neurotransmitter secretion. *Science* 287, 864-869.
- Voets, T., Toonen, R.F., Brian, E.C., de Wit, H., Moser, T., Rettig, J., Sudhof, T.C., Neher, E., and Verhage, M. (2001). Munc18-1 promotes large dense-core vesicle docking. *Neuron* 31, 581-591.
- Walch-Solimena, C., Blasi, J., Edelman, L., Chapman, E.R., von Mollard, G.F., and Jahn, R. (1995). The t-SNAREs syntaxin 1 and SNAP-25 are present on organelles that participate in synaptic vesicle recycling. *J Cell Biol* 128, 637-645.
- Walseng, E., Bakke, O., and Roche, P.A. (2008). Major histocompatibility complex class II-peptide complexes internalize using a clathrin- and dynamin-independent endocytosis pathway. *The Journal of biological chemistry* 283, 14717-14727.
- Wang, D., and Hiesinger, P.R. (2013). The vesicular ATPase: a missing link between acidification and exocytosis. *J Cell Biol* 203, 171-173.
- Wang, H., Kadlec, T.A., Au-Yeung, B.B., Goodfellow, H.E., Hsu, L.Y., Freedman, T.S., and Weiss, A. (2010). ZAP-70: an essential kinase in T-cell signaling. *Cold Spring Harb Perspect Biol* 2, a002279.
- Wang, Y., Okamoto, M., Schmitz, F., Hofmann, K., and Sudhof, T.C. (1997). Rim is a putative Rab3 effector in regulating synaptic-vesicle fusion. *Nature* 388, 593-598.
- Watanabe, S., Trimbuch, T., Camacho-Perez, M., Rost, B.R., Brokowski, B., Sohl-Kielczynski, B., Felies, A., Davis, M.W., Rosenmund, C., and Jorgensen, E.M. (2014). Clathrin regenerates synaptic vesicles from endosomes. *Nature* 515, 228-233.
- Watts, C. (1985). Rapid endocytosis of the transferrin receptor in the absence of bound transferrin. *J Cell Biol* 100, 633-637.

LITERATURE

- Weber, T., Zemelman, B.V., McNew, J.A., Westermann, B., Gmachl, M., Parlati, F., Sollner, T.H., and Rothman, J.E. (1998). SNAREpins: minimal machinery for membrane fusion. *Cell* 92, 759-772.
- Xu, J., Luo, F., Zhang, Z., Xue, L., Wu, X.S., Chiang, H.C., Shin, W., and Wu, L.G. (2013). SNARE proteins synaptobrevin, SNAP-25, and syntaxin are involved in rapid and slow endocytosis at synapses. *Cell Rep* 3, 1414-1421.
- Yamashiro, D.J., and Maxfield, F.R. (1987). Acidification of morphologically distinct endosomes in mutant and wild-type Chinese hamster ovary cells. *J Cell Biol* 105, 2723-2733.
- Yamashiro, D.J., Tycko, B., Fluss, S.R., and Maxfield, F.R. (1984). Segregation of transferrin to a mildly acidic (pH 6.5) para-Golgi compartment in the recycling pathway. *Cell* 37, 789-800.
- Zerial, M., and McBride, H. (2001). Rab proteins as membrane organizers. *Nat Rev Mol Cell Biol* 2, 107-117.
- Zhang, N., and Bevan, M.J. (2011). CD8(+) T cells: foot soldiers of the immune system. *Immunity* 35, 161-168.
- zur Stadt, U., Schmidt, S., Kasper, B., Beutel, K., Diler, A.S., Henter, J.I., Kabisch, H., Schneppenheim, R., Nurnberg, P., Janka, G., *et al.* (2005). Linkage of familial hemophagocytic lymphohistiocytosis (FHL) type-4 to chromosome 6q24 and identification of mutations in syntaxin 11. *Hum Mol Genet* 14, 827-834.

Publications

1. Chang HF, **Bzeih H**, Schirra C, Chitirala P, Halimani M, Cordat E, Krause E, Rettig J, Pattu V. Endocytosis of Cytotoxic Granules Is Essential for Multiple Killing of Target Cells by T Lymphocytes. *J Immunol.* 2016 Sep 15; 197(6):2473-84. PMID: 27527597
2. Chang HF, **Bzeih H**, Chitirala P, Ravichandran K, Sleiman M, Krause E, Hahn U, Pattu V, Rettig J. Preparing the lethal hit: interplay between exo- and endocytic pathways in cytotoxic T lymphocytes. *Cell Mol Life Sci.* 2016 Sep 1. PMID: 27585956
3. Pattu V, Halimani M, Ming M, Schirra C, Hahn U, **Bzeih H**, Chang HF, Weins L, Krause E, Rettig J. In the crosshairs: investigating lytic granules by high-resolution microscopy and electrophysiology. *Front Immunol.* 2013 Nov 27; 4:411. PMID: 24348478